NATIONAL ACADEMIES OF SCIENCE AND ENGINEERING

NATIONAL RESEARCH COUNCIL

of the

UNITED STATES OF AMERICA

UNITED STATES NATIONAL COMMITTEE

International Union of Radio Science

National Radio Science Meeting

11-13 January 1984

Sponsored by USNC/URSI
in cooperation with
Institute of Electrical and Electronics Engineers

University of Colorado
Boulder, Colorado
U.S.A.

National Radio Science Meeting
11-13 January 1984
Condensed Technical Program

TUESDAY, 10 JANUARY

2000-2400 USNC-URSI Meeting — Broker Inn

WEDNESDAY, 11 JANUARY

0900-1200

A Measurements and Standards for Microwave Antenna Systems	CR2-6
B-1 Electromagnetic Theory	CR2-28
B-2 Reflector Antennas	CR2-26
B-3 Guided Waves	CR2-28
G/H History of Ionospheric Research	CR0-30

1400-1700

A Time Domain Measurements	CR2-6
B-1 Transient Phenomena	CR1-46
B-2 Rough Surface Scattering	CR2-28
E The Radio Channel: Measurement, Modeling, and Communication	CR1-40
F Polarization Diversity Radars: Theory, Observations, and Techniques	CR1-42
G Modern Ionospheric Sounding Techniques	CR0-30
H Active Experiments in Space	CR2-26

1600

Commission H Business Meeting	CR2-26

1640

Commission A Business Meeting	CR2-6

1700

Commission E Business Meeting	CR1-40
Commission F Business Meeting	CR1-42

1730

Commission G Business Meeting	CR0-30

1900-2100

Student Paper Session	CR2-28

THURSDAY, 12 JANUARY

0830-1200

A Electromagnetic Measurements	CR2-6
B-1 Antennas and Arrays	CR1-46
B-2 Random Discrete Scatterers	CR2-28
C Information Theory	CR0-38

United States National Committee

INTERNATIONAL UNION OF RADIO SCIENCE

PROGRAM AND ABSTRACTS

National Radio Science Meeting
11-13 January 1984

Sponsored by USNC/URSI in cooperation
with IEEE groups and societies:

Antennas and Propagation
Circuits and Systems
Communications
Electromagnetic Compatibility
Geoscience Electronics
Information Theory
Instrumentation and Measurement
Microwave Theory and Techniques
Nuclear and Plasma Sciences
Quantum Electronics and Applications

Hosted by:

National Oceanic and Atmospheric Administration
National Bureau of Standards
National Telecommunications and Information Administration
University of Colorado at Boulder
and
The Denver-Boulder Chapter, IEEE/APS

NOTE:

Programs and Abstracts of the USNC/URSI Meetings are available from:

USNC/URSI
National Academy of Sciences
2101 Constitution Avenue, N.W.
Washington, DC 20418

at $2 for meetings prior to 1970, $3 for 1971-75 meetings, and $5 for 1976-84 meetings.

The full papers are not published in any collected format; requests for them should be addressed to the authors who may have them published on their own initiative. Please note that these meetings are national. They are not organized by the International Union, nor are the programs available from the International Secretariat.

MEMBERSHIP

United States National Committee

INTERNATIONAL UNION OF RADIO SCIENCE

Chairman:
Prof. Thomas B.A. Senior*
Vice Chairman:
Prof. Robert K. Crane*
Secretary:
Dr. Thomas E. VanZandt*
Immediate Past Chairman:
Dr. C. Gordon Little*

Members Representing Societies, Groups and Institutes:

American Geophysical Union	Dr. Donald A. Gurnett
American Astronomical Society	Dr. David E. Hogg
IEEE Antennas & Propagation Society	Dr. W. Ross Stoner
IEEE Communications Society	Prof. Raymond Pickholtz
IEEE Geophysics and Remote Sensing Society	Dr. Robert E. McIntosh
Optical Society of America	Prof. Herman A. Haus

Liaison Representatives from Government Agencies:

National Telecommunications & Information Administration	Dr. Douglass D. Crombie
National Science Foundation	Dr. Vernon Pankonin
National Aeronautics & Space Administration	Dr. Erwin R. Schmerling
Federal Communications Commission	Mr. William A. Daniel
Department of Defense	Dr. George L. Salton
Department of the Army	Lt. Col. Robert Clayton, Jr.
Department of the Navy	Dr. Leo Young
Department of the Air Force	Dr. Allan C. Schell

Members-at-Large:
Dr. Sidney A. Bowhill
Dr. David C. Chang
Dr. Donald T. Farley
Mr. John A. Klobuchar
Dr. Juergen Richter

*Member of USNC-URSI Executive Committee

Chairmen of the USNC-URSI Commissions:

Commission A	Dr. Helmut Hellwig
Commission B	Prof. Chalmers M. Butler
Commission C	Dr. Andrew J. Viterbi
Commission D	Drs. K.J. Button and A.A. Olin
Commission E	Dr. Arthur A. Giordano
Commission F	Dr. Earl E. Gossard
Commission G	Dr. Kenneth Davies
Commission H	Dr. Robert F. Benson
Commission J	Dr. Mark A. Gordon

Officers of URSI resident in the United States:
(including Honorary Presidents)

President	Prof. William E. Gordon*
Honorary President	Prof. Henry G. Booker*

Chairmen and Vice Chairmen of
Commissions of URSI resident
in the United States:

Chairman of Commission C	Prof. Jack K. Wolf
Vice Chairman of Commission G	Dr. Jules Aarons

Foreign Secretary of the U.S.
National Academy of Sciences — Dr. Walter A. Rosenblith

Chairman, Office of Physical
Sciences-NRC — Prof. William A. Fowler

NRC Staff Officer — Mr. Richard Y. Dow

Honorary Members: — Dr. Harold H. Beverage
Dr. Ernst Weber

*Member of USNC-URSI Executive Committee

DESCRIPTION OF THE

INTERNATIONAL UNION OF RADIO SCIENCE

The International Union of Radio Science is one of 18 world scientific unions organized under the International Council of Scientific Unions (ICSU). It is commonly designated as URSI (from its French name, Union Radio Scientifique Internationale). Its aims are (1) to promote the scientific study of radio communications, (2) to aid and organize radio research requiring cooperation on an international scale and to encourage the discussion and publication of the results, (3) to facilitate agreement upon common methods of measurement and the standardization of measuring instruments, and (4) to stimulate and to coordinate studies of the scientific aspects of telecommunications using electromagnetic waves, guided and unguided. The International Union itself is an organizational framework to aid in promoting these objectives. The actual technical work is largely done by the National Committee in the various countries.

The officers of the International Union are:

President:	W. E. Gordon (USA)
Past President:	W. N. Christiansen (Australia)
Vice Presidents:	A. L. Cullen (U.K.)
	A. P. Mitra (India)
	S. Okamura (Japan)
	A. Smolinski (Poland)
Secretary-General:	J. Van Bladel (Belgium)
Honorary Presidents:	G. Beynon (U.K.)
	H. G. Booker (USA)
	W. Dieminger (West Germany)
	I. Koga (Japan)
	J. A. Ratcliffe (U.K.)

The Secretary-General's office and the headquarters of the organization are located at Avenue Albert Lancaster 32, B-1180 Brussels, Belgium. The Union is supported by contributions (dues) from 38 member countries. Additional funds for symposia and other scientific activities of the Union are provided by ICSU from contributions received for this purpose from UNESCO.

The International Union, as of the XXth General Assembly held in Washington, D.C., in August 1981, has nine bodies called Commissions for centralizing studies in the principal technical fields. The names of the Commissions and their chairmen follow.

A. Electromagnetic Metrology
V. Kose (FRG)

B. Fields and Waves
H. G. Unger (FRG)

C. Signals and Systems
J. K. Wolf (USA)

D. Electronic and Optical Devices and Applications
J. Le Mézec (France)

E. Electromagnetic Noise and Interference
S. Lundquist (Sweden)

F. Remote Sensing and Wave Propagation
D. Gjessing (Norway)

G. Ionospheric Radio and Propagation
P. Bauer (France)

H. Waves in Plasmas
M. Petit (France)

J. Radio Astronomy
V. Radhakrishnan (India)

Every three years the International Union holds a meeting called the General Assembly, the next is the XXIst, to be held in Florence, Italy, in August/September, 1984. The Secretariat prepares and distributes the Proceedings of these General Assemblies. The International Union arranges international symposia on specific subjects pertaining to the work of one or several Commissions and also cooperates with other Unions in international symposia on subjects of joint interest.

Radio is unique among the fields of scientific work in having a specific adaptability to large-scale international research programs, since many of the phenomena that must be studied are world-wide in extent and yet are in a measure subject to control by experimenters. Exploration of space and the extension of scientific observations to the space environment are dependent on radio for their research. One branch, radio astronomy, involves cosmic phenomena. URSI thus has a distinct field of usefulness in furnishing a meeting ground for the numerous workers in the manifold aspects of radio research; its meetings and committee activities furnish valuable means of promoting research through exchange of ideas.

Steering Committee

S. W. Maley, Chairman
D. C. Chang
D. Cook
R. Y. Dow
P. L. Jensen
C. G. Little
T. B. A. Senior
T. E. Van Zandt

Technical Program Committee

T. E. Van Zandt, Chairman
R. F. Benson
C. M. Butler
D. C. Chang
K. Davies
A. A. Giordano
M. A. Gordon
E. Gossard
M. Grossi
H. Hellwig
A. Ishimaru
N. S. Nahman
M. Nesenbergs
A. D. Spaulding
C. Rush
M. Kindren, Secretary to the Committee

Wednesday Morning 11 Jan., 0900-1200

MEASUREMENTS AND STANDARDS FOR
MICROWAVE ANTENNA SYSTEMS
A We-AM CR2-6
Chairman: R. C. Baird

A-1
0900

A HORN-TYPE MILLIMETER WAVE NOISE STANDARD

W. C. Daywitt, 723.05
National Bureau of Standards
Electromagnetic Fields Division
Boulder, CO 80303

This talk describes the theory behind a 94 GHz noise standard that consists of a cyrogenically cooled carborundum absorber illuminating a specially designed pyramidal horn inside a conducting cavity. Development of the plane-wave scattering matrix theory of antennas has made it possible to derive an expression for the noise efficiency of the antenna with the cavity and absorber in the radiating near field. This expression and the uniform theory of diffraction were used to analyze this configuration for errors, an essential feature of precision standards work.

Because of the higher waveguide losses and surface roughness effects at millimeter wave frequencies, it is difficult to construct an accurate cryogenic, waveguide-type, noise standard, while errors in the horn-type standard being discussed are easily kept below 1%. Also, the horn-type standard can be duplicated at other frequency bands by simply replacing the horn in the standard.

Many cryogenic, horn-type noise sources are subject to back lobe radiation at room temperature. An estimate of the resulting noise temperature at 94.5 GHz assuming a common, commercially available horn shows an excess of 3% over the cryogenic temperature. Even with the aperture matching sections built into the present horn, there is an excess temperature of 0.7%; so to increase the accuracy the flare and aperture of the horn were encapsulated into the cavity containing the absorber. With this configuration the matching sections (along with a smooth waveguide-to-throat taper) served mainly to reduce internal horn reflections. With these reflections removed, the TE_{10} mode field pattern from the waveguide lead of the horn was maintained in the horn flare, allowing the attenuation to be calculated by treating the flare as a gradually enlarging waveguide. Subsequent 6-port reflectometer measurements indicated that combined reflections from the horn throat, flare, and aperture have a reflection coefficient magnitude less than 0.002 at 94.5 GHz.

A-2
0930

GAIN SUBSTITUTION MEASUREMENTS WITH SPHERICAL NEAR-FIELD SCANNING AND WITH COMPACT RANGE ILLUMINATION

Doren W. Hess and John R. Jones
Scientific-Atlanta, Inc.
P. O. Box 105027
Atlanta, Georgia 30348

A set of near-field measurements has been performed by combining the methods of non-probe-corrected spherical near-field scanning and gain standard substitution. A corresponding set of gain measurements has also been performed by the conventional method of compact range illumination. (The test antenna used was a particular 24 inch paraboloidal dish operated at 13 GHz.) Whereas a conventional error budget yields an accuracy for these measurements of approximately 1/2 to 1 dB, the precision and agreement between the two methods was less than 0.1 dB. As with relative pattern measurements, then, the non-probe-corrected spherical near-field scanning technique yields measurements in close agreement with the compact range method.

We also demonstrate a novel utilization of spherical near-field scanning which permits a gain comparison measurement to be performed with a single spherical scan. By mounting the gain standard antenna and the antenna under test with their ports coupled and their main beams oppositely directed, the near-field to far-field correction for both can be determined from a single scan. The time saving is a factor of 1/2.

A-3
1020

A NEW NEAR-FIELD TEST FACILITY FOR LARGE SPACECRAFT ANTENNAS

W.Chang, D.Fasold, C.-P.Fischer
Messerschmitt-Bölkow-Blohm GmbH (MBB)
Space Division
P.O. Box 80 11 69
8000 Munich 80, Fed. Rep. of Germany

Due to severe environmental constraints and the requirement for far-field measurement distances up to several kilometres it is a necessity to utilize in-door testing for modern spacecraft antennas. For this reason a cylindrical near-field test facility has been analyzed, defined and implemented. The facility will be used for the tests of the antenna module of the German direct broadcasting satellite TV-SAT (D. Fasold, M. Lieke "A Circularly Polarized Offset Reflector Antenna for Direct Broadcasting Satellites". Proceedings 13th European Microwave Conference, Nürnberg, Sept. 1983)

The facility has been designed for the test of high gain antennas with up to 5 m in diameter in the frequency range 1 ... 40 GHz. It provides high accuracy in the side-lobes (1 dB at -30 dB), cross-polarization (1.5 dB at -40 dB) and gain (0.2 dB). Because of the narrow beamwidth special interest has been given to the angular accuracy ($\leq$ 0.01 degr.). One of the key equipments is the linear probe positioner which is laser controlled for high probe position accuracy.

For the qualification of the facility, extensive comparisons and parametric tests have been performed in order to demonstrate the accuracy. The results of the qualification tests will be presented in the paper.

A-4 THE MEASUREMENT OF EIRP AND SATURATING FLUX DENSITY OF
1050 SATELLITE SYSTEMS USING PLANAR NEAR-FIELD MEASUREMENTS

Allen C. Newell
National Bureau of Standards
Electromagnetic Fields Division, 723.05
Boulder, CO 80303

Near-field measurements have been used successfully for a wide variety of antennas and frequency ranges to obtain gain, pattern and polarization data. In these measurements, however, the results have been a characterization of the antenna only. In a satellite system, as well as other complex systems, there is a need to include the transmitter or receiver as a part of the measurement and determine the total integrated system performance. Two such measurements are the determination of effective isotropic radiated power (EIRP) and the flux density incident on the antenna which will saturate the receiver. The near-field techniques have recently been extended to provide for the measurement of both these quantities.

These measurements are both related to the determination of antenna gain from near-field measurements where the information required is the relative near-field data, the gain of the probe, and the insertion loss $b_0'(\underline{P}_0)/a_0$, where a_0 is the input to the transmitting antenna, and $b_0'(\underline{P}_0)$ is the output of the receiving antenna when the probe is at the reference point $\underline{P}_0$.

In the total system measurements, it may be difficult or impossible to disconnect the antenna from the rest of the system for this insertion loss measurement. It is also often desirable to include the antenna/system interaction as part of the measurements. For these reasons, the two new techniques do not require the insertion loss measurement or any disconnection of the actual system. In both, relative near-field data and probe gain are still required. For the flux density measurement, instead of the insertion loss measurement, the probe is placed at the near-field reference point and a signal sufficient to saturate the receiver is transmitted from the probe. From a knowledge of the power level input to the probe and the above near-field data, the equivalent plane-wave flux density can be determined. For the EIRP measurements, the probe is also placed at the reference point, the system under test transmits its normal signal, and the power output of the probe is measured.

Details of the equations and measurement techniques for both of these applications will be described.

A-5
1120

A PLANAR NEAR-FIELD ANTENNA TEST FACILITY FOR PRECISION ALIGNMENT OF PHASED ARRAY ANTENNAS

W. T. Patton
Building 101-124
RCA
Moorestown, NJ 08057

The use of planar near-field measurement techniques to determine the radiation pattern characteristics of an antenna (A.C. Newell, R.C. Baird and P.F. Wacker, IEEE Transactions, AP-21, no. 4, 1973), has become a well known and accepted technique over the past decade. The use of an inverse transform of the far-field pattern to detect errors in a phased array aperture was suggested by Ransom (P.L. Ransom and R. Mittra, Phased Array Antennas, Artech House, 1973), and the use of this technique to align a phased array antenna (D. Staiman, Proc. 1979 Antenna Applications Symposium, Univ. of Illinois) has been demonstrated.

A new near-field test facility has been constructed which employs a novel spectrum merging technique to enhance the resolution of the inverse transform in the antenna aperture plane. This facility employs laser instrumentation to measure the translational and rotational position errors of the probe carriage and its support tower. The probe position errors are then compensated by a "k-vector" compensation technique (P.K. Agrawal, 1982 APS Symposium Digest, 218-221). Extensive calibration of the RF receiver linearity, and of the RF path phase errors are used to ensure highly accurate data. These measures are taken to obtain phase alignment data for each element of the array with an accuracy of better than one degree RMS.

This facility is currently in the final phase of verification testing and will soon begin testing and alignment of production array antennas.

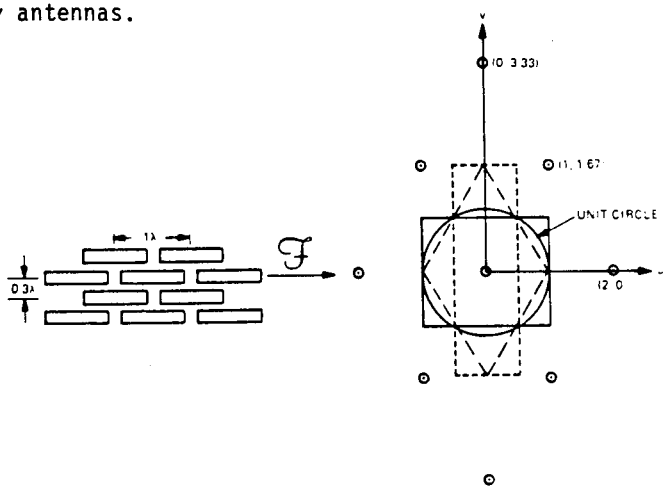

Triangular-grid array and its angular spectrum

ELECTROMAGNETIC THEORY
B-1 We-AM CR2-28
Chairman: Y. Rahmat-Samii, Jet Propulstion Laboratory,
California Institute of Technology,
Pasadena, CA 91109

B1-1
0900 STRUCTURE OF SURFACE POLARITON MODES IN AND NEAR SMALL PARTICLES

H. Weil and T.B.A. Senior
Radiation Laboratory
Department of Electrical and Computer Engineering
The University of Michigan
Ann Arbor, MI 48109

Resonant electric fields induced in small homogeneous particles are studied by numerical means. The fields are induced by an incident wave whose wavelength in the ambient medium greatly exceeds the particle dimensions but whose frequency lies within an absorption band of the bulk material of which the particle is composed. The resonant fields are a manifestation of the close coupling between electromagnetic and internal vibrational modes of the material which is the source of the enhanced absorption. Such coupled disturbances are called polariton modes and in particular this investigation is concerned with the effects of particle shape on the geometric structure of the induced polariton fields as well as that of the associated external near fields.

For a variety of rotationally symmetric objects Senior and Weil (Appl. Phys. B-29 (117) 1982) have investigated the dependence on particle shape of the relative strength of the various resonant modes as well as the precise frequencies within the bulk material absorption bands at which they occur. The present investigation is a continuation of that research to explore the field structure and is based on the same theoretical formulation. It involves an improved numerical solution of the integral equations governing the induced surface electrical potential from which the exterior near fields and the interior fields are then deduced.

A polariton mode may exhibit a complex and highly non-uniform structure at its resonant frequency even in a simply shaped body such as a capped cylinder. Illustrative results show the manner in which cellular regions of large and complex fields develop and move as the frequency approaches the resonance frequency. Near resonance the influence of a surface perturbation depends on its location relative to regions of internal field concentration near the surface.

B1-2
0920

THE WAVE-KINETIC FORMALISM WITHIN THE FRAMEWORK OF CATASTROPHE THEORY

Michael E. Sockell and Ioannis M. Besieris, Department of Electrical Engineering Virginia Polytechnic Institute and State University, Blacksburg, VA 24061; Ngo Dinh Hoc, Department of Electrical Engineering, Stanford University Stanford, CA 94305

Arising naturally in the study of one-dimensional pulse propagation in homogeneous dispersive media are certain classes of canonical diffraction catastrophe integrals due originally to Thom (Structural Stability and Morphogenesis Benjamin, Reading, MA, 1975) and Arnold (Russ. Math. Surys. 30, 1 1975). This is especially evident within the framework of the wave-kinetic formalism which utilizes a combined space-wavevector-time domain, called phase space, and incorporates the full dispersion relation $w=w(K)$. Wave propagation in this context is realized through the evolution of a phase-space distribution function, referred to as the Wigner distribution function, which, in turn, is intimately related to physically meaningful quantities, such as the pulse envelope, pulse spread, etc.

Except for scaling factors, the formal solution for the Wigner distribution function is shown to be a cuspoid diffraction catastrophe of infinite odd codimension. Depending on the order of approximation of the exact solution beyond the "semiclassical" or"quasiparticle" limit (e.g., Airy, Hyperairy, etc.) one recognizes caustic-like structures of finite codimension.

For illustrative purposes, specific analytical and numerical results will be presented for a canonical quintic dispersion medium ($w= -K^5/5$) corresponding to a linearized fifth-order Korteweg-deVries equation. In this case, the Wigner distribution function is related to the swallowtail diffraction catastrophe, whereas its projection onto the space-time domain (pulse envelope) is given in terms of the hyperairy function.

B1-3 ELECTROMAGNETIC VIRIAL THEOREMS
0940

Edward F. Kuester
Department of Electrical and Computer Engineering
Campus Box 425
University of Colorado
Boulder, Colorado 80309

In classical and quantum mechanics, the virial theorem has proved useful in calculations of energy and predictions of such relations as the ideal gas law (Yu.N. Demkov, Variational Principles in the Theory of Collisions, Oxford: Pergamon, 1963). For an eigenfunction $\psi(\bar{r})$ of the Schrödinger equation

$$-\nabla^2\psi + q(\bar{r})\psi = \lambda\psi$$

where $\bar{r} = x\bar{a}_x + y\bar{a}_y + z\bar{a}_z$, the virial theorem reads

$$\int (\nabla\psi)^2 dV = \tfrac{1}{2}\int (\bar{r}\cdot\nabla q)\psi^2 dV$$

where the integrals are carried out over all space. This relation allows the average kinetic energy associated with ψ to be expressed as an integral carried out only over those points in space where the potential q is not constant. This often results in more economical computations.

Using Fock's idea of variable scaling of a stationary functional (V.A. Fock, Z. Phys., 63, 855-858, 1930), we can use well-known stationary functionals from electromagnetic theory to derive virial theorems for electromagnetic fields as well. As an example, a resonant mode in a cavity occupying a volume V bounded by a perfectly conducting wall S obeys

$$\int_V (\mu\bar{H}\cdot\bar{H} - \varepsilon\bar{E}\cdot\bar{E})dV = \int_V \bar{r}\cdot[\nabla\varepsilon(\bar{E}\cdot\bar{E}) - \nabla\mu(\bar{H}\cdot\bar{H})]dV + \oint_S (\mu\bar{H}\cdot\bar{H} + \varepsilon\bar{E}\cdot\bar{E})\bar{r}\cdot d\bar{s}$$

A similar formula can be found for guided mode fields. As an indication of its application, we can derive an expression for the power carried by a mode of a step-index optical fiber in terms of an integral carried out only over the core-cladding interface.

B1-4 1000 TRANSIENT RESPONSE FROM A THIN DYKE IN THE EARTH FOR LINE AND LOOP SOURCES

A. Q. Howard Jr., K. Nabulsi and D. N'Guessan
Geo Electromagnetics Group
Department of Electrical and Computer Engineering
University of Arizona
Tucson, AZ 85721

A closed form solution to a thin tabular conductor in a lossy medium is presented. Impulsive current on a line or on an arbitrarily oriented loop sets up the time domain transient problem. The solution, which is an extension of 'Maxwell's Theorem' can be interpreted as a continuous superposition of moving images. The images move away from the observer and perpendicular to the plane of the target. For example in the loss free background case it is well known that the image moves with an apparent velocity $v_a = 2/(\mu\sigma d)$ where $\mu \cong 4\pi \times 10^{-7}$ is the magnetic permeability in henries/meter and σd is the conductivity thickness product of the sheet in MHOS. (Static and Dynamic Electricity, Third Ed., W. R. Smythe, McGraw-Hill, 1968, pp. 380-382). The transient numerical results presented have a geophysical application. This is because mineralization in the earth often occurs in cracks which are thin and approximately planar. The transient response is seen to be diagnostic of both the conductivity thickness product $W = \sigma d$ and the range R of the distance to the target.

REFLECTOR ANTENNAS
B-2 We-AM CR2-26
Chairman: R. J. Pogorzelski, TRW Space and Technology Group, Redondo Beach, CA 92078

B2-1
1040

DIFFRACTION ANALYSIS OF REFLECTOR ANTENNAS WITH MESH SURFACES

Y. Rahmat-Samii* and S. W. Lee+
*Jet Propulsion Laboratory, California Institute of Technology, Pasadena, CA 91109
+University of Illinois, Urbana, IL 61801

Applications of large reflector antennas for satellite communications and ground terminals have resulted in the use of mesh surfaces, due to their light weight, reduced wind effects and unfurlability. A close look at these mesh structures reveals that they have basically either strip/aperture or wire grid characteristics. The meshes, however, may have a variety of individual cell shapes based on their manufacturing construction. Accurate performance analysis of these mesh reflectors for multiple and contour beam applications demands that the effects of the mesh be properly accounted for in the vector diffraction analysis. This is particularly important when determining the cross-polarized patterns of these reflectors.

In order to properly incorporate the effects of meshes, the physical optics induced current on the reflector surface needs to be modified. This is done by first determining the reflection coefficient matrix for the prescribed mesh configuration and then by properly accounting for the local coordinate system of the mesh cells at each point on the curved reflector surface. So far, most of the analytical/numerical works have been based on a simplified wire-grid model, which uses Astrakhan's reflection coefficient matrix, without the proper incorporation of the mesh local coordinate system.

In this paper, a strip/aperture model has been used to formulate the reflection coefficient matrix for a variety of mesh cell configurations. This model uses aperture modes in a Floquet-type expansion and imposes proper boundary conditions to derive the reflection coefficient matrix. Next, the induced physical optics current on the reflector surface is modified to account for the mesh surface by carefully incorporating the orientation of the local mesh cell coordinates in the construction of the mesh-induced current using Eulerian angle transformations. Numerical results are obtained for both symmetric and offset reflector antennas with a variety of mesh configurations using the aperture/strip and wire-grid models. Detailed comparisons are made between these two approaches; in particular, attention is focused on the generation of cross-polarized fields.

B2-2 1100 ANALYSIS AND DESIGN OF A FREQUENCY-SELECTIVE REFLECTING SURFACE

J. J. Fratamico, C. A. Lindberg, A. J. Simmons
M.I.T. Lincoln Laboratory
Lexington, Massachusetts 02173

A subreflector which reflects one frequency band but is transparent to another is useful in the design of dual-frequency antennas. One approach is to use an array of resonant dipoles. Previous analysis (B. A. Munk, et al, IEEE Trans. AP, 19, 612-617, 1971) was based on dipole antenna and mutual coupling theory, or by an equivalent-circuit filter theory approach (J. A. Arnaud, F. A. Pelow, BSTJ, 54, 263-283, 1975). The theory described here is based on a moment method analysis. The obstacles analyzed consist of end-loaded crossed dipoles printed on a dielectric sheet in a square array. The effect of the dielectric sheet is included. The fields are expanded in an infinite series of 2-dimensional Floquet modes and the currents on the elements are represented by a number of segments with unknown coefficients. The reflected and transmitted plane wave fields are calculated, for a plane wave at arbitrary incidence, by application of the boundary conditions in the plane of the scattering obstacles, by numerical solution of the resulting matrix of equations. Extension of the results to a double-layer grid is carried out simply by means of transmission line theory, in which evanescent-mode coupling is ignored. The double-layer design improves the bandwidth and wide-angle reflecting properties. An experimental version of the reflector built to reflect a 5% band around 44 GHz showed good agreement with the theory. (See Figure)

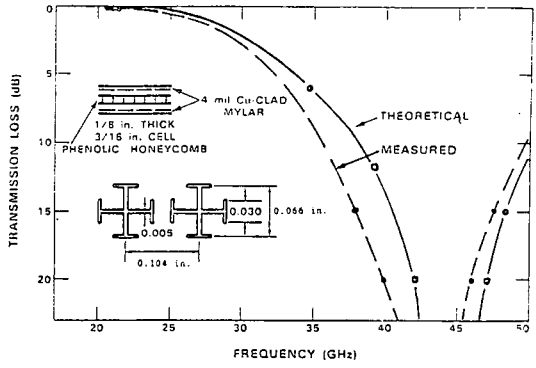

TRANSMISSION LOSS VS. FREQUENCY DICHROIC PANEL

B2-3 SCANNING AND COLLIMATION CHARACTERISTICS OF SYMMETRIC AND
1120 OFFSET BICOLLIMATED GREGORIAN REFLECTOR ANTENNAS: Jaganmohan B. L. Rao, Code 5372, Electromagnetics Branch, Radar Division, Naval Research Laboratory, Washington, DC 20375

A bicollimated Gregorian reflector antenna which can collimate a beam in two different directions and has better scan capabilities than an equivalent confocal reflector was proposed (J.B.L. Rao, "Bicollimated Near Field Gregorian Reflector Antenna," APS Symposium Digest, pp. 273-276, May 1982). A three dimensional ray tracing technique was developed (J.B.L. Rao, "Bicollimated Near Field Gregorian Reflector Antenna," NRL Report No. 8658, 9 Feburary 1983) to determine the aperture phase errors as the antenna beam is scanned to different angles by scanning the array feed. It is the purpose of this paper to report on the aperture phase error analysis for both offset and symmetric bicollimated reflectors. The analysis will show that almost perfect ring collimations are obtained for symmetric as well as offset configurations. Also, the scanning range of the offset configuration is almost circularly symmetric and is not noticeably inferior to its symmetric counterpart. In addition, the scanning ranges of the bicollimated configurations are about 45% more than their equivalent confocal configurations.

B2-4
1140

ADVANCES IN QUADRATIC PHASE INTEGRATION

R. J. Pogorzelski
TRW Space and Technology Group
One Space Park
Redondo Beach, CA 90278

In a recent symposium presentation, this author discussed an integration algorithm in the context of physical optics applied to a hyperboloidal subreflector (R.J. Pogorzelski, IEEE AP-S International Symposium, Los Angeles, June 1981). In this algorithm it is assumed that by removing an appropriate quadratic phase factor from the integrand one may render the remaining part slowly varying. One then approximates this slowly varying part by a polynomial of degree N thus casting the integral in the form

$$I = \sum_{n=0}^{N} A_n I_n \quad \text{where } I_n = \int_a^b x^n e^{j(\alpha x^2+\beta x+\gamma)} dx$$

A recursive algorithm was then introduced by which one may efficiently calculate the constituent integrals, I_n, beginning with the zero order one which is easily expressed in terms of Fresnel integrals. It was also suggested that the polynomial coefficients A_n be computed by first expanding in Chebyshev polynomials.

The present work concerns the mitigation of two difficulties inherent in the above scheme. First, the recursive algorithm beginning with the Fresnel integral and proceeding upward has been found to be unstable. Secondly, the triangular matrix transformation from the Chebyshev expansion to the desired polynomial one has been shown to result in an unnecessarily cumbersome integration algorithm.

The first difficulty has been overcome by using the recursive formula in the reverse direction proceeding downward from an asymptotic approximation to a high order integral. This technique not only stabilizes the calculation but also obviates the need for a Fresnel integral subroutine. The second difficulty above has been circumvented by derivation of a new recursive algorithm which applies to the constituent integrals resulting from the Chebyshev expansion as opposed to the polynomial one. This new recursive formula is unstable in both upward and downward directions. However, if it is represented in matrix form and decomposed into lower and upper triangular factors, a stable algorithm results.

GUIDED WAVES
B-3 We-AM CR2-28
Chairman: D. C. Chang, Department of Electrical and Computer Engineering, University of Colorado, Boulder, CO 80309

B3-1
1040 ON THE SOLUTION OF TWO-DIMENSIONAL ELECTROMAGNETIC FIELD PROBLEMS WITH COMPLEX IMPEDANCE BOUNDARIES

K.C. Gupta
Department of Electrical and Computer Engineering
University of Colorado
Boulder, CO 80309

In the analyses of microwave planar circuits and microstrip patch antennas, one comes across two-dimensional boundary value problems with reactive or complex impedance boundaries (because of fringing of the fields at the edges). Corresponding problems with electric or magnetic wall boundary conditions can often be solved by using two-dimensional impedance Green's functions which are available for several regular shapes.

An approximate method for solving a class of such problems will be discussed. The method involves the solution of the corresponding configuration with magnetic walls boundary condition as the first step. This configuration with magnetic walls is considered as a multiport component with several ports located all around the magnetic walls. The impedance wall is approximated by a lumped element network with an equal number of ports. Characterizations of the two-dimensional multiport component and that of the lumped element representation of the complex impedance boundary are combined together by using the segmentation method to yield the desired characterization of the component with the complex impedance boundary.

Applications of the method to microstrip antenna design will be presented.

B3-2
1100

QUASISTATIC LINE PARAMETERS FOR SLOTLINES

Edward F. Kuester and David C. Chang
Department of Electrical and Computer Engineering
Campus Box 425
University of Colorado
Boulder, Colorado 80309

Slotline consists of a dielectric substrate bounded on one side by a conducting ground plane in which a narrow, long slot has been cut to serve as a waveguide. Cohn and many others have published analyses of slotline requiring substantial computer time in order to obtain numerical results for the effective dielectric constant and characteristic impedance. Recently, Vainshtein et al. (Radio Eng. Electron Phys., 22(9), 36-43, 1977) have formulated integral equations for the slot fields in the quasistatic limit, and using variational techniques, obtain two sets of formulas for L and C (the inductance and capacitance per unit length of the line). Both formulas involve the corresponding parameters of the complementary microstrip line. Unfortunately, the two formulas give differing results, and the authors acknowledge the difficulty of deciding when one set of formulas will be more accurate than the other.

We use a more accurate trial function to refine Vainshtein's variatonal results, and obtain simple, closed-form expressions for L and C of the slotline. With the corresponding values of L and C for microstrip computed from simple formulas given by Kuester (IEEE Trans. MTT, Jan. 1984, to appear), we have expressions which are accurate for all values of substrate permittivity, substrate thickness and slot width, within the quasistatic assumptions. The expressions are completely programmable onto an HP-15C calculator, which will calculate values for the effective dielectric constant and characteristic impedance as well.

B3-3
1120

REFLECTION AND RADIATION FROM TRUNCATED DIELECTRIC WAVEGUIDES: J.S. Bagby and D.P. Nyquist, Dept. of Elec. Engr. and Sys. Sci., Michigan State University, East Lansing, MI 48824

An iterative technique for evaluating the reflection and radiation of an incident guided-wave field in a truncated dielectric waveguide is presented. The technique is based on an equivalent-polarization integral equation formulation.

The waveguide, which is assumed to be axially-symmetric with arbitraty transverse cross-section and transverse grading described by a refractive index contrast $\delta n^2(\vec{\rho})$, is plane-truncated at location z = 0. The guide supports a surface-wave field $\vec{E}(\vec{r}) = \vec{e}(\vec{\rho})\exp(-j\beta z)$ which is incident on the truncation. The total field satisfies the 3-d polarization integral equation

$$\vec{E}(\vec{r}) - \int \frac{\delta n^2(\vec{\rho}')}{n_c^2} u(-z') \overleftrightarrow{G}(\vec{r}|\vec{r}')\cdot\vec{E}(\vec{r}')\, dV' = 0$$

where $\overleftrightarrow{G} = PV(k_c^2\overleftrightarrow{I} + \nabla\nabla)\overleftrightarrow{G}_o + \overleftrightarrow{L}$, with $\overleftrightarrow{L}$ the appropriate depolarizing dyadic and G_o the free-space Green's function. By decomposing the total field $\vec{E}$ as $\vec{E} = \vec{E}^L + \vec{E}^R$, with $\vec{E}^L = \vec{E}\, u(-z)$ and $\vec{E}^R = \vec{E}\, u(z)$, we can write the above integral equation as

$$\vec{E}^R(\vec{r}) - \int \frac{\delta n^2(\vec{\rho}')}{n_c^2} \overleftrightarrow{G}(\vec{r}|\vec{r}')\cdot\vec{E}^L(\vec{r}')\, dV' = 0$$

for z > 0. If we assume a modal expansion for $\vec{E}$ with amplitudes a_n and $A(\vec{\xi})$, we can also show by use of an appropriateinverse-operator, $\mathcal{L}_n$, that

$$a_n = C_n^{-1} \int \vec{E}_n^+(\vec{r})\cdot\vec{E}^R(\vec{r})\, dV$$

where C_n is a normalization constant dependent on $\vec{e}_n(\vec{\rho})$ and the spatial transform of $\overleftrightarrow{G}$ at β_n. The iterative method is based on these last two equations. Given an initial guess at the partial field $\vec{E}^L$, they can be used to find a refined modal expansion for $\vec{E}^L$ and $\vec{E}^R$.

This method is applied to the slab waveguide, and extensive numerical results of the iterative scheme are presented and compared to the results of other techniques.

B3-4
1140 ON THE NONPHYSICAL POLE IN THE SPECTRAL REPRESENTATION OF THE VECTOR POTENTIAL FOR A LINE DIPOLE IN A DIELECTRIC SLAB: Krzysztof A. Michalski, Department of Electrical Engineering, University of Mississippi, University, MS 38677, and Chalmers M. Butler, Department of Electrical Engineering, University of Houston, Houston, TX 77004

The first step in formulating the integral equation for the current distribution on a conducting strip embedded in a dielectric slab is to find the magnetic vector potential due to a line current (TM excitation) or a line dipole (TE excitation) residing in the slab (K.A. Michalski and C.M. Butler, Radio Sci., 18, November-December, 1983). This potential has the form of a Sommerfeld-type integral with the integration path along the real axis in the spectral k_x-plane. An equivalent, and often more efficient representation of this integral is obtained by deforming the original path to a path around the branch cuts and the poles of the integrand. As is well know, the branch cut contributions can be physically interpreted in terms of lateral waves and the pole contributions in terms of surface waves or leaky waves. It is found, however, that in the TE case there is an additional pole present at $k_x=k_2$, where k_2 is the wave number of the slab dielectric, which is not associated with any physical phenomenon. Although this pole's contribution may be dominant in the spectral representation of the integral, it is annihilated when the harmonic operator is applied to obtain the electric field from the vector potential. Since, in the moment method procedure, the harmonic operator is approximated by finite differences, the contribution of this pole may introduce appreciable error to the final result. Therefore, it is expedient, in light of the nonphysical nature of this pole, to omit it in computing the vector potential.

HISTORY OF IONOSPHERIC RESEARCH
G/H We-AM CRO-30
Chairman: C. Stewart Gillmor, Wesleyan University, Middletown, CT 06457

G/H-1 0840 **THE FRIENDSHIP AND COLLABORATION OF BREIT AND TUVE IN IONOSPHERIC RESEARCH, 1923-1929:** C. Stewart Gillmor, Department of History, Wesleyan University, Middletown, CT 06457

Gregory Breit and Merle Tuve first met in 1923 and soon became good friends. Both had radio experience. Breit had studied radio and electronics with E. O. Hulburt at Johns Hopkins and worked in the Radio Section of the Bureau of Standards. Tuve had been interested in radio since his Boy Scout days and had been a noted ham operator. He graduated in E. E. from Minnesota, studying with C. M. Jansky, then stayed on to do an M. A. in Physics, becoming acquainted with Breit at that time. Tuve learned there from W. F. G. Swann of Swann and J. G. Frayne's unsuccessful experiments to sound the Kennedy-Heaviside Layer with radio pulses.

Tuve succeeded to a position as Instructor in Physics at Johns Hopkins in 1924. In July 1924 Breit became Mathematical Physicist at the Department of Terrestrial Magnetism, Carnegie Institution of Washington, and immediately began to plan a program to measure the height of the conducting layer, and to involve Tuve, and Johns Hopkins. Breit made several experiments in the early fall of 1924 and succeeded in getting funds for construction of a very large parabolic antenna and also in gaining a temporary position for Tuve for the summer of 1925. Promising results were noted by Breit in early January 1925 (Terr. Mag. Atmos. Elect., March 1925) and he continued experiments with commercial and Navy transmitters and with university colleagues. With Tuve's arrival at DTM in mid-June and with the collaboration of Hulburt and A. H. Taylor at the Naval Research Laboratory, experiments began using a Navy transmitter at Anacostia, a few miles from the DTM. Results were announced soon (Nature, 5 September 1925), describing the layer height measurements using echo sounding. Radar returns from aircraft flying into Bolling Field were often an annoyance at that time... Breit and Tuve continued joint ionospheric researches until Breit left for NYU in 1929, but their other work on hi-voltage and atomic physics, and Breit's interest in quantum theory drew them away from the ionosphere. Beginning in early 1927 they unsuccessfully tried to encourage rocket research to aid in upper atmosphere and ionosphere studies. Their last joint article on ionospheric physics was published in 1928.

This paper draws upon personal interviews and correspondence, and manuscript collections, including the Papers of M. A. Tuve.

G/H-2
0900

THE U.S. ROLE IN THE EVOLUTION OF BREIT AND TUVE IN IONOSPHERIC RESEARCH 1923-1929:

A. H. Shapley
4170 Pinon Drive, Boulder, CO 80303

G/H-3
0920

FORTY YEARS (1944-1984) OF U.S. IONOSPHERIC AND SOLAR FORECASTING INCLUDING DEVELOPMENT OF SOLAR-TERRESTRIAL PHYSICS DATA SERVICES

J. V. Lincoln, Author
2005 Alpine Drive
Boulder, CO 80302

The Interservice Radio Propagation Laboratory of NBS prepared weekly and later bi-weekly forecasts of ionospheric radio propagation for modification of the monthly median predictions issued months in advance. By 1944 a 24-hour warning service for ionospheric conditions over the North Atlantic was in operation. This developed into the North Atlantic Radio Warning Service with forecasts every six hours, including broadcasts on WWV. The North Pacific Radio Warning Service was established in 1952. These forecasts depended in a large part on knowledge of current solar activity and geophysical phenomena. In 1956 the publication of "Solar Geophysical Data" began. With the IGY the contents of SGD expanded and data services through the World Data Center system began. Now the short-term forecasts are the responsibility of the Space Environment Services Center of SEL, NOAA. The data services for solar-terrestrial physics are run by the National Geophysical Data Center of NESIS, NOAA.

G/H-4
0940

CHRISTIAN DOPPLER AND THE DOPPLER EFFECT

Kurt Toman, Propagation Branch
Rome Air Development Center
Electromagnetic Sciences Division
Hanscom AFB, MA 01731

A summary is given of Doppler's life and career. He was born 180 years ago on 29 Nov 1803 in Salzburg. He died on 17 Mar 1853 in Venice. The effect bearing his name was first announced in a presentation before the royal bohemian society of the sciences in Prag on 25 May 1842. Doppler considered his work a generalization of the abberation theorem as discovered by Bradley. With it came the inference that the perception of physical phenomena can change with the state of motion of the observer. Acceptance of the principle was not without controversy. In 1852, the mathematician Petzval claimed that no useful scientific deductions can be made from Doppler's elementary equations. In 1860, Ernst Mach resolved the misunderstanding that clouded this controversy. The Doppler effect is alive and well. Its role in radio science and related disciplines will be enumerated.

THE HISTORY OF NEAR-VERTICAL-INCIDENCE SKYWAVE (NVIS) COMMUNICATIONS: G. H. Hagn, Telecommunications Sciences Center, SRI International, 1611 N. Kent Street, Arlington, VA 22209

G/H-5
1020

Let us define near-vertical-incidence skywave (NVIS) propagation as pertaining to paths out to 500 km. The first NVIS studies go back to the original experimental verification of the existence of the ionosphere by Breit and Tuve in the mid 1920s. Indeed, vertical-incidence sounders were the primary tool for scientific study of the ionosphere before the advent of oblique-incidence sounders in the 1950s and satellites and rockets in the 1960s. However, the history of these tools is not the main thrust of this paper.

Radio amateurs pioneered the use of the NVIS mode for communications in the 1920s. Berkner and Wells verified parts of the magnetoionic theory (Appleton-Hartree equations) in a classic experiment at Huancayo, Peru in the 1930s, and their results suggested the potential importance of antenna orientation at low geomagnetic latitudes. Experiments by Herbstreit and Crichlow in the 1940s in Panama and New Guinea led to use of NVIS communications by the U.S. Army in South Pacific jungles during World War II to achieve greater ranges than could be achieved by HF or VHF groundwave modes. The NVIS mode was used by the UN forces in Korea in the early 1950s to overcome ground-wave diffraction losses in the mountains of Korea. The theory of "dipole orientation" at low geomagnetic latitudes was known during WW II, but the use of the ordinary mode (north-south orientation of the dipole near the geomagnetic dip equator) was not used operationally until the late 1950s in Malaya by the British Far East Land Forces. Theoretical considerations of dipole orientation by Piggott aided Shirley in his Malayan operations-research experiments regarding counterinsurgency warfare. NVIS communications was considered again by Busch as a way to overcome the operational range limitations imposed by "jungle loss," and he proposed the YoYo antenna for launching thw NVIS mode. Dipole orientation was independently rediscovered by Hagn in the early 1960s as it pertained to paths near the Kra peninsula in Thailand and the Mekong Delta area of South Vietnam. The U.S. Army Special Forces used dipole orientation on NVIS paths for their single-sideband (SSB) nets in Vietnam between fixed outposts and to patrols with manpack radios. The importance of antenna selection (for gain toward the zenith) and frequency selection (to be below the vertical-incidence critical frequency) to avoid an "operational skip zone" were reiterated through the experiments of Hagn and Vincent in Thailand and through the U.S. Army operational experience in Vietnam.

The threat of modern weapons (e.g., surface-to-air missiles) in the 1970s forced military helicopters to begin flying very low--at the nap-of-the-earth (NOE). NOE helicopter communications can be achieved using the NVIS mode when appropriate antennas are employed. Indeed, other modern threats have led to a rediscovery of HF communications in the 1980s, and the NVIS mode will receive added attention along with other longer distance modes of HF communications over the coming years. The resulting need for covering the NVIS mode more thoroughly in U.S. Army field manuals and training has recently been noted by Fiedler and Hagn. The history of this use of the ionosphere is just beginning.

G/H-6
1040

TRACING HF RADIO RAYS DIGITALLY: DEVELOPMENT AND IMPACT IN THE SIXTIES

T. A. Croft
Technology for Communications International
1625 Stierlin Road
Mountain View, CA 94043

As the decade of the fifties drew to a close, digital computers were beginning to come into common use at universities and research centers, but they were as yet little used in HF radio studies. The use of rays was almost exclusively limited to parabolic layer solutions for which approximate formulas were often the subject of intensive study. In the early sixties, several research workers independently tried a new and comparatively simple approach; a repeated application of Snell's law to trace the progress of rays within the ionosphere. This direct, brute force approach was on at least one occasion implemented by hand calculations, yielding a family of rays at the completion of a long and tedious number manipulation! But, of course, the brute force approach became practical and powerful only when the manipulation was done by computers, for which the work is naturally well adapted.

With the introduction of computer ray tracing, that branch of HF research dealing with the manipulation of parabolic ray equations died a sudden death. Problems that were previously intractable suddenly became easy to solve, and perhaps more importantly the solutions became more realistic because it was then feasible to use realistic ionospheric models with detailed structure based upon in situ measurement by rocket-borne instruments. The latter new technology developed alongside computer ray tracing and the two developments complemented one another.

Largely due to adequate funding by DoD, several independent avenues of investigation yielded ray tracing algorithms that stressed accuracy in all three dimensions, or the inclusion of geomagnetic and absorptive effects, or cost-effectiveness with various levels of compromise. It is reasonable to say that the technique reached its peak in the ESSA "Three-dimensional" program of 1966, designed to do almost everything for everyone! The program still endures in many guises, having been brought up to date by its authors in 1975.

G/H-7
1100

THE EVOLUTION OF THE INCOHERENT SCATTER RADAR TECHNIQUE

H. C. Carlson, Jr.
Air Force Geophysics Laboratory
Hanscom Air Force Base, MA 01731

The incoherent scatter radar technique as practiced is an example of living history still evolving and vital. At its initial conception it offered a unique capability of time continuous probing of topside ionospheric electron concentrations. It was conceived through the recognition, by Professor Williams E. Gordon in 1959, of the juxtaposition of a technological advance (high-power radar technology) and a scientific need. It was born through the joining of credable plans of implementation and agency missions.

Experiment and theory have alternately paced the other to steady progress for over two decades. The number of physically significant parameters the technique can measure has by now grown from one to twenty-six. Applications have advanced from discovery of basic ionospheric properties (for example the existence of several versus a single upper atmospheric gas temperature) in the 1960's, to detailed studies of the overhead ionosphere (from equatorial through auroral latitudes) in the 1970's, to embarking on the ambitious project of global coupling studies in the 1980's.

This evolution will be high-lighted, noting the tug and pull of theory and experiment each on the other as the scientific needs and experimental capabilities evolved.

Wednesday Afternoon 11 Jan., 1400-1700

TIME DOMAIN MEASUREMENTS
A We-PM CR2-6
Chairman: N. S. Nahman, National Bureau of Standards,
Electromagnetic Fields Division,
Boulder, CO 80303

A-1
1400

IDEALIZED ELECTRIC- AND MAGNETIC-FIELD SENSORS BASED ON SPHERICAL SHEET IMPEDANCES

Dr. Carl E. Baum
Air Force Weapons Laboratory
Kirtland AFB NM 87117

This paper considers the response of electric- and magnetic-field sensors in terms of spherical modal expansions to identify the electric- and magnetic-dipole terms which are associated with the ideal angular response to an incident plane wave. Considering an idealized an idealized spherical resistive sheet sensor, the dipole surface current densities are computed and band-width and figure of merit determined to optimize the choice of R_s.

For practical time domain and/or frequency domain sensors the response in general includes various multipole terms besides the desired dipole terms. Expanding the response in terms of spherical harmonics allows one to identify the dipole term and from this gives one a definition of upper frequency response. In addition a norm over the unit sphere of the difference between the actual response and the ideal response gives another way to define upper frequency response.

An example of a magnetic-sensor design which approximates the resistive-sheet sphere is also considered.

A-2
1420

TIME DOMAIN MEASUREMENTS OF PROPAGATING ELECTRIC WAVES IN STRIPLINE USING A SUB-PICOSECOND LASER-DRIVEN ELECTRICAL WAVEFORM SAMPLING OSCILLOSCOPE

Gerard Mourou
University of Rochester
Lab for Laser Energetics
Rochester, NY 14623

The electrooptic effect has been used in conjunction with 100 fs optical pulses to sample electrical transients with unprecedented resolution of 0.5 ps and sensitivity of 50 to 100 microvolts. The electrical material can be used in a traveling wave geometry or in an electrodeless manner. Applications of the technique to the characterization of electrical devices and to the study of short pulse propagation will be described.

A-3
1440

TIME DOMAIN MEASUREMENTS AND COMPUTER - SIMULATION OF AVALANCHE TRANSISTOR PULSERS

H. Geramifar, S. M. Riad and W. A. Davis
Department of Electrical Engineering
Virginia Polytechnic Institute and State University
Blacksburg, VA 24061

This paper presents a physically - based model for Avalanche Transistor Pulse Generators. The model is computer simulated and the simulation results are compared to the experimental data. The purpose of the study is to develop an understanding of the behavior of the avalanche transistor in the negative resistance region and thereby optimize the design of a new pulse generator.

Measurements on the pulsers are being performed in the time domain using a sampling oscilloscope. The computer simulation is achieved by a model for the avalanche transistor based on the relationships,

$$I_c = (\alpha I_B + I_{co}) / (\alpha - 1/M)$$

$$M = 1 / (1 - (V_{cB}/BV_{cBo})^n)$$

This model is implemented in the Transient Circuit Analysis Program (TCAP). It is planned to expand this work to the study of a variety of transient and switching devices.

A-4
1520

REDUCTION OF NOISE, CLUTTER AND SYSTEM BIAS IN TIME DOMAIN WAVEFORM DATA

B.Z. Hollmann, Code F12
Naval Surface Weapons Center
Dahlgren, Virginia 22448

703- 663 8557

The Naval Surface Weapons Center's (NSWC) time domain range has been previously described (B.Z. Hollmann, U.S. National Radio Science Meeting, 88, January 1981). A brief review description of the system is given here. In time domain range data-gathering systems, there are three inherent limitations: (1) noise, (2) clutter, (3) system bias. The question is: Given the waveforms acquired by the system, how do we infer the actual waveform of the transient scattered field? What is being done at NSWC to cope with these limitations is described.

In the case of noise, many samples of each point on the sampling oscilloscope trace are taken and averaged. This method is effective up to a certain point, at which computer roundoff errors limit the cleanness of the waveforms. How far we can go with the averaging process is briefly discussed. A two-part method for dealing with clutter is employed: (1) Eliminating internal reflections within the system as much as possible, and (2) signal processing to eliminate the remaining clutter. Progress and problems are described. The effects of transmitter-receiver antenna system bias on scattering data are addressed. One method used to correct for this bias is that of Lawton and Ondrejka (R.A. Lawton and A.R. Ondrejka, NBS Technical Note 1008, November 1978). The effectiveness and limitations of this, and other methods as time permits, are discussed. Plans for future efforts are suggested.

A-5
1540

$\mathcal{L}_2$ - APPROXIMATION OF IMPULSE RESPONSE FROM TIME LIMITED INPUT AND OUTPUT : THEORY AND EXPERIMENT

Tapan K.Sarkar, Soheil A. Dianat and Bruce Z. Hollmann*
Department of Electrical Engineering
Rochester Institute of TEchnology
Rochester, New York- 14623.
* Naval Surface Weapons center
Dahlgren, Virginia- 22448.

Since it is difficult to generate and propagate an impulse, often a system is excited by a narrow time domain pulse. The output is recorded and then a numerical deconvolution is often done to extract the impulse response of the object. Classically the fast Fourier Transform technique has been applied with much success to the above deconvolution problem. However when the signal to noise ratio becomes small sometimes one encounters instability with the FFT approach. In this paper, the method of conjugate gradient is applied to the deconvolution problem. Unlike the FFT approach, this new method solves the deconvolution problem in the time domain,with any desired degree of accuracy. Moreover, the method converges for any initial guess to the exact solution in a finite number of steps. Also for the application of the conjugate gradient method,the time samples need not be uniform like FFT. Computed impulse response utilizing this technique has been presented for measured incident and scattered fields from a sphre and a cylinder.

A-6
1600

TIME DOMAIN SPECTROSCOPY OF THICK FILM MATERIALS

A. M. Shaarawi, A. A. Riad and S. M. Riad
Department of Electrical Engineering
Virginia Polytechnic Institute and State University
Blacksburg, VA 24061

This paper presents a time domain experimental study to measure the dielectric properties of thick film materials. The material considered in this paper is the ceramic substrate (Alumina 96%). The work will be expanded to include thick film dielectric and resistor pastes.

The measurements are performed using the Time Domain Reflectometery (TDR) Technique. A sample of the ceramic substrate is laser cut to fit the spacing between the inner and outer conductors of a 50 ohm precision air line. The reflections from the sample inserted in the 50 ohm line (response waveform) and from ideal short (reference waveform) are both acquired and used in the analysis. The complex dielectric constant (as a function of frequency) is calculated using the equations developed by Cole, ("Evaluation of Dielectric Behavior by Time Domain Spectroscopy. II. Complex Permittivity", The Journal of Physical Chemistry, Vol. 79, No. 14, 1975, p. 1469). Calculations were made up to a third order approximation as determined by the dielectric sample thickness.

The problems caused by the delay between the acquired reference and response waveforms are discussed and some possible solutions are presented.

A-7
1620

PULSE DELAY MEASUREMENTS FOR LOSSY (PULSE DISTORTING) TRANSMISSION LINES

N. S. Nahman
National Bureau of Standards
Electromagnetic Fields Division
Boulder, CO. 80303

A discussion of the time domain measurement method for the time delay xT of lossy pulse distorting transmission lines where x and T are the line length (meters) and the delay (typically, in nanoseconds per meter). Corrections for pulse distortion employ the s^m, $0 < m < 1$, model (N. S. Nahman, IRE Trans. PGCT, CT-9, pp. 144-151, 1962). The interrelations between the time domain delay and the frequency domain phase shift are summarized in terms of the minimum and nonminimum phase components, the former being related to the attenuation. Applications to coaxial and shielded twisted-pair transmission lines are presented.

TRANSIENT PHENOMENA
B-1 We-PM CR1-46
Chairman: K. F. Casey, JAYCOR,
Fremont, CA 94538

B1-1
1400 **THE SINGULARITY EXPANSION REPRESENTATION OF THE FIELDS SCATTERED BY A FINITE-EXTENT PERFECTLY CONDUCTING OBSTACLE: S-PLANE INTERPRETATION**

L. Wilson Pearson
Department of Electrical Engineering
University of Mississippi
University, MS 38677

A recent presentation by Morgan, Van Blaricum and Auton (National Radio Science Meeting, Houston, TX, May, 1983) calls attention to the fact that the singularity expansion for the field scattered by a perfectly conducting finite-extent obstacle requires an entire function to be complete. Their development is based on the causal Green's function concept and ray-path arguments. The present presentation deals with this same issue from the point of view of the large-s asymptotic behavior of the electric field integral equation's resolvent.

The large-s asymptotic behavior of the EFIE resolvent has been estimated by Wilton (Electromagnetics, v.1, no. 4, 1981) based on a discretization of the integral equation using a method of moments scheme. Though non-rigorous, this result has led to interpretations of the coupling coefficents in the time-domain singularity expansion which are derivable by the causal Green's function approach (Pearson, Wilton, and Mittra, Electromagnetics, v. 2, no. 3, 1982). The consequences of the Wilton result on the far scattered field expansion are explored in the present presentation and are found to be consistent with the conclusions in the presentation by Morgan, et. al. The large-s information allows one to go further than the causal Green's function approach and construct alternative representations for the scattered field.

The alternative representations for the scattered field in the time and frequency domains are explored. It is observed that to separate the entire function explicitly in the frequency domain offers no computational advantage and that one does well simply to retain the frequency dependence arising in the radiation integral. In the time domain, three alternative representations are interesting to study. One contains the inverse transform of an entire function augmenting a "pure" singularity expansion--i.e. a residue series. The other two representations--one in terms of a "time dependent coupling coefficient" and one in terms of a "time dependent far-field natural mode"--are hybrid singularity expansions in that they account for the progressive wave character of, respectively, the incident field or the early-time of the scattered field. The time dependencies in these representationsare present only in the time interval during which resonances are establishing themselves on the scatterer.

B1-2
1420

ON THE IDENTIFICATION OF NATURAL FREQUENCIES OF A TARGET USING A MEASURED RESPONSE,

B. Drachman, Dept. of Math., Michigan State University, East Lansing, MI 48824

Let $E^s(t)$ be the late-time backscatter response of a target illuminated by a time limited excitation waveform $E^i(t)$. The response

$$E^s(t) = \sum_{\ell} a_\ell(\theta,\phi) e^{\sigma_\ell t} \cos(\omega_\ell t + \psi_\ell(\theta,\phi)) \qquad \text{for } t > T$$

where T is the sum of the duration of E^i and twice the transit time for E^i to sweep past the target. The terms $s_\ell = \sigma_\ell + j\omega_\ell$, a_ℓ, ψ_ℓ are the complex natural frequencies and the aspect-dependent amplitudes and phases.

$E^s(t)$ will be taken as a sampled function. The problem is to determine the number of terms, and variables a_ℓ, s_ℓ, ψ_ℓ to best fit the data. One method is Prony's Method. This problem is ill-conditioned. Instead, a sequence of problems is solved, starting with a well-conditioned problem, and converge to a well-conditioned approximation to the above problem: Let

$$p(x,t) = \sum_{j=1}^{N} x_{4(j-1)+1} e^{[4(j-1)+2]t} \cos x_{4(j-1)+3} t + x_{4(j-1)+4}$$

where $x_1 = a_1$, $x_2 = \sigma_1$, $x_3 = \omega_1$, $x_4 = \psi_1$, $x_5 = a_2, \ldots$, and

$$F(x,\tau_k) = \tau_k \frac{\sum_i [E^s(t_i) - p(x,t_i)]^2}{\sum_i E^s(t_i)^2} + (1 - \tau_k) \frac{\sum_j{}' (x_j - x_j^0)^2}{\sum_j x_j^2}$$

The second summation is taken over the natural frequency terms. When $\tau_k = 0$, $\{x\} = \{x^0\}$ is an initial guess for the unknown quantities. As $\tau_k \to 1$ through discrete values, the value of the vector x from the last step is used as initial value to minimize $F(x,\tau_{k+1})$ as a function of the vector x. As $\tau_k \to 1$, the solution to the minimization problem is used to determine σ_ℓ and s_ℓ.

B1-3
1440

PERTURBATION FORMULATION FOR NEARLY-DEGENERATE SEM MODES OF LOOSELY COUPLED BODIES

C-I Chuang, General Electric Co., and D.P. Nyquist, Michigan State University

A general form of electric field integral equations (EFIE's) for coupled bodies is expressed in terms of electric Green's dyadic and surface current density functions. For loosely coupled bodies with nearly-degenerate SEM modes, two leading terms in Taylor's series expansion of Green's dyadic about the natural frequency of isolated body are retained for perturbation formulation. The natural-mode current functions can be approximated by their isolated-body counterpart along with unknown amplitude coefficients. A set of equations for these coefficients are obtained from EFIE's. Condition on non-trivial solution leads to a zero determinant which is a function of ΔS, the amount of shift in the natural frequency due to coupling. The natural frequencies of coupled system are therefore determined.

This formulation is applied to a system of two skew-coupled, identical thin wires. ΔS is found to be $kN(So)/D(So)$, where So is natural frequency of isolated wire, $k=+1$ or -1 for antisymmetric or symmetric modes respectively, and

$$N(So)=\int_0^L\int I(u,So)Kc(u|u',So)I(u',So)du'du,$$

$$D(So)=\int_0^L\int I(u,So)\frac{\partial Ks(u|u',S)}{\partial S}\Big|_{S=So} I(u',So)du'du,$$

with Kc=coupling-kernel; Ks=self-kernel in EFIE, I=natural-mode current for isolated wire, and L=length of both wires. Numerical results are shown to agree well with those obtained by solving coupled EFIE's or Hallen-type IE's directly.

B1-4
1500

KILL-PULSE METHODS TO EXCITE SELECTED TARGET MODES, D.P. Nyquist, K-M Chen, E. Rothwell, and L. Webb, Dept. of Elect. Engrg., and B. Drachman, Dept. of Math., Michigan State University, East Lansing, MI 48824

The kill pulse (K-pulse) is a transient EM waveform which annuls (kills) specific natural-mode content in the backscatter-field response of a target which it illuminates. Incident wave E^i excites late-time backscatter response E^s according to $E^s = E^i * h_n$ for $t > T_E = T_k + 2T$ where all signals are causal, T_k is the finite duration of E^i, T is the maximal one-way transit time for the incident wavefront to sweep past the target, and h_n is the natural or free component of the impulse response

$$h_n(t) = \sum_{\ell=1}^{N} a_\ell(\theta,\phi) e^{\sigma_\ell t} \cos(\omega_\ell t + \psi_\ell(\theta,\phi)) \quad \ldots \text{ for } t>2T$$

with $s_\ell = \sigma_\ell + j\omega_\ell$ complex natural frequencies and a_ℓ, ψ_ℓ aspect-dependent amplitudes and phases. E^i is decomposed as $E^i = E^e + E^k$ where excitatory E^e, nonzero only for $0 < t < T_e$ is followed by E^k, nonvanishing for $T_e < t < T_k$; component E^k annuls the response due to prior E^e and satisfies the integral equation

$$\int_{T_e}^{T_k} E^k(t')h_n(t-t')dt' = -\int_0^{T_e} E^e(t')h_n(t-t')dt'$$

$$\ldots \text{ for } t>T_E.$$

Two alternative K-pulses are defined: i) "natural" pulse E^k when $T_e=0$, having non-trivial homogeneous solutions only for discrete durations T_k, which annuls its own response and ii) "forced" pulse E^k for $T_e > 0$ which annuls the response to E^e for (almost) any T_k. The natural K-pulse is unique, while its forced counterpart depends upon the choice of E^e and T_k. Both K-pulses are synthesized and compared for thin-wire targets; their suitability for target discrimination is assessed.

If the target impulse response is comprised of N natural modes but M of those modes are to be retained in the scatter field, then the K-pulse is synthesized such that E^k annuls N-M modes. The resulting K-pulse excites selected modal content in the target response, e.g., M=1 yields monomode response in a single natural mode. Results are presented for K-pulses synthesized from analytical natural frequencies as well as experimental data; their validity is confirmed by convolution with measured target responses.

B1-5
1540

SYNTHESIS OF K-PULSE AND SINGLE-MODE EXCITATION SIGNALS FROM EXPERIMENTAL IMPULSE RESPONSES OF TARGETS, Lance Webb, K-M Chen, D.P. Nyquist, Dept. of Elect. Engr., Mich. State Univ., E. Lansing, MI 48824, and Bruce Hollmann, Naval Surface Weapons Center, Dahlgren, VA 22448

It is difficult to synthesize the K-pulse and single-mode excitation signals for a complex radar target because it is difficult to theoretically determine its complex natural frequencies. Therefore, the only feasible approach is to synthesize these excitation signals from the experimental impulse response of the complex target combined with the application of some appropriate theoretical methods. Our approach consists of the following steps.

(1) Prony's method is applied to the sampled data of the measured impulse response [X] of the target. The coefficients of Prony polynomial are obtained. The ordered sequence of these coefficients can be shown to become the K-pulse [K] of the target, which eliminates the natural modes of the target and other noise.

(2) Find zeros of the sequence which represents [K]. From those zeros in the proper locations of the complex plane, the complex natural frequencies $[\varsigma_m]$ of the target can be calculated.

(3) At this step, the K-pulse $[K_N]$ which kills N natural modes of the target can be constructed by convolving N couplets $(1, -z_m)$ for m = 1,2,...N where $z_m = \exp[\varsigma_m \Delta T]$ and ΔT is the sample time interval:

$$[K_N] = (1, -z_1) * (1, -z_2) * ..... * (1, -z_N)$$

(4) The jth-mode excitation signal $[E_j]$ can be obtained by removing the couplet $(1, -z_j)$ from $[K_N]$ as

$$[E_j] = (1, -z_1) *....* (1, -z_i) * (1, -z_k) *....* (1, -z_N)$$

The above approach was used to construct the K-pulse and various single-mode excitation signals for the wire targets of various dimensions. To check the validity of these signals, the synthesized K-pulse and single-mode excitation signals were then used to convolve with the measured radar returns of the wire targets. The results were found to be satisfactory.

B1-6
1600

TARGET DISCRIMINATION USING THE K-PULSE CONCEPT AND PRONY'S METHOD, Lance Webb, K-M Chen, and D.P. Nyquist, Dept. of Elect. Engr., Michigan State University, E. Lansing, MI 48824, and Bruce Hollman, Naval Surface Weapons Center, Dahlgren, VA 22488

Empirical radar returns from experimental targets measured at NSWC are processed using Prony's method together with the K-pulse concept for the purpose of discriminating the targets.

The late-time response of the measured radar return [X] contains natural modes of the target but contaminated by noise and unwanted natural modes introduced by the system. To discriminate the targets, the following procedure, on discrete time basis, is used:

(1) The K-pulse [K] and the single-mode excitation signals [E] of the anticipated target are synthesized with our previously developed method. The jth-mode excitation signal $[E_j]$ is obtained by deleting the jth-mode from [K].

(2) Convolve [K] with [X] to form a convolved output [Y], $[Y] = [X]*[K]$. If the measured target is the right (anticipated) target, [Y] contains no natural modes [S] of the right target because they are eliminated by [K]. On the other hand, if it is a wrong target, [Y] contains natural modes of the wrong target and other noise.

(3) Obtain the Prony K-pulse $[K_p]$ for the convolved output [Y]. This Prony's K-pulse arises in an intermediate step of Prony's method when it is applied to [Y]. In fact, $[K_p]$ is the ordered sequence of the coefficients of the Prony polynomial.

(4) Convolve $[K_p]$ with the original radar return [X] to form an output [Z] where $[Z] = [X]*[K_p]$.

(5) Convolve $[E_j]$ with [Z] to form an output [M], $[M] = [Z]*[E_j]$. If the measured target is the right target, [M] should contain the jth-mode $[S_j]$ of the right target. On the other hand, if it is a wrong target, [M] will either be small or not resemble the jth-mode.

In the present scheme, Prony's method has been applied more than once to the radar return and different K-pulse sequences have been constructed in the process. It was found that the extreme sensitivity of Prony's method can be used to suppress certain types of noise and signal distortions.

B1-7
1620

COMPLEX FREQUENCY POLES OF RADAR SCATTERING FROM COATED CONDUCTING SPHERES

W. E. Howell, Naval Research Laboratory, Washington, D. C. 20375 and Catholic University, Washington, D. C. 20064 and
H. Überall, Department of Physics, Catholic University, Washington, D.C. 20064

The importance of poles in the radar scattering amplitude has been pointed out by C. Baum (in: Transient Electromagentic Fields, L. B. Felsen, ed., Springer, Berlin, 1976, vol.X, pp. 129-179) in the framework of the Singularity Expansion Method (SEM). These poles are located at the scatterer's complex eigenfrequencies, and are characteristic for its shape and composition; they are customarily presented as pole patterns in the complex frequency plane, or in the plane of the Laplace variable $s = \omega/i$. Numerous examples of such pole diagrams appear in the literature for the case of perfectly conducting targets. Due to their large imaginary parts, and corresponding little-pronounced resonances, proposed use of these poles for target recognition purposes has evoked some controversy.

In the case of dielectrically coated objects, the coating can produce prominent resonances in radar echoes (P. J. Moser, J. D. Murphy, A. Nagl, and H. Überall, Radio Science 16, 279-288, 1981) due to poles located near the real axis. We have evaluated complex pole patterns for dielectrically coated spheres, and obtain the movement of the poles under charges of the thickness and dielectric constant of the coating. The displacement of some pole layers towards the real axis with increasing coating thickness, and the formation of new pole layers near the axis is observed.

ROUGH SURFACE SCATTERING
B-2 We-PM CR2-28
Chairman: Gary S. Brown, Applied Science Associates, Inc.
Apex, NC 27502

B2-1 1400 MULTIPLE SCATTERING ON ROUGHENED PLANAR SURFACES IN THE HIGH FREQUENCY LIMIT

Gary S. Brown, Applied Science Associates, Inc., 105 E. Chatham St., Apex, NC 27502

The classical approach to modeling scattering from rough conducting surfaces in the high frequency limit comprises weighting the single scatter physical optics current by incident and scattering shadow functions which, in turn, force the current to zero whenever there is appropriate blockage of the incident or scattered rays. While the use of these shadowing functions has some physical basis, it clearly lacks a rigorous analytical justification. Consequently, its limitations are largely unknown. The purpose of this paper is to investigate, by analytical means, the adequacy of the shadowing approximation for the problem of scattering from a roughened planar surface.

The approach entails iterating the Magnetic Field Integral Equation (MFIE) for the surface current in the high frequency limit. Whenever the integral term in the MFIE is evaluated in this manner, two distinctly different types of stationary phase points on the surface arise. The first occurs independent of surface slopes and results in what is called incident shadowing, i.e., the blockage of one point on the surface by another point. The second type of stationary phase points depend very critically on the surface slopes because they give rise to the specular reflection of an incident ray from one point on the surface to another point. It is then shown that in order to rigorously derive simple first order multiple scattering effects on the current, it is necessary to iterate the MFIE to at least third order (with physical optics being the zeroth order iteration).

Retaining only first order multiple scattering effects in the current, the field scattered from the surface is computed. The results of this computation lead to the major contributions of this paper. It is shown that the field resulting from the first order multiple scattered ray on the surface is not, in general, zero in the forward shadowed direction. This is shown to be related to the possibility of focusing of energy reflected from one point on the surface to a second point and, consequently, the failure of first order multiple scattering, i.e., the first order iterative solution of the MFIE is not adequate and one must take higher order terms. Conditions are obtained for which forward scatter shadowing (to first order) is valid and they relate the curvature of the surface at the point of specular reflection the the separation distance between this point and second point at which the specularly reflected ray strikes the surface. Finally, it is argued that the use of a scatter shadow function approximation is truly justifiable only under single scatter conditions in which case it can be ignored.

B2-2 ROUGH SURFACE SCATTERING - SPECULAR REFLECTION
1420

S.M. Chitanvis and M. Lax *
Physics Department, City College of the City University of New York, N.Y. 10031
*Bell Laboratories, Murray Hill, N.J. 07974

We describe a Feynman-Dyson type Green's function theory for dealing with multiple scattering from very rough surfaces.

We derive algebraically, an exact compact expression for the average wave amplitude of our scalar theory. The average is expressed via cumulants. A natural expansion parameter for the exact average is $(1-n_{1/n_2})$ where n_1, n_2 are the refractive indices for the two media involved.

A new, simple method is given for obtaining the specularly replected intensity by looking at the asymptotic form of the average wave amplitude, far from the rough surface.

The details of the lowest-order, Bourret type approximation for the reflected intensity for a gaussian surface with correlations are worked out analytically in the limit of large height fluctuations. Graphs for the intensity show considerable deviation from previous approximations that involved no multiple scattering.

B2-3
1440

SCATTERING AND DEPOLARIZATION BY LARGE CONDUCTING SPHERES WITH VERY ROUGH SURFACES

Ezekiel Bahar and Swapan Chakrabarti
Electrical Engineering Department
University of Nebraska
Lincoln, NE 68588-0511

The purpose of this investigation is to determine the like and cross polarized scattering cross sections for large conducting spheres with very rough surfaces. Perturbation theory has been used to determine EM scattering by spheres with random rough surfaces provided that the parameter $\beta = 4k_o^2 \langle h_s^2 \rangle$ is much smaller than unity (where k_o is the wave numbers and $\langle h_s^2 \rangle$ is the mean square height of the rough surface of the sphere (D. E. Barrick, Radar Cross Section Handbook, Ch. 9, Plenum Press 1970). For large conducting spheres with $\beta << 1$, the total scattering cross sections are not significantly different from the physical optics cross sections for the smooth conducting spheres. In this paper the full wave approach is used to determine the scattering cross sections for spheres with roughness scales that significantly modify the total cross sections. The full wave approach accounts for specular point scattering and Bragg scattering in a self consistent manner and the total cross section are expressed as weight sums of two cross sections. (E. Bahar and D. E. Barrick, Radio Science, 18, No. 2, 129-137, 1983).

B2-4
1520

ROUGH SURFACE SCATTERING BASED ON THE EXTINCTION THEOREM

Dale Winebrenner and Akira Ishimaru
Department of Electrical Engineering
University of Washington
Seattle, Washington 98195

In recent years, the Ewald-Oseen extinction theorem (also called the extended boundary condition by many, including Waterman) has been used to study scattering from bounded scatterers and rough surfaces. Briefly, the extinction theorem mathematically expresses the statement that the surface fields on an illuminated body or surface must radiate in such a way as to extinguish the unperturbed incident field inside the body or below the surface. An example of its application is the T-matrix method for bounded scatterers.

Scattering from rough surfaces has also been studied using integral equations for the surface and scattered fields derived with the aid of the extinction theorem. Toigo, Marvin, Celli, and Hill (Phys. Rev. B 15(12), 5618-5626) studied the relationship of these exact integral equations to those derived using the Rayleigh hypothesis. Several other authors have derived a perturbation theory based on the same equations which avoids the Rayleigh hypothesis (cf. M. Nieto-Vesperinas and N. Garcia, Optica Acta, 28(12), 1651-1672; and G. S. Agarwal, Phys. Rev. B, 15(4), 2371-2382.

Limiting our discussion to the scalar wave scattering problem with Dirichlet or Neumann boundary conditions for clarity, we show how the Kirchhoff approximation is the zero-order approximation to the surface field and show how systematic higher order corrections may be derived. It is not necessary to pass to a high frequency limit a priori. The rough surface enters through its characteristic function in this formulation, and in general, the $n + 1$ point characteristic function occurs in the n^{th} correction to the Kirchhoff approximation. We discuss the nature and magnitude of these corrections and indicate how our formalism can be extended to problems with more general boundary conditions.

B2-5 A ROUGH SURFACE SCATTERING MODEL FOR LOW, MEDIUM, AND HIGH
1540 FREQUENCY APPLICATIONS: A. K. Fung and M. F. Chen, Remote Sensing Laboratory, University of Kansas, Lawrence, KS 66045

A model for scattering from a perfectly conducting randomly rough surface has been developed using the extinction theorem. Its validity is established by comparing its backscatter predictions with moment method solutions for one-dimensional, statistically known, rough surfaces. Two types of surfaces have been selected for consideration. One surface has Gaussian roughness spectrum and the other has a non-Gaussian spectrum with more high frequency components. At sufficiently low frequencies both the small perturbation solution and the extinction theorem solution agree with the moment method solution for the surface with Gaussian spectrum. At intermediate frequencies, only the extinction theorem solution agrees with the moment method solution while at high frequencies, both the Kirchhoff and the extinction theorem solution agree with the moment method solutions. For the surface containing high frequency roughness components, the low frequency behavior is similar to the previous surface. However, as frequency increases, the perturbation solution continues to provide reasonable trend agreements at large incidence angles, although the method should not work at these frequencies. This seems to imply that the frequency filtering effect is present whenever there are frequency components to be filtered. The extinction theorem solution follos the moment method solution at all frequencies considered.

B2-6 1600 SOME RECENT STUDIES ON RADIOMETRY OF ROUGH SURFACES: M. Nieto-Verserinas*, The Institute of Optics, University of Rochester, Rochester, NY 14627

This communication reviews recent work on the scattering of radiation by perfectly conducting rough surfaces. The theory has a vector nature and uses the small perturbation method based on the extinction theorem. This allows an analysis of the scope of the Kirchhoff approximation for the radiant intensity. As regard to the inverse problem, it is pointed out that low angle approximations are inconsistent with Lambertian distributions of radiant intensity, and thus the failure of constructing rough surfaces that reflect such distributions based on the Kirchhoff approximation is explained. Lambertian surfaces, however, may be obtained by means of the perturbation method. Such surfaces have correlation distance of the order of the radiation wavelength, although for scattering angles smaller than 30°, δ- correlated surfaces produce almost Lambertian-radiant intensity.

*Permanent address:
Institute de Optica, CS1C,
Serrano 121, Madrid-6, Spain

B2-7
1620

SCATTERING OF A SCALAR PARTICLE FROM A RANDOMLY ROUGH SURFACE OF BUMPS

A.R. McGurn[+], A.A. Maradudin[‡], V. Celli[*]

[+]Department of Physics
Western Michigan University
Kalamazoo, MI 49008

[‡]Department of Physics
University of California
Irvine, CA 92717

[*]Department of Physics
University of Virginia
Charlottesville, VA 22901

The low energy scattering of a scalar particle from a hard surface consisting of a random array of bumps which are all of the same shape is calculated. The scattering as a function of energy is shown to have a resonance and the energy width of the diffuse scattering is shown to be dependent on the concentration of bumps and the final momentum. The effects on the diffuse scattering of certain processes which are important in Anderson localization phenomena (Phys. Rev. 109, 1492-1505, 1958) are determined.

B2-8 Discussion
1640

THE RADIO CHANNEL: MEASUREMENT, MODELING, AND COMMUNICATION

E We-PM CR1-40

Chairman and Organizer: A. A. Giordano, GTE Systems Group, Strategic Systems Division, Westborough, MA 01581

E-1
1400

DETECTION OF WEAK SIGNALS IN NON-UNIFORM, NON-GAUSSIAN NOISE FIELDS

David Middleton
127 E. 91st Street
New York, NY 10128

Threshold detection of signals subject to doppler "smear" and fading in non-Gaussian, non-uniform noise fields is discussed. Because of non-uniformity (i.e., incomplete spatial correlation) of the interference field, beam-forming by (M) multiple sensors distributed (arbitrarily) in such fields can achieve additional improvement over local beam forming or single-sensor processing, in addition to the required temporal processing (N-samples) at each element. Coherent, incoherent, and composite threshold detection algorithms are described for generally non-Gaussian fields, under the postulate of independent sampling of the received space-time noise field. The minimum detectable signal is generally proportional to $(J')^{-1}(=[M'N']^{-1})$, where $M' \leq M$ and $N' \leq N$ are, respectively, the effective number of spatially and temporally independent (noise) samples, provided signal waveform coherence is maintained. The latter can be partially or totally destroyed by doppler-smear and rapid fading. Explicit results for optimum and sub-optimum detectors are presented and the effects of dependent sampling on performance are noted. These algorithms provide canonical examples of generalized, adaptive beam-forming and signal processing.

E-2
1420

NEW RESULTS ON HIGHER ORDER ATMOSPHERIC NOISE STATISTICS

J. R. Herman, A. Giordano and X. DeAngelis
GTE Sylvania Systems Group
Strategic Systems Division
One Research Drive
Westborough, MA 01581

Digital recording of medium frequency atmospheric radio noise with wideband equipment over three seasons has provided a permanent raw data base for use in statistical analyses of noise characteristics and system performance simulations. Preliminary studies have indicated that use of nonlinear receivers in real noise result in less performance improvement over linear receivers than is predicted by noise models. The reason for this is suspected to lie in the nature of the noise pulse statistics. These are therefore examined in terms of receiver bandwidth and digital sampling rates for a variety of noise conditions.

E-3
1440

SUBTERRANEAN MEASUREMENTS OF VLF RADIO NOISE AND SIGNALS

R. Vargas-Vila, J. R. Herman and X. DeAngelis
GTE Sylvania Systems Group
Strategic Systems Division
One Research Drive
Westborough, MA 01581

To ascertain the effects of a multi-layered, multiple conductivity earth on VLF radio noise and signals propagating from the earth's surface to underground receivers, a series of measurements were conducted under Seboyeta Mesa in an adit (type of tunnel) about 70 miles northwest of Albuquerque, NM. These measurements of signal and noise intensities using both E-field and H-field probes were taken as a function of tunnel penetration and used to determine attenuation rates as a function of frequency and depth through the earth. Data for the various layer thicknesses and composition were obtained from bore hole samples. These data were used in conjunction with the resulting attenuation rates to determine the various layer conductivities.

A multiple uniform transmission line propagation model, analagous to plane wave propagation through a homogeneous medium was employed to take into account the multi-layer conductivity effects on the subterranean radio wave propagation. It was found that a loop antenna responsive to the magnetic field component gave better performance than a linear probe responsive to the electric field.

E-4 1520 RELIABILITY OF ATMOSPHERIC RADIO NOISE PREDICTIONS

D.B. Sailors
Ocean and Atmospheric Sciences Division
Naval Ocean Systems Center
San Diego, CA 92152

Measured radio noise values at widely separated geographical locations are compared with predicted atmospheric noise values for five frequencies between 0.495 and 20.0 MHz. The measured noise data were the seasonal 4-hr time block values, averaged over each 4-hr period for the 3 months of the season and were for the years 1960 and 1965. The cooperative measurements of received noise power were made under the direction of the National Bureau of Standards Central Radio Propagation Laboratory (Crichlow, NBS Technical Note 18 series and subsequently ESSA Technical Report IER 18-ITSA series, 1959).

Atmospheric noise values were predicted using noise models with their worldwide atmospheric noise representation at 1 MHz, as presented in CCIR Report 322 (1963), produced by numerical mapping techniques developed by D. H. Zacharisen and W. B. Jones (OT/ITS Research Report 2, 1970). Included in these models were simplified atmospheric noise models suitable for use in estimating noise on a minicomputer (D.B. Sailors and R.P. Brown, Radio Sci, 18, 625-637, 1983). The frequency dependence in these models was represented by a power series of least squares fit to the frequency dependence curves in CCIR Report 322 (D. L. Lucas and J. D. Harper, NBC Technical Note 318, 1965). For a realistic assessment of the reliability of radio noise prediction, galactic noise and quiet rural man-made noise were estimated using the curves in CCIR Report 322 to eliminate measured data more likely from these latter sources.

As a whole the measured values were higher than the predicted values, and models with the least number of coefficients were least accurate. The bias of the models was generally lower during the 1960 period than in the 1965 period. For 1960 during winter, the most accurate model was 0.5 dB low; for 1965 this same model was 5 dB low. This difference in bias for the two years was considerably less during the summer and fall seasons. For models with a small number of coefficients, the bias was 2 to 5 dB greater during 1965 than in 1960. The rms error was larger during the 1965 period than in the 1960 period. For the winter season in 1960, the rms error was 6.7 dB for the most accurate model; in 1965 it had an rms error of 9 dB.

E-5
1540

ADAPTIVE COMBINING AT VLF/LF

David F. Freeman
GTE Sylvania Systems Group
Strategic Systems Division
One Research Drive
Westborough, MA 01581

Adaptive Interference Cancellation (AIC) combines signals from multiple antennas so as to improve SNR without the use of either external navigational information or internal bit decision feedback. In environments with strong directional interference, AIC provides improvements very near optimum (i.e., that offered by LMS combining). Different formulations of the defining equations and the effects on performance are considered.

POLARIZATION DIVERSITY RADARS: THEORY, OBSERVATIONS, AND TECHNIQUES

F We-PM CR1-42

Chairman and Organizer: R. A. Kropfli, Wave Propagation Laboratory, NOAA, Department of Commerce, Boulder, CO 80303

F-1
1320 **METEOROLOGICAL AND RADIO WAVE PROPAGATION STUDIES USING TWO-CHANNEL CIRCULARLY-POLARIZED RADARS WITH CROSS CORRELATION MEASUREMENT CAPABILITY.** A. Hendry, Division of Electrical Engineering, National Research Council of Canada, Montreal Road, Ottawa, Ontario, Canada K1A 0R8.

Two-channel radar systems that provide for simultaneous measurement of the intensities of the orthogonal components of the echo yield a second target characteristic in addition to the reflectivity which is measured by one-channel systems. If the relative phase angle and the degree of cross correlation of the components are measured, two other parameters of the radar target are obtainable. Switching the polarization state of the transmitted wave further increases the amount of information which may be obtained about the target.

This paper will include a brief general discussion of the features of such polarization diversity radars, with emphasis on circularly-polarized systems, and a review of the parameters of meteorological targets which are measurable with them. The capabilities of these radars will be illustrated by an overview of the results obtained at the National Research Council of Canada Laboratory, where circularly-polarized radars operating at 1.8 and 3.2 cm have been used for meteorological and atmospheric radio wave propagation studies. Included will be a discussion of remote identification of precipitation particles and of the determination of differential propagation factors from the radar data.

Recent results taken with polarization switching of the 3.2 cm radar will be presented. These results include comparisons of the differential reflectivity, obtained from linear polarization measurements, with the equivalent factor calculated from circular polarization data.

F-2
1400

OBSERVATIONS OF A SEVERE HAILSTORM WITH A POLARIZATION DIVERSITY RADAR

R.G. Humphries Atmospheric Sciences Department
Alberta Research Council
4445 Calgary Trail South
Edmonton, Alberta, Canada
T6H 5R7

The Alberta Research Council's S-band polarization diversity radar transmits circularly polarized radiation and measures the circular depolarization ratio, the magnitude of the cross-correlation and the phase difference of the signals in the main and orthogonal receiver channels. These parameters have been obtained for a severe hailstorm and have been analyzed for a period of several hours of the storm's lifetime.

Several fine scale reflectivity patterns (B.L. Barge and F. Bergwall, Second WMO Scientific Conference on Weather Modification, 341-348, 1976) have been identified and tracked. The development of precipitation within these patterns is related to the polarization observations.

F-3
1420

DUAL WAVELENGTH AND DUAL POLARIZATION RADAR METEOROLOGICAL RELATIONSHIPS

K. Aydin[1], T. A. Seliga[1], and M. Arai[2]
[1]Atmospheric Sciences Program and
Department of Electrical Engineering
The Ohio State University
Columbus, OH 43210
[2]Kokusai Denshin Denwa Co. Ltd.
Tokyo, Japan

Rainfall disdrometer measurements are used to establish empirical relationships between reflectivity factors (backscattering) and specific attenuations at 3 and 10 cm wavelengths of electromagnetic waves. The computational results demonstrate the importance of polarization of the waves in understanding scattering and propagation characteristics. Comparisons between the disdrometer-derived relationships and those obtained from model drop size distributions indicate that a gamma distribution with m = 2 produces a best fit to the empirical results. Finally, the capability of radar differential reflectivity measurements at S-band to predict X-band scattering and attenuation is tested successfully with dual-wavelength radar measurements obtained with the CHILL radar during the SESAME '79 field program.

F-4
1440

SELECTED FEATURES OF DUAL POLARIZATION DIFFERENTIAL REFLECTIVITY MEASUREMENTS DURING MAYPOLE

T. A. Seliga[1], V. N. Bringi[2], R. Carbone[3], P. Herzegh[3], and K. Aydin[1]
[1]Atmospheric Sciences Program and
Department of Electrical Engineering
The Ohio State University
Columbus, OH 43210
[2]Department of Electrical Engineering
Colorado State University
Ft. Collins, CO 80523
[3]Field Observing Facility
National Center for Atmospheric Research
Boulder, CO 80303

As part of a collaborative research program to extend the multi-parameter measurement capabilities of the CP-2 radar system, a May Polarization Experiment (MAYPOLE) was conducted near Boulder, Colorado during May-June 1983. The purpose of this first MAYPOLE field program was (1) to test the operational characteristics of a new fast-switching dual polarization, differential reflectivity (Z_{DR}) capability at S-band, and (2) to compare in-situ aircraft-derived observations of hydrometeors with multi-parameter radar measurements. Measurements were obtained under several meteorological conditions, including both upslope, stratiform and convective regimes. Selected features of these will be presented as PPI and RHI profiles of (Z_H, Z_{DR}) and Doppler velocity. Implications of the measurements for quantitative and qualitative interpretation of the data will be noted.

F-5
1520

EARLY RESULTS OF A COMPREHENSIVE POLARIZATION EXPERIMENT WITH 10 CM AND 8 MM WAVELENGTH RADAR

W.R. Moninger and R.A. Kropfli
NOAA/ERL/Wave Propagation Laboratory
Boulder, Colorado 80303
and V. Bringi, Colorado State University
Ft. Collins, Colorado 80521

In the past, there have been conflicting results of polarization measurements made with different wavelength radars in different meteorological settings. As an example of this, observations near the melting layer of high differential reflectivity indicating the alignment of deformed hydrometeors is at odds with the observation of low correlation between the main and cross channels of circularly polarized radars indicating low degree of alignment. These discrepancies as well as others concerning the details of the relative positions and thicknesses of the bright band, the depolarization band, and the low correlation band remain unresolved. The ability of dual-polarization techniques to distinguish liquid from ice in clouds is still much in question.

As a step in resolving these points, an experiment focused on the interpretation of a variety of polarization signatures was conducted in May, 1983. This experiment had the following major components:

1) The NCAR CP-2 radar with differential reflectivity capability.

2) The NOAA K-band dual-polarization radar with polarization switching.

3) The NOAA FM-CW radar for high resolution probing of the melting layer.

4) The NOAA dual-channel radiometer for total liquid water detection.

5) The Wyoming King Air aircraft with two sets of crossed PMS probes.

This presentation will focus on the preliminary results obtained with the NOAA K-band radar and the NCAR CP-2 radar.

F-6
1540

COHERENT, DUAL-POLARIZED OBSERVATIONS OF THE RADAR RETURN FROM PRECIPITATION.

Paul R. Krehbiel and Marx Brook,
Geophysical Research Center, New Mexico Tech,
Socorro, NM 87801

Simultaneous, coherent observations of the backscattered return from precipitation in both the transmitted and orthogonal linear polarizations have been used to compute Doppler spectra and cross-spectra for the two polarizations. Observations were obtained from strong precipitation echoes in several convective storms and from the bright band of a weakly precipitating storm. 65 spectra have been examined at elevation angles ranging from vertical to near horizontal. The spectra of the returns in the orthogonal polarization were often dominated by 'cross-talk' from the larger returns in the transmitted polarization. The cross-talk was determined from the data itself to have been 22-27 dB below the return in the transmitted polarization and was probably caused by the antenna feed. The orthogonal spectra were often enhanced relative to the cross-talk, however, indicating the presence of detectable orthogonal returns. The enhanced return usually peaked at a different Doppler frequency than the cross-talk, indicating that the spectra were different in the two polarizations. Enhanced returns were most often observed near horizontal incidence. In this case the maximum orthogonal return was typically 15-20 dB below that in the transmitted polarization. In several instances where the Doppler spectra were narrow, the orthogonal return was enhanced on both sides of the cross-talk peak in a manner suggestive of amplitude (or frequency) modulation, such as would be produced by oscillating drops. Except in bright bands, few enhancements were observed at vertical incidence. Only 2 of 17 vertical observations showed an enhanced orthogonal return; these occurred in a localized precipitation echo at 1-2 km range above the radar. The orthogonal return peaked 17-18 dB down on the low frequency side of the Doppler spectrum, i.e. for the smaller particles (assuming that the spectra were not aliased). Bright bands produced the strongest orthogonal returns; at vertical incidence the orthogonal return was largest for the particles with the largest fall velocity, where it was was only 10 dB below the return in the transmitted polarization. The cross-spectra were expressed in terms of the coherency and phase of the signals vs. frequency. The coherency was high (0.8-0.9) in the presence of cross-talk and decreased when the orthogonal returns were enhanced. The phase could be measured only when the coherency was high; it sometimes increased linearly with frequency over a part of the Doppler spectrum. We believe that this was caused by a non-uniform distribution of particles across the antenna beam.

F-7
1600

POLARIZATION CHARACTERISTICS (Z_{DR} AND LDR) OF NCAR'S CP-2 METEOROLOGICAL RADAR

Jeff Keeler, Charles Frush, and Brian Lewis
Field Observing Facility
National Center For Atmospheric Research
Boulder, Colorado 80307

NCAR's Field Observing Facility has implemented a 10 cm differential reflectivity (Z_{DR}) capability on its CP-2 radar and will have added the ability to measure the linear depolarization ratio (LDR) at 3 cm by May 1984. The Z_{DR} function uses a Raytheon fast ferrite switch and typically operates in the mode of changing polarization on consecutive pulses. When more than one pulse of the same polarization is transmitted (and received) anomolies in the polarization angle and switch isolation appear. Measurements from a polarized source on the Boulder Atmospheric Observatory tower are being used to characterize these anomolies, and these will be reported.

The LDR measurement will employ the use of two separate "polarization twist" Cassegrain antennas with beams matched to the main lobe of the 10 cm beam used for Z_{DR}. The polarization characteristics of these antennas have been accurately measured on the National Bureau of Standards near-field antenna test range. Separate X-band (3 cm) receivers each having a sensitivity comparable to the S-band (10 cm) portion of CP-2 will receive the horizontal (co-polar) and vertical (cross-polar) return. The two IF signals will be sent down a common transmission line to the processor for LDR measurements approaching -30 dB. We will describe our LDR design and performance expectations plus report on the antenna modifications.

F-8
1620

DIFFERENTIAL REFLECTIVITY ARTIFACTS RESULTING FROM BEAM PATTERN EFFECTS

Paul H. Herzegh, Charles F. Frush, and
Richard E. Carbone
Field Observing Facility
National Center for Atmospheric Research
Boulder, Colorado 80307

Differential reflectivity (Z_{DR}, in dB) is given by the ratio of reflectivity measured at horizontal polarization to that measured at vertical polarization for the same measurement volume. Ideally, positive and negative values of Z_{DR} obtained in precipitation correspond to a predominance of vertically-aligned prolate or oblate hydrometeors, respectively. However, mismatch of the radar beam pattern at horizontal and vertical polarizations can yield significant positive and negative Z_{DR} artifacts, particularly in situations where there are strong gradients and low values of reflectivity. In such cases, Z_{DR} measurements may bear no relation to the shapes of hydrometeors within the pulse volume, and the use of Z_{DR} to derive meteorological parameters (such as precipitation rate or hydrometeor phase and type) will produce misleading results.

In this paper, beam pattern measurements at horizontal and vertical polarizations for the S-band section of the National Center for Atmospheric Research CP-2 radar are described. Using these beam pattern measurements, the distribution, sign and magnitude of Z_{DR} artifacts are calculated for a range of typical reflectivity patterns. A variety of Z_{DR} measurements obtained in rain and snow by the CP-2 radar are examined, and the features of these measurements (determined to be artifacts resulting from beam pattern effects) are highlighted. Finally, some general guidelines for the analysis of Z_{DR} measurements obtained in low reflectivity/high gradient regions are discussed.

MODERN IONOSPHERIC SOUNDING TECHNIQUES
G We-PM CRO-30
Chairman: Charles M. Rush, NTIA/ITS,
Boulder, CO 80302

G-1
1340 PHILOSOPHY AND DESIGN OF THE DIGISONDE 256

K. Bibl, B.W. Reinisch and D.F. Kitrosser
University of Lowell Center for Atmospheric Research
Lowell, MA 01854
J. Buchau
Air Force Geophysics Laboratory
Hanscom AFB, MA 01731

The Digisonde 256, designed to be the combination of a scientific instrument and a routine ionosonde, needs all its basic features simultaneously to fulfill either of its main tasks: automatic real-time monitoring and scaling of the ionospheric parameters, or scientific investigation of the ionosphere for geophysical and radio propagation studies. High speed discrete Fourier transform techniques determine the complex doppler spectra, while polarization and incidence angle measurements are made by appropriate antennas and antenna array controls. Digital recording after very fast pre-processing permits post-processing of the data for separation of multi-dimensional parameters in compressed time-series and for emphasis of special events. Remote operation control, real time ionogram analysis and remote data transfer enables central operation of a sounder network for world-wide real-time monitoring of the ionosphere. Ease of maintenance and built-in-test procedures provide a highly reliable system.

G-2 A DIGITAL IONOSONDE FOR REMOTE OPERATION:
1400 J.C. Schlobohm, Associate Director
Radio Physics Laboratory,
SRI International, Menlo Park, CA 94025

A digital ionosonde has been developed that can operate unattended for months at a time. The measured data can be sent automatically to a central processing point at which the data from several ionosondes can be analyzed together. The ionosondes can be controlled remotely in order to select the frequency range over which they will sound and the interval between soundings. The data can be stored locally at the ionosonde on floppy disks for up to a week or on magnetic tape for several months. Data can be retrieved either in real time or after the fact from disk or tape.

The height resolution of the digitized ionogram is 75 m with a maximum measurable height of 800 km. The ionosonde transmits pulses in the shape of a cosine on a pedestal in order to reduce interference to others. In addition, it checks each frequency before it transmits to minimize the likelihood of transmitting on a frequency that is already in use. A multiple-pulse verification scheme validates that the response measured is a return from the ionosphere rather than the result of interfering signals.

Good separation of O- and X-ray returns is achieved by using a cross-polarized receiving antenna and subsequent processing.

Software has been developed for the central processing system to eliminate sporadic data points and multiple-hop returns and to convert the ionogram data into a true-height electron-density profile.

G-3 RESEARCH POTENTIAL OF DIGITAL IONOSONDES
1420

Adolf K. Paul
Naval Ocean Systems Center
Ocean and Atmospheric Science Division
Code 5321
San Diego, CA 92151

Modern digital ionosondes with the capability of measuring amplitude and phase for each echo offer new opportunities for ionospheric research, especially, if an array of receiving antenna is used. The principles of extracting new information from this kind of data will be summarized and some results of practical applications will be shown. Further, the relevance of this information to HF propagation will be discussed.

G-4
1440

DIGITAL HF RADAR OBSERVATIONS OF EQUATORIAL SPREAD F

Paul E. Argo
Atmospheric Sciences Group
Earth and Space Sciences Division
Los Alamos National Laboratory
Los Alamos, New Mexico 87545

The F-region irregularities that generate spread-F were first observed by a vertical incidence ionosonde (Booker and Wells, J. Geophys. Res. 43, 249, 1938). Although many observations of spread-F with ionosondes have been documented, analysis of the data has been hampered by the fact that the classical ionosonde has provided only virtual range versus frequency, ignoring not only signal amplitude but also the direction of arrival and motion of the reflecting region. The hf radar, by accurately measuring the returned echo phase and amplitude at four separated antennas allows determination of the reflecting region location and motion for each returned echo. This, in turn, provides a picture of the spread-F irregularity region never before seen. The mapping of localized regions of small scale irregularities, and their motion across the sky, indicate that modern sounders may in fact be more useful during disturbed conditions than undisturbed because it is precisely during these disturbed periods that echo returns from other than directly overhead are available to the ionosonde.

This paper will discuss three separate and distinct spread-F events; the first will be the standard post-sunset spread-F, usually identified as "range" spreading. The next two events will be isolated post-midnight occurences of "frequency" spread-F. It will be shown that the differences between these spread F types relate directly back to the morphology of the reflecting regions.

G-5
1500

GEOPHYSICAL OBSERVATIONS WITH DIGITAL IONOSONDES

J. Buchau
Air Force Geophysics Laboratory
Hanscom AFB, MA 01731
B.W. Reinisch and K. Bibl
University of Lowell Center for Atmospheric Research
Lowell, MA 01854

The multi-demensional signal characteristics of ionospheric echoes, such as amplitude, doppler shift and spectrum, polarization and angle of arrival, determined and recorded by the digisonde series digital ionospheric sounders have provided new insight into the structure and properties of the disturbed latitudes. Single antenna measurements on board a moving or stationary aircraft have unraveled previously unknown structures of the polar cap ionosphere and shed light on the spatial relation of the mid-latitude F-region trough and the auroral E-layer. Spaced antenna measurements at the equator and at Goose Bay now permit to determine details of the development of equatorial F-region depletions or plumes and of trough-type disturbances at high latitudes. Artificial disturbances caused by rf heating of the ionospheric plasma, measured by an airborne digisonde, can be unfolded in their three-dimensional structure. Compressed presentation of selected parameters of digital ionospheric data, based on processing routines developed around single or combined characteristics of the data, allows to survey large amounts of data from specific aspects, such as their direction or velocity. Detailed case studies using digisonde data, supported by other related experiments, establish the occurrence patterns of certain ionospheric phenomena like equatorial plumes, polar cap F-layer arcs and polar cap patches.

G-6
1540

INTERPRETATION OF PHASE INFORMATION FROM A DIGITAL IONOSPHERIC SOUNDER

M.J. Jarvis and J.R. Dudeney
British Antarctic Survey
Natural Environment Research Council
Madingley Road
Cambridge CB3 OET
England

This paper describes the method used by the British Antarctic Survey for the interpretation of phase information from a NOAA HF sounder (AIS) at Halley, Antarctica. It compares and contrasts this method with alternative phase processing methods. Particular regard is made to the evaluation of data from high latitude stations where data aliasing in such parameters as skymap echolocation and doppler shift is frequent.

The requirement to be able to dealias high latitude data enabling unambiguous tracking of large scale features such as the mid-latitude F region ionospheric trough is satisfied using user-interactive graphics. An example of this technique is demonstrated on Halley data. Such techniques can usefully be applied to data from stations of all latitudes where significant gradients in electron density are present.

G-7
1600

SOME SCIENTIFIC ADVANCES USING A DIGISONDE AT GOOSE BAY, LABRADOR

B.W. Reinisch and K. Bibl
University of Lowell Center for Atmospheric Research
Lowell, MA 01854
J. Buchau
Air Force Geophysics Laboratory
Hanscom AFB, MA 01731

After one decade of development it is now possible to routinely determine the vertical electron density profiles from the digital ionograms in real time. Correct identification of the overhead E and F traces was a very difficult task which we solved even for disturbed ionospheric conditions. The ARTIST (automatic real time ionogram scaler with true height) operates with the Goose Bay digisonde since March 1983, allowing for the first time to monitor the diurnal variations of the electron density profile in real time and to compare the profiles with the ionograms.

To measure the ionospheric drift, the digisonde at Goose Bay (64.6N geomagnetic) was operated in the spaced antennae doppler drift mode in between ionograms for 12-hour periods around local midnight. While the drift velocity vector varied substantially both in magnitude and azimuth, a clear trend was observed. Drift velocities of 100-200 m/s were directed toward the west before local midnight and toward the east afterward. This result correlates well with the direction of the sunward return flow of the polar cap plasma convection driven by the magnetospheric dawn-to-dusk electric field. It appears, therefore, that the HF doppler drift technique measures the convection velocity vectors.

G-8 1620

A HIGH RESOLUTION OBLIQUE SOUNDER FOR HF CHANNEL PROBING

L.S. Wagner and J.A. Goldstein
Naval Research Laboratory
Washington, D.C. 20375

A wideband, oblique incidence, coded-pulse HF radio sounder has been developed for studying the detailed pulse response of the HF extended line-of -sight channel. The sounder can be operated in a narrow band mode with an equivalent pulse width of 8 μs, or in a broad band mode with an equivalent pulse width of 1 μs. The sounder uses a pulsed, PSK modulation with a pulse duty factor of 25 percent. The PSK modulation is governed by a maximal length pseudo-noise sequence with a repetition period of approximately 8 ms and consisting of 255 chips in the narrow band mode and 2047 chips in the wideband mode. Correlation processing at the receiver results in the recovery of the channel pulse response with a processing gain of 24 or 33 dB depending on the mode. Signal digitization, correlation processing, data selection and data recording are done in real-time and continuous measurements are made over time periods limited only by the capacity of the magnetic tape storage medium ($\sim$15 min).

Measurements have been made on two mid-latitude paths of 126 and 250 km in southern California. Observations of 1 hop F2 and Es modes reveal structural details heretofore unresolved. Results show a great variety of responses of the skywave modes, depending on time of day, season, and structure of the ionosphere as characterized by near real-time ionograms. Evidence of the patchy structure of Es, interference effects between "O" and "X" modes, short term periodic oscillations of group delay and the distinctive "fingerprint" of the dispersed skywave return when viewed with a phase coherent sounder system are some of the interesting effects that are observable with the current system.

G-9 EXPERIMENTAL RADAR SYSTEM CLUTTER STATISTICS

1640 Kurt Toman, Propagation Branch
Rome Air Development Center
Electromagnetic Sciences Division
Hanscom AFB, MA 01731

For a high-frequency over-the-horizon radar system, unwanted radar echoes are associated with a moving, turbulent field-aligned ionospheric irregularity structure. The power of these echoes depends on the combined action of the earth's magnetic field and an electric field build-up during geomagnetic disturbances. The result is transient, intensified irregularity movement. At the radar, this effect produces signal clutter. In assessing the statistical phenomenology of clutter caused by moving ionospheric irregularities, observed spectra are grouped statistically in approach, recede and flat type spectra using selected flatness criteria. Flat spectra appear prevalent at high geomagnetic latitudes where intense disturbances are more likely to occur. The statistics of approach and recede spectra appears to map out a plasma flow above the surveillance area with receding motion generally dominating approach motion except during hours around local midnight.

ACTIVE EXPERIMENTS IN SPACE
H We-PM CR2-26
Chairman: P. R. Williamson, STAR Laboratory,
Stanford University, Stanford, CA 94305

H-1
1400 EFFECTS OF CHEMICAL RELEASES BY THE STS-3 ORBITER ON THE IONOSPHERE, J. S. Pickett, G. B. Murphy, W. S. Kurth (Department of Physics and Astronomy, University of Iowa, Iowa City, Iowa 52242) and S. D. Shawhan (Code EE-8, NASA Headquarters, Washington, D.C. 20546)

The Plasma Diagnostics Package (PDP) which was flown aboard STS-3 as part of the Office of Space Science first payload (OSS-1) recorded various chemical releases from the orbiter. Changes in the plasma environment were observed to occur during water dumps, flash evaporator system (FES) releases and maneuvering thruster operations.

While not intended to be scientific ventures, the orbiter water dumps and flash evaporator operations are, in effect, chemical releases and provide opportunities to study the effects of relatively large releases of water on the ionospheric environment. Examples of some of the effects noted by the PDP during STS-3 include plasma density irregularity ($\Delta N/N$) increases as great as two orders of magnitude as measured by a spherical Langmuir Probe and enhancement of the broadband orbiter-generated electrostatic noise ($0.1 < f < 100$ khz) as measured by the plasma wave instruments. In the case of the flash evaporator operations, the $\Delta N/N$ turbulence spectrum is strongly peaked at frequencies below about 6 Hz while for water dumps the turbulence spectrum is much broader and extends to higher frequencies.

The orbiter's primary and vernier thruster operations provide additional opportunity to study a large number of (smaller) chemical releases in the form of monomethyl hydrazine and primary reaction products in the ionosphere. The thruster firings are accompanied by increases in the electron density of up to three orders of magnitude as well as neutral pressure increases to as high as 10^{-4} Torr from the nominal 10^{-7} Torr. During thruster operations, perturbations in the spacecraft potential are observed, particularly when measured relative to the plasma potential in the wake. Thruster activity also stimulates electrostatic noise with a spectrum which is most intense at frequencies below 10 kHz. Further measurements to study the effects of water dumps, FES releases and thruster operations will be made by the PDP on Spacelab-2.

H-2
1420 CHARACTERISTICS OF STRONG PLASMA TURBULENCE CREATED BY THE STS ORBITER, G. B. Murphy, N. D'Angelo, W. S. Kurth, J. S. Pickett (Department of Physics and Astronomy, University of Iowa, Iowa City, IA 52242) and S. D. Shawhan (Code EE-8, NASA Headquarters, Washington, D.C. 20546)

Using a fixed biased spherical probe, the Plasma Diagnostics Package (PDP) on STS-3 observed a high degree of $\Delta N/N$ turbulence in the plasma surrounding the shuttle. The spectra of this turbulence show some variability with ram angle of the vehicle, but are primary flat to high frequency. The intensity of the turbulence is enhanced by thruster operation and water dumps and is most intense where the plasma density gradient is highest. The turbulence shows a correlation with the Broadband Orbiter-Generated Electrostatic (BOGES) noise observed by the PDP wave receivers. Discussion of the characteristics of the turbulence will be followed by a brief summary of current theories about the generation of strong turbulence and plasma waves by large vehicles moving at supersonic velocity through a plasma.

H-3
1440

CONVERSION OF NEUTRAL ACOUSTIC WAVES INTO MHD WAVES IN THE IONOSPHERE

Paul A. Bernhardt
John H. Wolcott
Dwight G. Rickel
David J. Simons
Atmospheric Sciences Group
Earth and Space Sciences Division
Los Alamos National Laboratory
Los Alamos, NM 87545

Large near-earth disturbances such as severe thunder storms, volcanic eruptions, earthquakes, high explosive detonations and atmospheric nuclear tests launch neutral acoustic waves which propagate to ionospheric altitudes. The acoustic waves produce direct modification of the ionospheric plasma densities which can be detected as Doppler frequency changes in reflected HF radio transmissions.

The neutral acoustic waves couple into the plasma via ion-neutral collisions. The three magnetohydromagnetic waves [i.e., the Alfven wave, the fast (magnetosonic) wave, and slow (ion-acoustic) wave] may be excited by the neutral acoustic waves. The ion-acoustic waves are rapidly dissipated by Landau and viscous damping. The Alfven and fast MHD waves can propagate undamped to the topside ionosphere for detection with satellite magnetometers.

The conversion of neutral acoustic waves into MHD waves is studied using numerical simulation. Plane acoustic waves are propagated vertically from below the ionosphere. The amount of acoustic wave energy that is coupled into MHD waves is computed as a function of wave frequency, magnetic field direction and ionospheric plasma density profile.

H-4
1520

THEORY FOR LOW FREQUENCY RADIATION FROM PULSED ELECTRON BEAMS

K.J. Harker and P.M. Banks
Space, Telecommunications, and Radioscience Laboratory
Stanford University
Stanford, CA 94305

A previous study of electromagnetic radiation in the band between the lower hybrid and the electron cyclotron frequency from a pulsed electron beam (Harker and Banks, "Radiation from Pulsed Electron Beams in Space Plasmas", to be published in Radio Science) is extended to the low frequency region below the lower hybrid frequency. The electrons are assumed to follow an idealized helical path through a space plasma in such a manner as to retain their respective positions within the beam. This leads to radiation by coherent spontaneous emission. The waves of interest in this region are the slow (compressional) and fast (torsional) Alfven waves. The radiation per unit frequency interval and per unit solid angle is determined for these low frequency waves as a function of both propagation and ray angles, electron beam pulse width and separation, total number of pulses, and beam current, voltage, and pitch angle. These results provide a useful theoretical basis for planning future electron beam experiments in space plasmas.

H-5
1540

PRODUCTION OF LOWER HYBRID WAVES AND FIELD-ALIGNED PLASMA DENSITY STRIATIONS BY THE INJECTED VLF WAVES

M. C. Lee
Regis College Research Center
Weston, Mass. 02193
S. P. Kuo
Polytechnic Institute of New York
Long Island Center
Farmingdale, N. Y. 11735

The VLF waves injected from the ground-based transmitters may change from linear to circular polarization (i.e., whistler modes) on their paths through the neutral atmosphere and into the ionosphere. These VLF waves, if intense enough, may excite two lower hybrid waves and a magnetically field-aligned zero frequency mode via the purely growing instabilities. This process is dominantly controlled by the thermal focusing force effect, since the favorably excited modes have large scale lengths (λ) in the sense that $\lambda^2 >> (2\pi v_{te})^2/\Omega_e \omega_r$, where λ, v_{te}, Ω_e, and ω_r are the scale lengths of the excited modes, the electron thermal velocity, the electron gyrofrequency, and the lower hybrid frequency, respectively. The expected perturbations in the ionosphere (or magnetosphere) as a consequence are as follows. The excited lower hybrid waves may accelerate the electrons and induce particle precipitation and airglow. The production of field-aligned density striations gives rise to the irregularities in the ionosphere (or in the magnetosphere depending on the wave frequency of the injected waves) and may cause the radio wave scintillations.

STUDENT PAPER SESSION
We-PM CR2-28
1900-2100

ELECTROMAGNETIC MEASUREMENTS
A Th-AM CR2-6
Chairman: H. Hellwig

A-1 0900 ON THE PRACTICALITY OF RESONANCE-BASED IDENTIFICATION OF SCATTERERS: J. R. Auton and M. L. Van Blaricum, General Research Corporation, Santa Barbara, CA; and M. A. Morgan, Naval Postgraduate School, Monterey, CA

The practicality of resonance-based identification of electromagnetic scatterers is explored through measurements performed at the Transient Scattering Laboratory, Naval Postgraduate School, Monterey CA. Measurements of the monostatic scattering for the two stick-model scatterers shown below were obtained. These scatterers are representative of two different aircraft that are to be discriminated or identified. Numerical predictions for these same scatterers were carried out to validate the measurements and quantities derived from the measurements. Clusters of natural frequencies (Laplace-domain poles) have been formed for each scatterer with data from different measurements. The mutual exclusiveness of the clusters is an indication of the practicality of resonance-based identification.

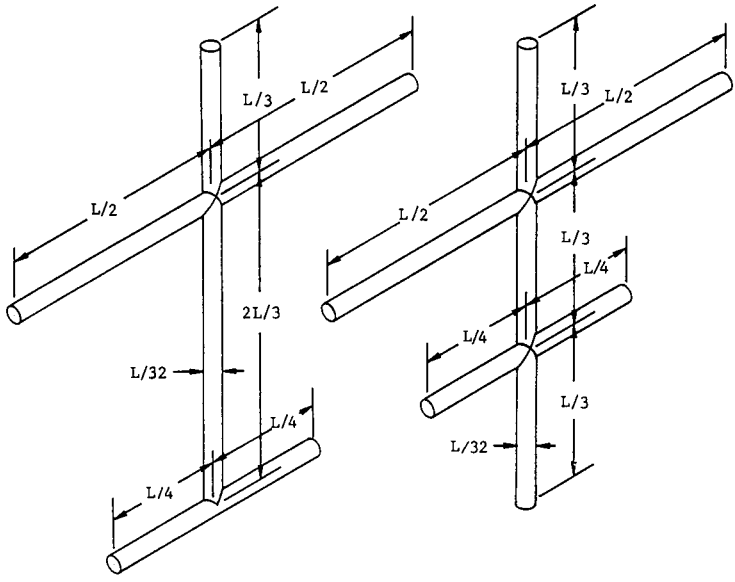

A-2 0920 FOURIER ANALYSIS OF NOMINAL ELECTROMAGNETIC PULSES FROM HIGH ALTITUDE NUCLEAR BURSTS, TIME ZERO TO 10 MILLISECONDS

J.A. Marks and T.L. Brown
Dikewood, Division of Kaman Sciences Corporation
1613 University Boulevard, N.E.
Albuquerque, New Mexico 87102

A nominal four-part electromagnetic pulse time history is devised from the open literature dealing with high altitude nuclear bursts. The four part time history consists of (1), prompt gamma signal, (2), scattered gamma signal, (3), neutron inelastic signal, and (4), the residual decay of these effects. A Fourier analysis of the time-tied and filtered time history is done. Variations in the spectrum are found by individually varying each of the four physics processes.

A-3 IMPROVED USNO MASTER CLOCK: W. J. Klepczynski, U.S. Naval
0940 Observatory, Washington, DC 20390

Two VLG-11B hydrogen masers were recently acquired for the purpose of improving the physical realization of UTC (USNO), a mathematically derived time scale of the U.S. Naval Observatory. The paper will briefly report on how the time scale is formed and how the hydrogen masers will be utilized to drive the Master Clock, the real-time physical realization of UTC (USNO).

In addition, short- and intermediate-term time domain measurements of the relative stability of the two masers will be presented. The measurement system utilized in this study consisted of an HP 9826 controller, and HP 5370A counter, and a Boulder Scientific Model 106C, High Resolution Mixer/Heterodyne Measurement System.

A-4 1020 MEDIUM AND HIGH FREQUENCY (MF AND HF) GROUND ELECTRICAL PARAMETERS MEASURED DURING 1982 AT SEVEN LOCATIONS IN THE UNITED STATES WITH THE SRI OWL PROBE KIT

G.H. Hagn and J.C. Gaddie
Telecommunications Sciences Center
SRI International
1611 North Kent Street
Arlington, Virginia 22209

The ground "constants" available in handbooks pertain to the MF broadcast band for generic types of soil, and they can be quite misleading when used for other bands. SRI International developed an open-wire line (OWL) probe kit to measure ground electrical constants (i.e., relative dielectric constant and conductivity) as a function of frequency in the LF, MF, HF and VHF bands. This kit was used at six U.S. Army bases and at a University of Alaska Geophysical Institute site near Fairbanks to measure surface ground electrical parameters as a function of frequency in the MF and HF bands. The soil types varied from dry desert sand to thawed loess overlaying permafrost. The resulting data are compared to generic curves of ground electrical parameters vs frequency developed by SRI (G.H. Hagn, B.M. Sifford, and R.A. Shepherd, "The SRICOM Probabilistic Model of Communications System Performance -- A User's Manual for Engineers, Applications Programmers, and Systems Programmers," Final Report, Contract NT-81-RC-16011, SRI International, Arlington, Virginia, May 1982) as replacements values for current handbook values for propagation model predictions and antenna computations using models such as the Numerical Electromagnetic Code (NEC).

A-5
1040

MATCHING THE HOT-CARRIER DETECTOR

J. N. Brittingham and L. F. Jelsma
Lawrence Livermore National Laboratory
P. O. Box 5504, L-156
Livermore, California 94550

Because of its large output signal voltage as compared to other microwave detectors, the hot-carrier detector is being developed at Lawrence Livermore National Laboratory as a high field detector. This detector is a germanium crystal which is used to measure the electric field. When placed in a rectangular waveguide, a special matching method is required because the old approaches of introducing metal objects into the guide might initiate arcing for high fields. Therefore, to overcome this, we have chosen dielectrically-filled guide sections as a matching technique. The method is to use lossless, homogeneous, isotropic dielectrically-filled rectangular guides which fill the entire guide. The first two matching procedures which we investigated was the single dielectric slab and double dielectric slabs. In the second case, there is a void between the two slabs; also between the last and load.

We chose to study these problems by writing a numerical code which uses the scattering matrix theory for dielectrically-filled rectangular guides. This code uses the analytical formulation of the matching section along with the measured reflection coefficient data to predict the cascade effect. The code was experimentally verified for the single slab matching section. Then the code was used to assess the bandwidth of both matching techniques.

This paper describes the analytical development and measurement along with the results of the two methods.

A-6
1100

THERMAL PATTERNS OF INDUCED SURFACE CURRENTS ON FLAT PLATES

John P. Jackson
Kaman Sciences Corporation
Colorado Springs, Co 80933
Robert W. Burton, Ronald M. Sega
Department of Electrical Engineering
University of Colorado
Colorado Springs, Co 80907

Infrared detection of induced surface currents has advanced rapidly. Substantial progress has been made in the theoretical modeling of resonant patterns in plexiglass. These patterns can be observed with the infrared technique and compared to theory. Provisions have been made to account for conductivity which has also been examined in a trans insulator/conductor regime. The goal is to have a theoretical capability to evaluate the infrared detection capabilities at all conductivites.

The theoretical model assumes that the observed resonant patterns are in essence diffraction patterns set up by internal reflections in the plexiglass squares. We consider the plexiglass square as an aperture into which the microwaves propagate and then calculate the amplitude and phase of the wave reflected internally back towards the front surface. We make this calculation using Kirchoff's formulation of Huygen's Principle. Reflections both from the rear surface and sides of the plexiglass are treated by image theory where the image has the strength and phase as determined by the reflection coefficient. The reflection coefficient off the rear wall is calculated by the Fresnel reflection equations but, owing to polarization complexities, the reflections off the sides are treated as phenomenological parameters to be inputed. The diffracted/reflected wave is then recombined with the incident plane wave at the front surface and the resulting interference pattern calculated, displayed on the computer CRT screen, and photographed.

A-7 1120 Ka-BAND UNILATERAL FINLINE PIN DIODE MODULATORS: David P. Wilson, Electronic and Electrical Engineering Department, California Polytechnic State University, San Luis Obispo, CA

Ka-band amplitude modulator design for high dielectric constant substrates is presented. The modulators consist of PIN diodes shunt mounted on unilateral finline. Substrate material is 0.010" thick alumina (ε_r=9.6). Impedance transformation from waveguide to narrow-gap finline and higher-order mode considerations are discussed. Measurements confirm computer predicted performance. A representative set of measured characteristics include: minimum insertion loss = 1.7 $\pm$ 0.5 dB; on/off ratio = 48 $\pm$ 6 dB; transition time to maximum insertion loss state $<$ 10 ns. Ideas for realization of absorptive tapered bias unilateral finline PIN modulators conclude the paper.

ANTENNAS AND ARRAYS
B-1 Th-AM CR1-46
Chairman: E. F. Kuester, Department of Electrical and Computer Engineering, University of Colorado, Boulder, CO 80309

B1-1
0840

ELECTROMAGNETIC RADIATION FROM SOURCES IN OPEN CYLINDRICAL STRUCTURES WITH ARBITRARY, LINEAR MEDIA

H. Blok and A. T. de Hoop
Schlumberger-Doll Research
P.O. Box 307, Ridgefield, CT 06877 U.S.A.

Electromagnetic radiation in open cylindrical structures has many applications in such fields as optical communication (optical waveguides) and geoscience (boreholes). For the transfer of electromagnetic signals, such structures can be often regarded as a cascading of a number of uniform waveguide sections. The excitation and transmission properties of the structure as a whole are fully known, once the transmission properties of each uniform section and the transfer properties of the junction between two successive sections are known. In the present paper, we present a unified approach to characterizing the transmission properties of an open cylindrical structure of arbitrary cross section and with an arbitrary (i.e. in general bi-anisotropic and lossy), linear, transversely inhomogeneous medium by the modal constituents as they are excited by equivalent surface-current distributions located in the end planes of a section. The orthogonality relations of, as well as the normalization conditions for the modal constituents in the field representation are proved to follow from the excitation of the field by a radiating point source. This reasoning immediately proves the completeness of the modal expansion for the field excited by a source. As can be expected, the modal constituents are made up of the discrete surface-wave modes and the continuous radiation modes. The Lorentz normalized orthogonal transverse field distributions of the modal constituents show up in the expressions for the tensorial Green's functions in a natural way. In the literature, the discussion on the modal expansion of the tensorial Green's functions is restricted to separate geometries [e.g. Felsen and Marcuvitz, *Radiation and Scattering of Waves*, Chap. 3, Prentice-Hall, Inc. 1973; Snyder, IEEE MTT-19 (8), 720-727, 1971; Shevchenko, *Continuous Transitions in Open Waveguides*, The Golem Press, Boulder, 1971. The discussion on the orthogonality and normalization of radiation modes is restricted either to lossless structures [e.g. Sammut, J. Opt. Soc. Am., 72 (10), 1335-1337, 1982; or they lack a correct proof of the orthogonality [e.g. Manenkov, Radio-phys. Quantum Electron., 13, 578-586, 1970 and IEEE MTT-29, 906-910, 1981. The present analysis is devoid of such restrictions; it can be considered as a generalization of the approaches by Nyquist, et al. J. Opt. Soc. Am., 71 (1), 49-54, 1981, and Vassallo, J. Opt. Soc. Am., 73 (5), 680-683, 1983.

B1-2
0900

A UNIQUENESS THEOREM FOR NEAR-FIELD ARRAY SYNTHESIS

David A. Hill
Electromagnetic Fields Division
National Bureau of Standards
Boulder, Colorado 80303

In synthesizing a prescribed field distribution within a given volume, it is more convenient and efficient to work with the field on the surface than the fields within the volume. For time-harmonic fields the tangential vector, $\underline{F} = \underline{E}_{tan} - \eta\, \hat{n} \times \underline{H}$, where $\hat{n}$ is the unit normal into the region, can be used to drive the following uniqueness theorem. "The electromagnetic fields in a source-free region are uniquely specified by $\underline{F}$ over the boundary." The proof requires that the constitutive parameters of the region be continuously differentiable, but it does not require loss in the region as do proofs involving the tangential components of only $\underline{E}$ (or $\underline{H}$). η can be any positive quantity, but it is most natural to define it as the intrinsic impedance when the region is homogeneous and lossless. $\underline{F}$ is essentially the combined field uantity which has been used to eliminate internal resonances in the integral equation solution for the current on a perfectly conducting scatterer (J.R. Mautz and R.F. Harrington, AEU, 32, 157-164, 1978).

A near-field array synthesis technique which minimizes the mean squared error in $\underline{F}$ over the surface has been developed. The technique has been applied to the problem of producing a plane wave field in a test volume for electromagnetic susceptibility testing of equipment. Plane wave synthesis in the near field of a spherical array was previously applied to antenna pattern measurements (J.C. Bennett and E.P. Schoessow, IEE Proc., 125, 179-184, 1978), but in that case the field error was minimized over a planar cut through the test volume. By minimizing the error in $\underline{F}$ over the closed surface, we find that the plane wave quality of $\underline{E}$ and $\underline{H}$ is good throughout the entire test volume. A remaining task is to obtain a quantitative relationship between the surface errors in $\underline{F}$ and the volume errors in $\underline{E}$ and $\underline{H}$.

B1-3
0920

THE DISCRETE CONVOLUTION METHOD AND ITS APPLICATION TO ARRAYS

Htay L. Nyo
Roger F. Harrington
Arlon T. Adams
Department of Electrical and Computer Engineering
Syracuse University
Syracuse, NY 13210

The discrete convolution method is an iterative method for the treatment of electromagnetic problems. The moment method equation is first reformulated as a convolution equation:

$$\vec{Z} * \vec{J} = \vec{V} ,$$

where $\vec{V}$ are known excitations, $\vec{J}$ are unknown currents, and $\vec{Z}$ are impedance functions. The solution is obtained by an iterative technique using the discrete Fourier Transform. The method is particularly useful for linear and planar arrays. Solution time is proportional to k n log n where n is the number of unknown currents and k depends upon the class of problem treated. The result is a rapid computation of array parameters. The discrete convolution method is described and typical results for large linear and planar arrays are presented.

B1-4
0940

NONUNIFORM TRANSMISSION LINE MODEL FOR CIRCULAR MICROSTRIP ANTENNAS

G-L Lan and D. L. Sengupta
Radiation Laboratory
Department of Electrical and Computer Enginering
The University of Michigan
Ann Arbor, MI 48109

An equivalent nonuniform transmission line circuit model is developed for the input impedance of a circular microstrip antenna excited by a coaxial probe. The theory is based on radial waveguide considerations applied to the circular cavity section with its edge terminated by proper radiating admittance. Each orthogonal mode is represented by a single radial transmission line and the input impedance is then obtained by adding the impedances of the lines at the output terminal. The reactive boundary admittance is determined from the electric and magnetic energies stored in the fringing fields, whereas the conductive boundary admittance is approximated by lumping the copper, dielectric and radiation losses to the edge of the antenna.

Numerical results for the first two lowest resonant modes have been calculated for circular microstrip antennas with variable radius, thickness and feed locations. The theory has also been applied to the microstrip half-disk and ring antennas. The calculations are compared with experimental data showing a good agreement.

B1-5
1000

COAXIALLY-DRIVEN THIN-WIRE, SLEEVE DIPOLE ANTENNAS

David C. Chang
Electromagnetics Laboratory, Campus Box 425
University of Colorado
Boulder, CO 80309 and
Lawrence W. Rispin
M.I.T. Lincoln Labs.
Cambridge, MA 02139

Because of the self-contained nature of the feedline structure, sleeve dipole antennas have many important applications in telemetry and portable antenna systems. While these antennas at resonance resemble, as they must, closely to a conventional linear dipole antenna, the detailed characteristics both in terms of bandwidth and input impedance can differ significantly due to the presence of any additional concentric coaxial lines used as external tuning elements. For instance, in the case of a sleeve monopole antenna with a decoupling choke, the structure acts like a dipole antenna only at resonance when the choking action restricts current flow to a finite section on the outer surface of the coaxial feed-line.

Before we can analyze this class of composite coaxial antenna structures, we need to first examine the effect of the junction created by the truncation of the outer conductor of a thin-wire coaxial line, using the well-known Wiener-Hopf method. We found that the junction has essentially no effect upon an antenna current incident from the extended portion of the inner conductor. However, when the antenna current is incident from the truncated outer conductor, the junction discontinuity now acts like a secondary voltage source exciting currents in all three regions of the truncated coaxial line. The same situation exists when current is incident from the coaxial region except for a reversal in sign. Analytic expressions for the reflected and transmitted currents are obtained in closed-form following a similar procedure to the one we used for the reflection from the end of a semi-infinitely long dipole antenna.

Numerical results have been obtained for an isolated sleeve dipole antenna, a sleeve monopole antenna with a gorund plane and an infinite sleeve monopole antenna with a decoupling choke. Good agreements were obtained with experimental data whenever available. Issues regarding the effect of the characteristic impedance of the coaxial-line, the location of the feed point and the effectiveness of a decoupling choke will be addressed in the presentation.

B1-6
1040

ANALYSIS OF A CYLINDRICAL ANTENNA IN A CIRCULAR APERTURE IN A SCREEN

Chalmers M. Butler and Anthony Q. Martin
Department of Electrical Engineering
University of Houston
Houston, Texas 77004
Kryzsztof A. Michalski
Department of Electrical Engineering
University of Mississippi
University, Mississippi 38677

An analysis of a finite-length cylindrical antenna which extends through the center of a circular aperture in a perfectly conducting planar screen separating two dissimilar half spaces is presented. The screen is of infinite extent and is planar while the half spaces are homogeneous, of semi-infinite extent and can be lossy. The screen and the cylinder are perpendicular. The cylinder is excited by the traditional slice generator. Coupled integral equations for the cylinder current and aperture electric field are derived and solved numerically. Data are presented for numerous cases of interest and are compared with special-case results available in the literature. When the two media are the same and when the screen is at a position where the charge density on the cylinder would have been maximum if the screen were not present, the effect of the presence of the screen is strong. On the other hand, when the screen is placed at a zero charge position, its presence has almost no effect on the cylinder current provided the cylinder is thin relative to the wavelength. As expected, when the upper medium is free space and the lower medium is a good conductor, the cylinder current replicates that on a monopole above ground plane, since the aperture is effectively shorted. The cylinder current and aperture electric field are investigated carefully as a function of aperture radius. As this radius becomes larger and larger, the structure under consideration here approaches the so called ground stake antenna, i.e., the cylindrical antenna partially in one half space and partially in that below. Results for the ground stake antenna and the present structure are in close agreement for large values of aperture radius.

B1-7 1100 APPROXIMATE FORMULAS FOR THE FAR FIELDS AND GAIN OF OPEN-ENDED RECTANGULAR WAVEGUIDE: Arthur D. Yaghjian, Electromagnetic Sciences Division, Rome Air Development Center, Hanscom AFB, MA 01731

Approximate formulas are derived for the far field and gain of standard, open-ended, unflanged, rectangular waveguide probes operating within their recommended usable bandwidth of frequencies. (Such probes are commonly used in making probe-correlated near-field antenna measurements.) The formulas, which yield forward far-field power patterns and on-axis gains of X-Band and larger waveguide probes to within about 2 dB and 0.2 dB accuracy, respectively, assume ($\sin\phi - \cos\phi$) azimuthal angular dependence and an E-plane pattern given by the traditional aperture integration of the TE_{10} mode in the Stratton-Chu equations. The H-plane pattern is estimated by two different methods. The first, and less accurate, method uses a purely E-field aperture integration to estimate the H-plane pattern. The second method uses an electric field integral equation (EFIE) to show that fringe currents near the shorter edges of the guide can be well-approximated by isotropic line sources. The amplitude of these line sources is then determined more simply by equating the total power radiated into free space to the net input power to the waveguide.

B1-8
1120

RADIATION BY A PROBE INTO A SUBSTRATE

C. L. Chi and N. G. Alexopoulos
Electrical Engineering Dept.
University of California
Los Angeles, CA 90024

The radiation properties of a probe in a substrate are considered. The probe is of arbitrary thickness and it can be greater, equal or smaller than the substrate thickness. Surface wave effects in the substrate are accounted for in the computation of probe current distribution and input impedance. Applications of the developed algorithm in various antenna configurations which include the probe will be discussed.

B1-9 TRANSITION RADIATION AT A FINE-WIRE MESH
1140

K. F. Casey
JAYCOR
39510 Paseo Padre Parkway, Suite 310
Fremont, CA 94538

Transition radiation is produced when a charged particle passes through an interface between two media or, as in the present paper, an impedance sheet. It has been proposed that this radiation might be useful for electron-beam diagnostics. In this paper we consider the transition radiation emitted when a charged particle passes through a wire mesh, a structure described by a spatially dispersive sheet impedance. It is found that the passage of the charged particle through the mesh causes a spherical wave to be radiated from the impact point and a surface wave to be propagated outward on the mesh.

We present analytical results and numerical data showing the behavior of the space and surface waves in the time and frequency domains, and estimate the total energy radiated by the process. We also briefly address the problem of "tailoring" the equivalent sheet resistance and inductance to in some sense optimize the transition radiation pulse.

RANDOM DISCRETE SCATTERERS
(Special Session)
B-2 Th-AM CR2-28
Chairman: L. Tsang, Department of Electrical Engineering, University of Washington, Seattle, WA 98195

B2-1 0900 WAVE SCATTERING BY A BOUNDED LAYER OF RANDOM DISCRETE SCATTERERS: Y. Q. Jin and J. A. Kong, Department of Electrical Engineering and Computer Science, and Research Laboratory of Electronics, Massachusetts Institute of Technology, Cambridge, MA 02139

A strong fluctuation theory for wave propagation through a bounded layer of random discrete scatterers is applied to the active remote sensing of earth terrain and atmospheric precipitations (snowfall, rain). By taking into account the singularity of the dyadic Green's function and introducing an auxiliary permitivity, the strong fluctuation theory has been developed to deal with dense random media and random scatterers with large permitivity contrast against background medium. The effective permitivity of such random medium is calculated without consideration of the boundary effect. The correlation functions of discrete scatterers which may have different constituents or size distribution are derived with a three dimensional probability analysis. Using the distorted Born approximation and the mean dyadic Green's functions of the two-layer model with the effective propagation constant in the far field approximation, we have calculated the backscattering cross section per unit area, bistatic scattering coefficients, cross-polarized backscattering cross sections per unit area, and studied the reflectivity factor, attenuation, and transmission of coherent and incoherent waves.

In remote sensing applications a snowpack is modeled as a bounded layer of random spherical discrete scatterers. The dry snow is a mixture of ice particles and air, and the wet snow has an additional constituent of water drops. The functional dependence of backscattering and bistatic scattering on wavelength, observation angle, polarization, snow depth, fractional volume, wetness is established. The theoretical results show the increasing trend for the like-polarized and cross-polarized backscattering and bistatic scattering coefficients with increasing frequency, snow depth, fractional volume, and gradually approaching saturation. In general the scattering of vertically polarized wave decreases more rapidly than the horizontally polarized wave due to more transmission through the background medium. Wetness causes the decrease of backscattering while large particle size causes more scattering. Based on the measured ground-truth data, the theoretical results are matched favorably with experimental results.

We also study the reflectivity factor, and the attenuation and transmission through the atmospheric precipitation (snowfall, rain) with this model. With the precipitation rates R given by Gunn-Marshall for snowfall, and by Marshall-Palmer for rain, the reflectivity factor Z is obtained from the strong fluctuation theory. It is shown analytically that our Z-R relationship is consistent with the empirical expression $Z = aR^b$ under single

scattering and weak fluctuation assumption. The attenuation of coherent wave and transmission of coherent and incoherent waves through a layer of snowfall are calculated theoretically and the results are shown to match attenuation data versus snow mass concentration at frequencies 35, 95, 140, and 217 GHz.

B2-2
0920 SCATTERING OF ELECTROMAGNETIC WAVES FROM A HALF SPACE OF NONSPHERICAL PARTICLES

L. Tsang
Department of Electrical Engineering
University of Washington
Seattle, Washington 98195

The scattering of a plane electromagnetic wave obliquely incident on a half space of nonspherical dielectric particles is studied. The orientation of the particles is described by a probability density function over the Euler angles of rotation. Particle positions are assumed to be random with a defined pair distribution function.

To investigate coherent wave propagation, the quasi-crystalline approximation is applied to truncate the hierarchy of multiple scattering equations. This gives the generalized Lorentz-Lorenz law and the generalized Ewald-Oseen extinction theorem. By solving the Lorentz-Lorenz law, it is found that the coherent wave can be described by two characteristic waves with two propagation constants. In the limit of low concentration of particles, the results agree with that of Foldy's approximation. The coherent reflection coefficient for the half space medium is calculated by solving the generalized Ewald-Oseen extinction theorem. For media that are not azimuthal symmetric, the coherent reflectivity is different for the two independent polarizations even at normal incidence. The incoherent scattered field is calculated with the distorted Born approximation and generally gives a nonzero depolarization term in the backscattering direction.

B2-3
0940

MILLIMETER WAVE PROPAGATION IN VEGETATION: THEORY

F. Schwering, G. M. Whitman and R. A. Johnson
U S Army Communications-Electronics Command/CENCOMS
Fort Monmouth, NJ 07703

A theoretical model of mm-wave propagation in woods and forests will be presented. The model is based on the theory of radiative energy transfer and takes multiple scattering effects into account while interference effects are neglected. The main purpose of the model is to establish overall effects and assist in the interpretation of the results of a recent experimental investigation on mm-wave transmission through vegetation.

The theory models vegetation as a statistically homogeneous random medium of discrete scatterers. The medium is characterized by its scatter cross section per unit volume σ_s, its absorption cross section per unit volume σ_a and its average scatter function (phase function). Both isotropic scattering and strong forward scattering (with an isotropic background) have been considered. The fact that the scatter objects in vegetation have a wide variey of sizes and shapes, and no preferred orientation suggests an isotropic scatter function, while the observation that these scatterers are large compared to a mm-wavelength points to a scatter function with a strong forward component.

The transport equation has been solved numerically for both cases. The results show that the range dependence of the received signal strength is characterized by a high attenuation rate at short distances into woods and by a lower attenuation rate at large distances, and that substantial beam broadening occurs at large vegetation depths. These effects which are confirmed by the experimental results can be described in terms of the strongly attenuated coherent field component, which dominates at short distances, and the less attenuated incoherent field component, which determines the field intensity at large distances into woods. Lateral wave effects, on the other hand, are not expected to exist at mm wavelengths.

Comparison of theoretical and experimental results indicates that vegetation at mm-wavelength is a strongly scattering medium ($\sigma_s >> \sigma_a$) and that the assumption of a scatter function with a strong forward component is more realistic than the isotropic option.

Theoretical results on range dependence and beam broadening will be presented and compared to measured data.

B2-4 1000 MILLIMETER WAVE PROPAGATION IN VEGETATION: EXPERIMENTS

E. J. Violette and R. H. Espeland
U S Department of Commerce
NTIA/ITS
Boulder, CO 80303

A test series was conducted on mm-wave propagation in woods and forests. A primary purpose of the experiments was determination of the dependence of the received signal strength on pathlength through vegetation (range dependence).

In naturally forested areas, the density of vegetation is nonuniform and difficult to describe in terms of foliage depth. To perform the experiments under well defined conditions, a uniformly planted, well-established orchard of pecan trees near Wichita Falls, Texas, was selected as a test site. Comparative measurements were made over path lengths of 0.1 to 0.9 km (with 1 to 35 trees on path) through the trunk region and the canopy region of the trees, both under summer and winter conditions (trees with and without leaves). The experiments were conducted at three frequencies simultaneously, i.e., at 9.6, 28.8 and 57.6 GHz.

Test results show that the range dependence of mm-waves in woods is not determined by a simple exponential decrease at constant attenuation rate. Rather, a high attenuation rate at short distances into vegetation transforms into a much lower attenuation rate at large distances. The transition between these two regions is rather sharp, in particular at mm-wave frequencies and for trees in leaf. The experiments have shown, furthermore, that substantial beam broadening occurs at large distances into woods; that polarization effects are negligible; that signal strength within vegetated areas fluctuates substantially with antenna position and pointing; and that leaves have a strong effect on path attenuation in the mm-wave region while their effect at microwave frequencies is much reduced.

The experiments will be described in detail; test results will be presented and interpreted. The investigation was sponsored by the U S Army Communications-Electronics Command at Fort Monmouth, NJ.

B2-5
1040

CURRENT FLOW IN HETEROGENEOUS MEDIA

James R. Wait, Geo Electromagnetics Group
Department of Electrical Engineering
University of Arizona
Tucson, AZ 85721

It is now well known that the effective conductivity and permittivity of earth materials in situ are strong functions of frequency. This isparticularly true at ELF and VLF. The physical mechanisms are not clearly understood but it is clear that change of conduction from electronic to electrolytic in the case of disseminated mineralization is a major source of the dispersion. A simple phenomenological model that has met with success is the ensemble of coated metallic spheres or spheroids. The interface impedance is then fitted into the boundary value problem in a straight-forward fashion (e. g. Chap. 2 in GeoElectromagnetism by J. R. Wait, Academic Press, 1982). Assuming more realistic electrochemical descriptions of the metal-electrolyte interface and non-spherical particle shapes, the dependence on volume loading, particle orientation , and texture can be examined. We also consider a model for dispersion in clay like media where the influence of bound ions on the particle surface can be modelled as a conductive sheath which, in general, may be complex and highly dispersive. Finally we consider a general particle model where the sheath effects can be treated as a combined interface impedance and interface admittance. In the context of potential theory this model allows for the simultaneous discontinuity of potential and normal current flow at the surface of the particle. Such effective electrochemical boundary conditions can be further generalized to include the electromagnetic surface impedance that plays a role when the problem is no longer quasi-static in nature. Such an example is a long metal conductor buried in the earth. Then the induced eddy currents add their share of the overall dispersion as seen by an external observer. (e. g — see M. S. theses by P. W. Flanagan and J. T. Williams, University of Arizona, 1983 and abstracts from Commission B meeting of URSI in Houston May, 1983) Some of the analytical details of this type of boundary problem are described in Electromagnetic Wave Theory (by J. R Wait, Harper and Row, 1984).

B2-6 1100 COLE PLOTS FOR INHOMOGENEOUS POLARIZABLE MEDIA

James R. Wait and Thomas Gruszka
GeoElectromagnetics Group
Depts of Electrical Eng. and Applied Mathematics
University of Arizona, Tucson, AZ 85721

In the induced polarization method of geophysical exploration, the frequency dispersion of the constitutive electrical properties of the media is exploited. It has been found that a wide variety of rock types can be represented in terms of the Cole-Cole form for the complex resistivity $\rho(i\omega)$ as follows:

$$\rho(i\omega) = \rho_o \left(1 - m_o[1 - [1+(i\omega\tau)^k]^{-1}]\right)$$

for a time constant τ sec, [e.g. see W.H. Pelton, S.H. Ward, P.G. Hallof, W.R. Sill, and P.H. Nelson, Geophys. 43, 588-603, 1978]. Here ρ_o, m_o, and k are the DC resistivity, chargeability, and dispersion parameter for the homogeneous region under consideration. When ρ is plotted in the complex plane, circular arcs are formed that are very convenient for diagnostic studies. The concept can be extended, in principle, to inhomogeneous regions by introducing "dilution factors" that weight the contributions from the individual homogeneous parts. Such a weighted superposition works amazingly well in many cases. The basic mathematical formulation has its roots in the basic work of Harry Seigel (Geophys. 24, 547-565, 1959). We have examined the general validity of the dilution concept in the case of layered earth models where each region has its own Cole-Cole representation. The resultant complex ρ plots exhibit very clearly when the dilution theory is an adequate scheme. As suggested earlier the dilution is really only a first order modification and, to be formally correct, one should also incorporate "distortion" effects (J.R. Wait, Can. Jour. Phys. 36, 1634-1644, 1958 and IEEE Trans. GE-19, 231-234, 1981). The present paper makes an attempt to show how one should interpret field frequency response data for the complex resistivity when the regions may be strongly polarizable and simple dilution theory is not valid. The role of the associated inductive coupling will also be discussed.

B2-7
1120

USE OF WIDEBAND CHANNEL PROBE FOR CLUTTER CROSS SECTION MEASUREMENT

K.V.N. Rao
James W. Coffey
Electromagnetic Techniques Branch
Electromagnetic Sciences Division
Rome Air Development Center
Hanscom AFB, MA 01731
and
John Austin
MIT Lincoln Laboratory
P.O. Box 73, Lexington, MA 02173-0073

This paper describes the novel use of an S-band pseudo-noise channel probe to measure the bistatic clutter cross section of wooded hills and pine tree clusters. Terrain reflectivity measurements have been generally made using FM-CW radars, pulse radars or, more recently, synthetic aperture imaging radars. Channel probes are conventionally used to determine the multipath delay profiles, muiltiple delay spreads, and doppler spreads in tropospheric and mobile communication links. The S-band channel probe measurement system previously described (John Austin at the 1983 International Symposium of IEEE AP-S meeting at Houston, TX in May 1983) is used to make the measurements reported in this paper. This system provides 5 nanosecond resolution in time of arrival measurement between direct and multipath components of the received signal. This high resolution permitted us to resolve discrete reflecting targets in range. The cross sections of conducting corner reflectors and spheres were measured at approximately 0° bi-static angles. The bistatic clutter cross sections of pine tree clusters and wooded hills in the Ft. Devens, MA area were also measured. The advantages and disadvantages of the channel probe in conducting bistatic reflectivity measurements will be discussed.

B2-8 Discussion
1140

INFORMATION THEORY

C Th-AM CR0-38

Chairman: Jack Wolf, Department of Electrical Engineering, University of Massachusetts, Amherst, MA

C-1 0900 DIGITAL SIGNAL IN COMMUNICATION: VLSI OR MICROPROCESSORS?: Andrew J. Viterbi, M/A-COM LINKABIT, INC., 3033 Science Park Road, San Diego, CA 92077

The answer to this rhetorical question is obviously both. Depending on application, speed, variety of processing tasks, either or both custom VLSI and general purpose microprocessors might be used for digital signal processing. Case studies in the author's experience will be discussed dealing with such applications as digital satellite modems and terminals, error-correcting coding, data encryption, video scrambling, speech compression, and data networking. Future trends will be predicted.

C-2 AUTOMATIC-REPEAT-REQUEST ERROR CONTROL SCHEMES: Shu Lin,
0930 Department of Electrical Engineering, University of Hawaii at Manoa, Honolulu, HI 96822

Error detection incorporated with automatic-repeat (ARQ) is widely used for error control in data communication systems. This method of error control is simple and provides high system reliability. If a properly chosen code is used for error description, virtually error-free data transmission can be attained.

This paper surveys various types of ARQ and hybrid ARQ schemes, and error detection using linear block codes.

C-3
1030

HIGH DATA RATE REED SOLOMON ENCODERS FOR THE SPACE CHANNEL

J. C. Morakis, Aerospace Data Standards Office
Applied Engineering Division
W. Miller, Instrument Electronic System Branch
Instrument Division
NASA/Goddard Space Flight Center
Code 730.4
Greenbelt, MD 20771

The Reed-Solomon (R/S) (255,223) code is being considered by NASA/Goddard Space Flight Center for inclusion as a concatenated coding standard. (The inner code is a short constraint length convolutional code, constraint length 7 Rate 1/2)

This paper discusses a new implementation of a conventional non-bit-serial architecture for high rate R/S encoders with the channel data stream in either the conventional or the trace orthogonal (dual) field representation (see E.R. Berlekamp. IEEE Trans on Information Theory, IT28, 869-874, 1982).

These techniques replace the 8-bit symbol feedback multipliers by transmission gates or ROM's resulting in eight times higher data rates and easily replicable circuits for VLSI design.

C-4 1100 CAPACITY AND ERROR EXPONENT FOR A DIRECT DETECTION POISSON CHANNEL: A. D. Wyner, Bell Laboratories, Murray Hill, NJ 07974

We consider the following channel. The channel input in a T-second interval is a waveform $x(t)$, $0 \le t \le T$, which satisfies $0 \le x(t) \le B$, and $\int_0^T x(t)\,dt \le \alpha B T$, $0 \le \alpha \le 1$. The channel output is a Poisson process with intensity parameter $\lambda(t) = x(t) + \lambda_0$. This channel is a model of a "direct-detection" optical channel with B and αB, the maximum and average input power, respectively. The parameter λ_0 represents "dark-current." We calculate the complete error exponent as a function of α, B, and λ_0. Thus, this channel is one of the very few for which the exponent is known exactly. Further for transmission rates R less than the "cutoff rate" R_0 we exhibit an explicit code which achieves error probability

$$P_e \le \exp\{-(R_0 - R)T\}.$$

RADAR BACKSCATTER: CLEAR AIR AND SEA SURFACE
F Th-AM CR1-42
Chairman: E. K. Smith

F-1
0900

ANISOTROPIC BACKSCATTER FROM THE CLEAR AIR

A. T. Waterman, T-z Hu
STAR Laboratory,
Stanford University
Stanford, CA 94305
P. Czechowski, Max Planck Institute for
Aeronomy, Lindau, FRG

Several measurements made with ST (stratosphere-troposphere) radars have indicated a variation of echo strength with zenith angle. One possible explanation for such observations is anisotropic backscattering. The present paper uses a model suggested by Gage & Balsley (Rad Sci 15, 243-257, 1980), and drawn from earlier works of Staras and of Booker & Gordon; it attempts to fit the model to measurements made at Arecibo using the 47MHz SOUSY transmitter (Röttger et al, JATP 43, 789-800, 1981) in the 1000-ft diameter antenna. Eight zenith angles (from 1.7 to 11.7 degrees off vertical) and two azimuths (north and east) were used in these measurements.

The results are not wholly definitive, since only two azimuths were used, but they do place limits on the degree of anisotropy, both horizontally and vertically. In the former case the limits are fairly broad, but in the latter they are more restrictive. For most of the heights covered, from 12 km up to the tropopause around 17 km, the ratio of the minor axis to the major axis of the vertical anisotropy ellipse lay between 0.1 and 0.3.

F-2 SIGNAL STATISTICS OF VHF RADAR ECHOES FROM CLEAR AIR
0920

D. R. Sheen and C. H. Liu
Department of Electrical Engineering
University of Illinois at Urbana-Champaign
Urbana, IL 61801

Signal statistics of VHF radar returns from vertical pointing observations of the clear air are investigated. In particular, the signal signature, its Doppler spectrum and statistical distribution are examined. It is found that the most important factors that characterize the statistics of the signals are the width of the spectrum and the Nakagami m-coefficient for the intensity distribution. Using these factors as criteria, two types of signals are found. One corresponds to volume scattering arising from isotropic turbulence or multiple thin layers. The other corresponds to return from single layers. Examples of the different scattering/reflection processes will be shown. Numerical modeling is used to simulate the scattering/reflection processes. From the simulation, it is demonstrated that echo signals from some range gates are consistent with the picture of reflection from a single, curved, diffusive layer, causing focusing and defocusing of the signals.

F-3
0940

PHASE SYNCHRONIZING LARGE ANTENNA ARRAYS USING THE SPATIAL CORRELATION PROPERTIES OF RADAR CLUTTER

E.H. Attia and B.D. Steinberg
Electrical Engineering Department
360 Moore School of Electrical Engineering
University of Pennsylvania
Philadelphia, PA. 19104

Interest has developed in using large, thinned, random or periodic antenna arrays in applications that require a very narrow beam such as high-accuracy tracking, direction finding or high resolution radar imaging. Since large structures are very likely to flex with time, the need arises for techniques for the real time self-calibration of the antenna system. In (B.D. Steinberg, IEEE Trans. Antenn. & Prop., 29, 740-748, 1981), a bistatic radar imaging system is described, where adaptive retrodirective beamforming techniques focus the array upon a point source, following which the focused beam is moved in range and angle to a target area and scanned across the target. The need for a point source (e.g., a corner reflector or a beacon) for system calibration limits its use especially in uncontrolled environments.

We present two techniques for self-calibrating such a system in the absence of a point source, capitalizing on the spatial correlation properties of radar clutter. We show that if the spatial autocorrelation function of the field (as measured by adjacent element pairs) is ensured to be real and positive in the neighborhood of the origin, both periodic and random arrays can be synchronized forming retrodirective beams pointing at the axis of symmetry of the radar transmitter, provided that the inter-element spacing does not exceed some limit (the order of the size of the transmitting aperture). If the spatial autocorrelation function is complex, we show that we can still synchronize a periodic array with a residual beam pointing error.

Both computer simulations and actual sea clutter data (collected by the Naval Research Laboratory) verify the theory and the practicality of the algorithms.

F-4
1020 A SEMI-EMPIRICAL MODEL FOR DOPPLER SPECTRAL FEATURES OF MICROWAVE RADAR SEA SCATTER: Dennis B. Trizna, Radar Techniques Branch, Naval Research Laboratory, Washington, D.C. 20375

A semi-empirical model is developed for Doppler spectral features of near grazing microwave radar sea scatter, which introduces a fetch dependence to explain the scatter in radar data previously published in the open literature. Constants for the model are determined from empirical curve fitting model equations to plotted surface truth data of wind speed, wave height and period in various combinations against one another. These constants are then employed in equations for the Doppler shift and the bandwidth of the peak of the sea scatter spectrum, which are thus independently predicted as a function of measured wind speed and wave parameters. It appears that the contributions to the Doppler shift of the radar return for the vertically polarized transmit/receive combination can be represented entirely by large wave orbital motions, Stokes and wind drift currents, and the classical Bragg scatter Doppler shift, all of which are included in the two scale model of radar sea scatter. However, additional sea mechanisms are necessary to explain the larger Doppler shifts reported for the horizontal transmit/receive and the cross polarized combinations, possibly the same that are found to produce stronger "sea spike" or "bursts" for horizontal polarization.

F-5
1040

A COMPARISON OF OPTICAL AND RADAR MEASUREMENTS OF C_n^2 HEIGHT PROFILES

Jean Vernin, Department of Astrophysics,
University of Nice, Nice, France and
John L. Green, T. E. VanZandt, W. L. Clark
and J. M. Warnock, NOAA, R/E/AL3,
325 Broadway, Boulder, CO 80303

Height profiles of the magnitude of the refractivity structure constant (C_n^2) were measured simultaneously by an optical double star scintillometer and a VHF ST radar. The optical instrument was located at the Sunset radar site, near Boulder, CO. The importance of this comparison is that these two techniques use radically different electromagnetic wavelengths and are based on different physical principals. The optical technique measures the transmission characteristics while the radar technique measures the scattering properties of a turbulent atmosphere.

The optical profiler analyses the scintillation of light from a double star produced by the turbulent inhomogeneities in the atmosphere. Each component of the double star projects a separate Fresnel diffraction pattern on the ground. Their separation is proportional to the altitude of the turbulent layer. Real time processing of these moving patterns is performed by a correlator, enabling retrieval of both the height and the strength of the turbulence from 4 km above sea level up to the lower stratosphere. It is a passive remote sounding method working under "clear air turbulence" circumstances, at night, and only sensitive to the fluctuations of the microstructure of the temperature field.

The Sunset radar is a pulsed Doppler radar with a wavelength of 7.4 m. C_n^2 can be inferred from the radar reflectivity at large antenna beam zenith angles, which is due to the scattering of the radar pulse by inhomogeneities of radio refractivity of scale 3.7 m. These inhomogeneities are caused by turbulent fluctuations of the temperature field and in the troposphere also by fluctuations of the humidity field.

F-6
1100

DIURNAL AND SEASONAL VARIABILITY OF C_n^2 OBSERVED BY THE VHF DOPPLER SUNSET RADAR AND COMPARISON BETWEEN OBSERVED AND MODEL PROFILES

J. M. Warnock, J. L. Green, T. E. VanZandt
and K. S. Gage
NOAA/ERL, R/E/AL3
325 Broadway
Boulder, CO 80303

In 1981 the Sunset radar system was improved to allow absolute measurement of the turbulence structure constant of the radio refractive index, C_n^2 (Green et al., Preprint Vol., 21st Conf. on Radar Meteorology, Sept. 19-23, 1983, Edmonton, Alta., Canada, pp 144-147). Using the improved Sunset radar we conducted an observing program to study the seasonal and diurnal variability of C_n^2 during Jan-Feb and June-July 1982. Good agreement is found between the average observed profiles and model profiles of C_n^2 computed from standard radiosonde balloon data (VanZandt et al., Preprint Vol., 20th Conf. on Radar Meteorology, Nov. 30-Dec. 3, 1981, Boston, pp 129-135).

Preliminary results of this study show that during the summer, in the middle troposphere, C_n^2 may increase by two orders of magnitude from dawn to midafternoon. Model calculations show that an increase in the vertical gradient of humidity accounts for most of this diurnal variation. Furthermore, day-to-day variations in C_n^2 during the summer are due primarily to the variations in the humidity structure, whereas such variations during the winter are due primarily to variations in the wind field structure.

RADIO PROPAGATION
G Th-AM CRO-30
Chairman: Adolf Paul, NOSC, San Diego, CA

G-1
0900 MEDIUM FREQUENCY SKYWAVE PROPAGATION CHARACTERISTICS OF SIGNALS RECEIVED AT FAIRBANKS, ALASKA

Robert D. Hunsucker and Brett S. Delana, Geophysical Institute, University of Alaska, Fairbanks, Alaska 99701, John C. H. Wang, Office of Science and Technology, Federal Communications Commission, Washington, D.C. 20554, and George H. Hagn, SRI International, 1611 North Kent Street, Arlington, Virginia 22209.

Since September 1981 an F.C.C.-sponsored medium-frequency (MF) skywave monitoring program has been in continuous operation at the Geophysical Institute of the University of Alaska. The equipment and antennas are located at the Ace Lake field site approximately 2.5 miles due west of the Geophysical Institute. The system is built around a commercial general purpose receiver modified for accurate AGC output. The receiver frequency is automatically stepped through 16 channels every five minutes by the system programmer. Recordings are continuously made on ten or more standard broadcast stations plus one HF transmission, and time information and are recorded on digital tape cassettes. These data are then transferred on a weekly basis to a data base on our VAX 11/780 computer. A noise source has also been provided for periodic system calibration. Three antennas have been utilized during the program to date: 1) A 615-foot longwire, 2) a 40-foot vertical monopole with ground screen, and 3) a 106-foot top-loaded vertical with ground screen. Extensive measurements and computer modelling efforts have been made on the antenna systems and results will be presented. Daily, seasonal and sunspot variation effects on measured MF skywave signal strengths will be presented. The summer/winter and magnetic activity effects are profound on medium and long-distance paths to Fairbanks. Observations were started in September 1981 when the smoothed monthly sunspot number was 143, and we hope to continue the program until the minimum of Solar Cycle 21, thus providing the F.C.C. with the full range of MF skywave signal strengths for these paths and latitudes.

G-2 0920 MUF/MOF FACTORS AND FOT BANDS OBSERVED DURING A ONE-MONTH TEST IN CONUS UNDER THE GEOMAGNETICALLY-DISTURBED CONDITIONS OF THE SUMMER OF 1982

L.O. Harnish, D.L. Worthington,
D.R. Uffelman, and G.H. Hagn
Telecommunications Sciences Center
SRI International
1611 N. Kent Street
Arlington, Virginia 22209

The frequency that is optimum for traffic (FOT) has traditionally been computed as 0.85 times the monthly median predicted MUF. This factor is an estimate of the factor required so that the operating frequency would be below the MUF on 90 percent of the days of the month. It is well known that on any given day this definition of optimum can be misleading (e.g., K. Davies, Ionospheric Radio Propagation, NBS Monograph 80, U.S. Government Printing Office, Washington, D.C., 1 April 1965).

A one-month test was conducted on 3 east-west paths in the continental United States (CONUS) between Ft. Bragg, NC and Ft. Knox, KY (696 km); Ft. Leavenworth, KS (1439 km); and Ft. Lewis, WA (3830 km). AN/TRQ-35(V) chirpsounders were operated on each path at least once an hour on 29 days between 6 July and 9 August 1982. The resulting ionograms were scaled to determine the maximum observed frequency (MOF) and the upper and lower frequencies of a FOT band defined using criteria for a digital system. Significant sporadic E (E_s) existed during daytime on the shorter two paths, so two FOT bands were defined: 1) F-layer, and 2) Total. The ratio of the FOT band edges to the MOF were computed versus time of day for each path. This paper summarizes the MOF factor results obtained during the geomagnetically disturbed period during the summer of 1982. It is concluded that an F-layer MOF factor which is a function of time of day and path length would provide better predictions during a disturbed period than any one number such as 0.85.

G-3
0940

MULTIPLE PHASE-SCREEN SIMULATION OF HF WAVE PROPAGATION IN THE TURBULENT IONOSPHERE

Yean-Woei Kiang and C. H. Liu
Department of Electrical Engineering
University of Illinois at Urbana-Champaign
Urbana, IL 61801

In a turbulent medium with stratified background, an equation for the modified complex amplitude, u, is derived. It reduces to a parabolic equation as the wave is incident along the direction of the stratification. The solution at the turning point can be derived by properly choosing the reference fields to represent the upgoing and the downcoming waves. Based on this parabolic equation, one can make use of the multiple phase-screen method to simulate the high frequency wave propagation in the turbulent ionosphere. Several one-dimensional random phase screens are numerically generated and placed at different heights along the propagation path adding random phases to the wave passing through them. The fluctuating wave field u on the ground is produced through the diffraction due to these screens. For plane wave case, the various statistical properties of the field, such as average field, field correlation, scintillation index, etc., can be readily computed using appropriate spatial averaging under the ergodicity assumption. Shifting each phase screen horizontally by different amount and then investigating the cross-correlation of field on the ground, one can study the effect of the velocity profile on the drift pattern on the ground. The contribution of electron density fluctuation at different heights to the scintillation can be examined by adjusting the strength of each phase screen. The beam wave case is also studied under certain limitations.

G-4
1020

WINTER NIGHTTIME ENHANCEMENTS OF IONOSPHERIC ELECTRON CONTENT IN THE TROUGH REGION

R. Leitinger*, Air Force Geophysics Laboratory
Bedford, MA 01731

The trough in ionospheric electron content can be considered as the transition region from mid latitude to high latitude behavior. Its position and its latitudinal profile are very sensitive to the level of (local) geomagnetic activity. Under quiet and very slightly disturbed conditions one finds a smooth latitudinal profile with a well defined but rounded minimum which moves equatorward in the evening and poleward in the morning, reaching a minimal latitude of about 60° magnetic around midnight magnetic. The minimal latitude decreases with increasing magnetic activity but often the latitudinal profile changes radically: in the latitude region where one expects the trough minimum one finds strongly enhanced F-layer ionization reaching sometimes peak values exceeding the solar EUV controlled early afternoon values. The enhancements are confined to a latitude of a few degrees but are rather extended in longitude and have a typical lifetime of several hours. One extensive case study showed that the enhancements occurred at the equatorward border of a bright diffuse aurora and were produced by a strong flux of soft precipitating electrons, in another case an equatorward movement of the enhancement was revealed. The studies were based on Differential Doppler observations from a chain of stations in Europe but there is evidence on winter nighttime enhancements in Faraday effect records from a suitably located station in eastern North America. Since the Faraday effect was observed on the signals of a geostationary satellite no information on the latitudinal profile can be derived but the records can be used to gain insight into the temporal behavior of the phenomenon.

*NAS/NRC Senior Resident Associate. Permanent Address: University of Graz, Austria.

G-5 1040 MODELLING OF QUASI-PERIODIC DIFFRACTION PATTERNS OBSERVED IN EQUATORIAL VHF SCINTILLATIONS

S. J. Franke and C. H. Liu
Department of Electrical Engineering
University of Illinois at Urbana-Champaign
Urbana, IL 61801

Quasi-periodic diffraction patterns have been observed in VHF scintillations recorded at Ascension Island in 1981. The patterns occur most often at the beginning or the end of a scintillation patch and are shown to be caused by irregularities associated with the "walls" of equatorial plasma bubbles. By using the amplitude signatures observed simultaneously at VHF L-band and C-band we are able to model the irregularity structures. Based on the modeling results we find evidence for vertical coherence in the irregularities which cause the diffraction patterns. Previous radar and scintillation studies have indicated that the walls of the plasma bubbles are vertically coherent (elongated). Our observations, however, pertain to irregularities in the several hundred meter scale size regime which may be imbedded in the larger scale "walls".

COHERENT WAVE-PARTICLE INTERACTIONS IN THE MAGNETOSPHERE

H Th-AM CR2-26

Chairman: U. S. Inan, STAR Laboratory,
Stanford University, Stanford, CA 94305

H-1
0840

WAVE-PARTICLE INTERACTIONS IN PLANETARY MAGNETOSPHERES

W.S. Kurth
Department of Physics and Astronomy,
University of Iowa
Iowa City, IA 52242

Numerous types of wave-particle interactions have been found to be important in the terrestrial magnetosphere. These include ion and electron cyclotron harmonic waves and whistler mode chorus and hiss. With the Voyager flybys of Jupiter and Saturn, we now have observations of several of these types of waves in non-terrestrial environments. The similarity between the terrestrial waves and their Jovian and Saturnian counterparts is quite striking. The effects of these waves on the energetic plasma populations in the Jovian and Saturnian magnetospheres are apparently as important as they are at the Earth.

We survey various types of wave-particle interactions observed in the Jovian and Saturnian magnetospheres and compare with the terrestrial analogs. Particular emphasis will be placed on observations of chorus emissions found in the inner magnetospheres of all three planets. A relatively new coherent wave-particle interaction common to these three planetary magnetospheres will also be discussed. This new phenomenon is an interaction between chorus waves and electrons via the Landau resonance which results in the production of bursts of electrostatic noise near the local electron plasma frequency.

H-2
0900

VLF Wave-Particle Experiments in the Magnetosphere from Siple Station, Antarctica

R. A. Helliwell
U. S. Inan
J. P. Katsufrakis
C. R. Carlson
Space, Telecommunications and Radioscience Laboratory
Stanford University
Stanford, CA 94305

New data on VLF wave-particle interactions in the magnetosphere have been obtained from Siple Station, Antarctica, and its conjugate point at Roberval, Que., using a recently lengthened (from 21 km to 42 km) dipole transmitting antenna. Two classes of experiment are described. In the first, the coherence of the injected waves is varied by employing two or more frequency components. For two components with $\Delta f = 20$–40 Hz growth is a minimum for both components. As one of the input waves is reduced in strength, the output increases and strong harmonics of the difference frequency Δf are seen. In addition new half-harmonic components are generated, typically at $f_2 + \Delta f/2$, where f_2 is the upper input frequency. Harmonic generation is attributed to partial triggering of emissions at each beat minimum. The half harmonic $(\Delta f/2)$ is attributed to partial suppression of one emission by the preceding emission. Other experiments, such as precursor excitation, pseudo-random noise simulation, and gap triggering will be shown.

In the second class, the transfer function of the magnetosphere is measured as a function of radiated power, f and df/dt, where f is the frequency of the injected signal. Preliminary data suggest that the low-frequency cutoff for temporal growth of the signal is controlled primarily by the flux of energetic electrons that interact with the signal near the magnetic equatorial plane at L = 4.3. An observed variation of the low-frequency cutoff with df/dt is interpreted in terms of the energy dependence of the electron distribution function.

For fixed f, the maximum output varies nonlinearly with injected signal power. At any given time there is a certain input signal level B_t below which temporal growth is small and there is no triggering. Above this threshold temporal growth (~ 100 dB/s) up to 20–30 dB above the initial input signal is observed, followed by the triggering of rising emissions. These results are interpreted in terms of a feedback model with a loop gain of G that varies with the input signal B_{in}.

For small B_{in}, $G < 1$ and the system behaves like an amplifier. For $B > B_t$, $G > 1$ and the system behaves like an oscillator whose growth rate depends on the time delay around the loop.

H-3 0920 WHISTLE-WAVES, CYCLOTRON MASERS, AND FREE-ELECTRON LASERS FROM THE SAME VIEWPOINT: W. B. Colson, Quantum Institute, University of California, Santa Barbara, CA 93106; and S. K. Ride, Johnson Space Center, Houston, TX 77058

In the whistler-wave interaction, the cyclotron maser, and the free-electron laser, electrons travel in approximately helical orbits so that there is better coupling to the transverse electromagnetic wave. However, the actual laser process in each case comes from quite a different interaction. We review each mechanism with a particularly simple approach to illustrate their essential differences. Recent work on free-electron lasers has extended this theory to a much more sophisticated non-linear, multimode model.

H-4
0940 **THREE-DIMENSIONAL PARTICLE CODES FOR THE SIMULATION OF MAGNETOSPHERIC WAVE PHENOMENA**

O. Buneman
STAR Lab
Stanford University
Stanford, CA 94305

Computer simulation of magnetospheric waves calls for particle codes rather than fluid codes (because of the long mean free paths) for full electromagnetics and for three-dimensionality in most applications. Such codes have recently been developed under the impetus of fusion plasma research (O. Buneman et al, J. Comput. Phys., 38, 1-44, 1980). The most advanced such code traces some five million charged particles through a grid of $2 * 128^3$ meshpoints on which all six field components are recorded. The fields are updated by Maxwell's equations in Fourier space each time step.

Significantly, the first test through which such a code is put is a problem which was originally posed and solved in magnetospheric reseach: What is the fluctuation spectrum of a uniform hot plasma embedded in a uniform external magnetic field? If the code can manifest the wealth of modes, from Alfven waves to Landau-damped Langmuir oscillations, it may be considered credible.

Examples of the dispersion curves yielded by runs with these codes will be shown, and the major difficulties encountered in building the codes, such as data management problems, will be described.

H-5
1000

THE PERSISTENT PROBLEM OF PLASMASPHERIC HISS

L. R. O. Storey
STAR Laboratory
Stanford Electronics Laboratories
Stanford, CA 94305

The present status of the quasi-linear (Kennel-Petschek) theory of the origin of plasmaspheric ELF/VLF hiss is examined critically, in the light of recent theoretical developments and of satellite measurements of wave distribution functions.

H-6
1040 HEATING OF THERMAL HELIUM BY LOW FREQUENCY ELECTROMAGNETIC WAVES

Maha Ashour-Abdalla, Department of Physics,
University of California, Los Angeles, CA 90024

Observations obtained in the equatorial magnetosphere from both GEOS-1 and -2 show a relationship between the presence of ULF waves in the Pc-1 frequency range and the presence of suprathermal He^+ ions. In order to understand these observations we have simulated the processes by which energetic and anisotropic protons generate ULF electromagnetic waves which subsequently interact with the cold particle population.

To simulate the heating of the He^+ ions, we have used a one-dimensional hybrid code in which the electrons are treated as an inertialess fluid, while a kinetic treatment was used for the ions. The simulation model assumes a periodic system with uniform magnetic field. The parameters of the simulation are $n(He^+)/n(H^+_{cold}) = 0.2$, $n(H^+_{hot})/n(H^+_{cold}) = 0.1$, initial cold energy = 3 eV, initial hot proton parallel energy = 17 keV, initial temperature anisotropy = 1, or $T_\perp/T_\parallel = 2$.

It was found that early in the simulation ion cyclotron waves grow at a rate which agrees with values obtained from a linear stability analysis. Later the electromagnetic waves attain large amplitudes $\delta B/B_0 = .01$. Both the cold protons and cold Helium are heated. The Helium is preferentially heated in the perpendicular direction. Analysis of the phase space plots show a tendency for He^+ ions to be trapped by the wave. The saturation mechanism of the waves and the heating of the helium ions will be discussed.

H-7
1100

The Third-Hop Whistler Anomaly: Possible Evidence for the Dependence of Magnetospheric Wave Amplification Upon df/dt

D. L. Carpenter
Space, Telecommunications and Radioscience Laboratory
Stanford University
Stanford, CA 94305
D. Sulic
Geomagnetic Institute
Grocka, Yugoslavia

Multi-hop (echoing) magnetospheric whistlers observed at a ground station usually exhibit a decrease in peak intensity with increasing hop number. However, on occasions other behavior is observed, including the occurrence of an amplitude maximum in the third-hop appearance of the whistler. Several case studies have been made based on data from the conjugate stations Siple, Antarctica and Roberval, Canada (L $\sim$4.3) and from Halley Station, Antarctica (L $\sim$4.2). The anomalous effect can apparently persist for periods of several hours in duration. Most events involve coupling from path to path near the ionospheric endpoints, rather than repeated propagation on the same path. In all four cases studied the final, third-hop, path was in the immediate vicinity of the plasmapause when the latter was near L = 4. Details of the anomaly do not appear to be understandable in terms of screening of the first-hop from the observing station by some process such as reflection by a sporadic E-layer. We suggest that the anomaly is primarily the result of amplification of the whistler wave as it becomes increasingly dispersed through multi-hop propagation. Occurrence near the plasmapause suggests that the process depends upon relatively high fluxes of interacting particles. Between the first and third hop, the magnitude of the frequency-time slope of the observed whistlers near the frequencies of interest ($\sim$2.5 kHz) decreased from $\sim$3 kHz-s^{-1} to $\sim$1 kHz-s^{-1}. For a comparable change in the slope of transmitted frequency ramps, Siple active experiments have revealed significant increases in overall wave growth.

It is likely that the path coupling involved in the anomaly is relatively common, more so than previously realized. The whistler waves, although weakened by typical propagation losses, are apparently able to sustain themselves during the coupling process until a suitable magnetospheric location and sufficiently gradual frequency-time variation are achieved. Then, as in the case of Siple transmitter experiments and as evidenced by echoing periodic emissions, it may be possible for the weak signal to be amplified by of order 30 dB.

H-8
1120

AKR BEAMS

W. Calvert
Department of Physics and Astronomy
The University of Iowa
Iowa City, IA 52242

The auroral kilometric radiation (AKR) produced by wave feedback [Calvert, J. Geophys. Res., 87, 8199, 1982] should occur in relatively narrow monochromatic beams, much like those of an optical laser oscillator. Moreover, since the AKR oscillations presumably occur at numerous discrete sites, the overall emission pattern must be a composite of the beam patterns, rather than the pattern of a single source, and this would account for certain previously-unexplained aspects of the AKR observations. For instance, it would account for the ISEE and JIKIKEN observations of overlapping discrete spectral components, and, provided the angular distribution of the beams is relatively sparse, it would explain why those satellites tend to show only a few such components at a time. Moreover, it would explain the wide range of observed AKR amplitudes [Gurnett, J. Geophys. Res., 79, 4227, 1964; Kaiser and Alexander, J. Geophys. Res., 82, 3273, 1977], since the beam nulls and skirts should produce a substantial modulation. The observed amplitude distributions, in fact, would suggest multilobe beams which sometimes fill up to a few percent of the composite emission pattern per kilohertz, even when the peak amplitudes of all the beams are assumed to be the same. In other words, it seems that the apparent strength of AKR is determined more by the density and orientation of the beams than by the individual beam strengths. Finally, a sparse distribution of beamed sources would also account for the troublesome variability of AKR observed with ISIS-1, since the beams should typically sweep past the satellite in less than a second.

H-9
1140

AURORAL KILOMETRIC RADIATION SOURCE REGION ELECTRON DENSITY STRUCTURE

Robert F. Benson
Laboratory for Planetary Atmospheres
Goddard Space Flight Center
Greenbelt, MD 20771

The maximum value for the plasma to electron gyrofrequency ratio $(f_N/f_H)_{max}$ has been found to always be less than 0.4 and to typically be less than 0.2 during the generation of x-mode auroral kilometric radiation (AKR). For o-mode AKR, on the other hand, $(f_N/f_H)_{max}$ can approach 0.9. These values correspond to the minimum altitude of the AKR source region which was found to extend down to 2400 km. The $(f_N/f_H)_{max}$ values are in excellent agreement with previously published results of the maximum instability temporal growth rates, obtained from the AKR Doppler shifted cyclotron mechanism, as a function of f_N/f_H.

The above results were obtained from ISIS 1 topside sounder data recorded during 12 apogee (~3500 km) nighttime auroral zone passes. The AKR propagation mode was determined by comparing the minimum frequency of the natural noise with sounder-stimulated wave cutoff phenomena.

Each of the 12 satellite passes recorded AKR and encountered regions of low electron density, i.e., $N_e < 100$ cm^{-3}. The extent of the low density regions ranged from a few degrees to more than 20^o along the satellite orbit (88^o inclination). Within the wide density depletions, i.e., those that extended over many degrees of latitude, there was no significant enhancement of the ambient f_N/f_H value. These results, which were limited by the ~100 km spatial resolution corresponding to the spacing between topside sounder ionograms, were substantiated on a much finer spatial scale (~10 km) using in situ measurements from the on-board Langmuir probe which were available for 10 of the 12 passes.

The observed lack of significant density enhancements within AKR source region density cavities provides additional confidence that the observed intense AKR is cyclotron x-mode radiation rather than plasma frequency o-mode radiation.

H-10 1200 Generation of Z Mode Radiation by Diffuse Auroral Electron Precipitation

P.B. DUSENBERY (Dept. of Astrophysical, Planetary, and Atmospheric Sciences, Univ. of Colo., Boulder, CO 80309)
L.R. LYONS (Marshall Space Flight Center, NASA, Huntsville, Al 35812)

High altitude (4-5 R_E, geocentric) measurements of Z mode radiation have recently been made by the DE 1 satellite in the northern polar magnetosphere in regions where $\omega_{pe}/\Omega_e < 1$ where ω_{pe} and Ω_e are the electron plasma and gyrofrequency, respectively. This cold plasma wave mode is bounded by the L=0 cutoff frequency and the upper hybrid resonant frequency. The frequency of occurrence of Z mode radiation is very broad in local time and not as intermittent as AKR and is ~ 3 orders of magnitude less intense than AKR. These properties suggest that Z mode radiation and AKR may not have a common source, especially at the high altitudes sampled by DE 1.

We propose that Z mode radiation is electromagnetic, not electrostatic and is generated by diffuse auroral electron precipitation assuming that a loss cone exists in the upgoing portion of the distribution due to diffuse electron interactions with the atmosphere. Z mode waves observed by DE 1 will be shown to have come from above the satellite and so must be propagating downward, along the earth's magnetic field direction. In addition, we shall determine theoretically the cutoff value of ω_{pe}/Ω_e for the generation of Z mode waves. The results are consistent with the recent DE 1 observations of high altitude Z mode radiation.

SOLAR RADIO ASTRONOMY
J Th-AM CR1-42
Chairman: Mukul R. Kundu, Astronomy Program,
University of Maryland, College Park, MD

J-1
0840 RECENT ADVANCES IN SOLAR RADIO ASTRONOMY

M. R. Kundu
Astronomy Program
University of Maryland
College Park, MD 20742

An account will be presented of recent advances in Solar Radio Physics, using instruments such as the Very Large Array, Westerbork Synthesis Radio Telescope, the Clark Lake Multifrequency Radioheliograph. The spatial location of microwave burst emitting sources in a flaring loop will be discussed. The magnetic field topology in flaring regions from the VLA intensity and polarization maps, and their use in testing of flare models will be presented. The ring structures in sunspot associated microwave active regions and their interpretations from combined radio and X-ray data will be presented. Finally, from the Clark Lake radioheliograph data, evidence will be presented that type III electron streams propagate in dense coronal streamers.

J-2 THE OWENS VALLEY FREQUENCY-AGILE INTERFEROMETER
0900 G. J. Hurford,
California Institute of Technology,
Pasadena, Ca., 91125

The solar interferometer of the Owens Valley Radio Observatory has recently been converted to frequency-agile operation to function as a high-resolution interferometric spectrometer over the frequency range, 1 to 18 GHz. The system uses two moveable, 27 m diameter parabolic antennas deployed along a T-shaped baseline up to 670 m east-west or 490 m north-south. The antennas are equipped with phase-locked receivers capable of switching their observing frequencies in less than 50 ms between any of 86 different frequencies (harmonics of 0.2 GHz) in the 1 to 18 GHz range. Each receiver has two feeds which can be interchanged in less than 500 ms to permit observations in either right- or left-circular polarization.

Observations consist of observer-defined frequency/polarization sequences in which successive integration periods of 25, 50 or 100 ms can be used for observing or for frequency/polarization changes. Each integration yields the amplitude and phase of the interferometric signal as well as the total power from each antenna. Since the order and cadence of the frequency-polarization sampling is arbitrary, considerable flexibility exists for defining observing sequences to match specific scientific objectives. All data are fully calibrated with respect to cosmic sources.

The instrument was motivated by the need for better spectral resolution observations of the solar microwave spectrum which contains significant information on plasma parameters, magnetic field strengths and characteristics of accelerated electrons in solar flares and active regions. Early results to be presented include the observation of relatively narrow bandwidth structures in the spectrum of microwave bursts and the measurement of magnetic field strengths in the solar corona near sunspots. The imaging potential of the frequency-agile system will also be briefly discussed.

J-3
0920

OBSERVATIONS OF THE RADIO SUN WITH THE CLARK LAKE MULTIFREQUENCY RADIOHELIOGRAPH,

T.E. Gergely
Astronomy Program
University of Maryland
College Park, Maryland 20742

The Clark Lake Radioheliograph can be used to produce images of the Sun in the frequency range 110-20 MHz. The spatial resolution of the instrument ranges from ~ 3.6 at the highest observable frequency to 20′ at the lowest; the highest time resolution currently available is .64 sec. We present observations obtained during the summer of 1982, during quiet periods, or low level of activity. We find that even during quiet periods (i.e. in the absence of Hα flares or meter-decameter noise storms) weak bursts, possibly of type III, are observed during a substantial fraction of the time. Such bursts are too weak to show up on high time resolution dynamic spectra. We eliminate such weak bursts to derive the brightness distribution and the diameter of the "quiet" Sun, and compare it to white light observations of the corona. Finally, we show some examples of the type III, or type III-like bursts. We show that when seen close to the limb, the burst sources are elongated along the limb at all frequencies. Some implications of these observations are discussed.

J-4
0940

SPACECRAFT OBSERVATIONS OF THE RADIO SUN AT KILOMETER WAVELENGTHS

R. G. Stone, J. Fainberg, J. L. Bougeret
Laboratory for Extraterrestrial Physics
NASA/Goddard Space Flight center
Greenbelt, Maryland 20771

Space observations of traveling solar radio bursts at hectometer and kilometer wavelengths correspond to the height range from about 10 R_o to 1 AU from the Sun. Observations from the ISEE-3 satellite, provide the azimuth and elevation angles of the radio source centroid as well as the source angular size at each observing frequency. Tracking type III bursts provides the three dimensional trajectory of the exciter and thus the large scale interplanetary magnetic field topology, as well as the electron density. Storms of type III events are shown to arise in streamer structures extending to distances of 100 R_o. These observations have also been analyzed to determine solar wind acceleration as a function of height. Type II bursts provide information about interplanetary shock waves and their speed as a function of distance.

J-5
1020

VERY LARGE ARRAY OBSERVATIONS OF CORONAL LOOPS AND RELATED OBSERVATIONS OF SOLAR TYPE STARS

Kenneth R. Lang, Associate Professor of Astronomy
Department of Physics
Tufts University
Medford, MA 02155

V.L.A. measurements at 21 cm wavelength with 10 s time resolution delineate the structure and evolution of coronal loops immediately prior to the emission of solar bursts. Emerging magnetic loops, transient brightening, and preburst heating within coronal loops occur minutes before solar bursts. Motions of plasma within coronal loops and changing magnetic structure have been observed during the bursts. [R.F. Willson and K.R. Lang, Ap. J., to be pub. (1984).]

Multiple wavelength observations of the quiescent emission of solar active regions delineate the temperature (total intensity) and magnetic (circular polarization) structure at different heights in coronal loops. At 6 cm and 12 cm wavelength, the circular polarization maps act as coronal magnetograms. At 21 cm wavelength the V.L.A. can map the entire solar disk with 2.6" angular resolution. These maps reveal the ubiquitous coronal loops whose emission may be attributed to the thermal bremsstrahlung of a typical coronal loop. The heights of the quiescent emission may be inferred from angular displacements from photospheric features on Hα or offband Hα photographs. [Lang, Willson and Gaizauskas, Ap. J. 267, 455 (1983); Lang and Willson, Astr. Ap., to be pub. (1984).]

The V.L.A. has been used to search for 6 cm emission from nearby active stars of late spectral type. Radio emission has been confirmed or discovered from several UV Cet flare stars, or RS CNv stars. Nevertheless, the majority of nearby solar-type stars do not have detectable radio emission, particularly those with magnetic field strengths as high as 2,000 gauss [R.F. Willson, R. Pallavicini and K.R. Lang, Astron. J., to be published (1984)].

The Arecibo Observatory has been used at 21 cm wavelength to observe bright, rapid, highly polarized spikes from the M dwarf star AD Leo. Rise times of $\tau \sim 200$ ms provide an upper limit to the linear size of $L < 6 \times 10^9$ cm for the emitter, and for a symmetric source a lower limit to the brightness temperature of $T_B \geq 10^{13}$ K. [K.R. Lang, J. Bookbinder, L. Golub and M.M. Davis, Ap. J. (Lett.) 272, L15 (1983)].

V.L.A. observations of coronal loops and related observations of solar type stars are supported under the anticipated renewal of grant AFOSR-83-0019 with the Air Force Office of Scientific Research.

J-6
1040 THREE DIMENSIONAL STRUCTURES OF TWO SOLAR ACTIVE REGIONS FROM VLA OBSERVATIONS AT 2, 6 and 20 CM WAVELENGTHS

R. K. Shevgaonkar
Astronomy Program
University of Maryland
College Park, Maryland 20742

Three dimensional structures of two active region groups are determined from observations with the Very Large Array (VLA) at 2, 6 and 20 cm. One of the groups exhibits a single magnetic loop of length ~ 10^{10} cm. The 2 cm radiation is mostly thermal bremsstrahlung and originates from the foot points of the loop. The 6 and 20 cm radiations are dominated by low harmonic gyro-resonance radiation and appears from the upper portion of the legs or the top of the loop. The loop broadens towards the apex. The top of the loop is not found to be the hottest point but two temperature maxima on either side of the loop apex are observed, which is consistent with the model proposed for long loops. From 2 and 6 cm observations it can be concluded that the electron density and temperature can not be uniform in a plane perpendicular to the axis of the loop; the density should decrease away from the axis of the loop.

J-7
1100

PARTICLE ACCELERATION IN SOLAR FLARES: INFERENCES FROM SOLAR RADIO OBSERVATIONS

E.W. Cliver
Plasmas, Particles, and Fields Branch
Space Physics Division
Air Force Geophysics Laboratory
Hanscom AFB, MA 01731

We review recently reported observations made with ground based radiometers and interferometers and space borne radio telescopes that provide possible insights into the process(es) by which ions and electrons are accelerated during solar flares. Emphasis is given to measurements by ground based patrol instruments, particularly the Radio Solar Telescope Network (RSTN) of the USAF. Topics to be discussed include: the relationship between impulsive phase emission and shock formation and ion acceleration in solar flares, shock waves as a candidate fast coronal propagation agent for solar protons, and electron acceleration and radio emission during the relaxation stage of large flares.

J-8
1120

SIMULTANEOUS OBSERVATION OF A CORONAL TRANSIENT AND TYPE IV SOLAR RADIO BURST

D.E. Gary,
Solar Astronomy 264-33,
California Institute of Technology
Pasadena, CA 91125
G.A. Dulk, University of Colorado, L.L. House, HAO/NCAR, and D.M. McLean, CSIRO Radiophysics Division

The coronal transient event of 1980 June 29, 0233 UT, was well observed by the HAO Coronagraph/Polarimeter aboard SMM and at meter radio wavelengths by the Culgoora Radioheliograph. The radio event consisted of a strong Type II (shock wave related) burst, followed by weak Type IV (storm) continuum. We discuss the details of the Type IV portion of the event in light of the two competing emission mechanisms--plasma emission (at the 2nd harmonic) and gyro-synchrotron emission. In support of the first alternative we find the following.

1) The 80 MHz Type IV source moves along the densest part of the transient in conjunction with the rising of the relevant (40 MHz) plasma level.

2) Both the 80 and 43 MHz sources are associated at all times with coronal features whose inferred densities are high enough to account for the emission as harmonic plasma emission.

3) The polarization of the 80 MHz source is consistent with harmonic plasma emission.

4) At times the spectrograph record shows weak Type III-like bursts that imply acceleration of electrons from the lower corona to energies of a few keV.

We find that gyro-synchrotron emission is a possible mechanism only if more stringent requirements are met, viz., that the density of electrons of energy greater than 10 keV is about 10% of the ambient density, that the average energy is about 40 keV, and that the magnetic field strength at 2.5 solar radii is about 2.8 gauss. We conclude that this Type IV event is likely due to plasma emission at the 2nd harmonic of the plasma frequency. We briefly discuss how well this mechanism accounts for other observations of Type IV bursts.

Thursday Afternoon, 12 Jan., 1400-1700

NETWORK ANALYZERS: ACCURACY AND STANDARD TEST METHODS
A Th-PM CR2-6
Chairman: R. C. Powell

A-1
1400

NBS PLANS ON AUTOMATIC NETWORK ANALYZERS

Cletus A. Hoer
Microwave Metrology Group
National Bureau of Standards
Boulder, CO 80303

The Microwave Metrology Group of NBS plans in the near future to cover the complete frequency range from 100 kHz to 100 GHz with dual six-port Automatic Network Analyzers (ANAs). Progress to date and designs for the millimeter wave ANAs will be outlined.

A new least squares solution for the six-port parameters has been devised and is now being tested. The new solution optimally takes advantage of the redundancy in an n-port reflectometer where $n \geq 6$. The equations to be solved have been reformulated in such a way that modern statistical approaches may be applied, yielding a variance associated with each parameter being solved for. In addition to providing valuable diagnostics, the solution provides a straightforward approach to propagating the errors through the calibration and measurement process to come up with a rigorous estimate of the uncertainty of the final measured results. The mathematics also suggest a new model for a six-port or four-port reflectometer.

Future plans also call for expanding the scope of calibration services offered by NBS on these new ANAs to include the following items which are not now calibrated.

- Components with 3.5 mm connectors to 26 GHz.
- Non-insertable devices such as waveguide-to-coax adapters.
- Shorts, opens, and beaded or beadless standard air lines for ANA calibration kits.
- Three-port couplers for obtaining power levels above and below the nominal 10 mW where the standard thermistor mounts operate.

A-2
1430

AUTOMATIC RF TECHNIQUES GROUP ROUND ROBIN TESTS ON AUTOMATIC NETWORK ANALYZERS

W. D. Seal and A. L. Lance
TRW Defense and Space Systems Group
One Space Park
Redondo Beach, California 90278

The Automatic RF Techniques Group has established a Round Robin Test Program to show the correlation of Automatic Network Analyzer measurements performed on standards which have been measured by the National Bureau of Standards. This discussion of the program includes a description of the standards, methods of measurement and automatic data transfer, information feedback and presentation of measurement results.

A-3
1520

The Proposed IEEE Standard on Network Analyzers, 100 kHz to 18 GHz

by

Bruno O. Weinschel, Chairman of IEEE Standards Committee for ANA's, P. O. Box 576, Gaithersburg, Maryland 20877

Since 1971, the above standard has gone through five re-issues. It broadly defines a network analyzer. The frequency range is limited by those connectors which are covered by U.S. or I.E.C. standards which contain air dielectric in the mating space.

Major error sources are discussed, including some which are less known, such as the "Fletcher Effect." Methods to test the source impedance, linearity, ability to computer correct for improper source and load impedance of the ANA are discussed. Verification of performance by certifiable standards for transmission and phase measurements are treated. The treatment of de-embedding or the measurement of non-insertable devices has been omitted.

The proposed standard is in the last stage of coordination within the committee and will then be processed by the IEEE Standards Board.

A-4 BEATTY TYPE 3, 5, AND 7 mm IMPEDANCE STANDARD: M. Maury 1550

A-5
1620

ERRORS DUE TO THE 'FLETCHER EFFECT' IN ANA MEASUREMENT

by Lawrence Fletcher
Weinschel Engineering Co., Inc.
One Weinschel Lane
Gaithersburg, Maryland 20877

Automatic Network Analyzers depend for their accuracy on careful calibration methods and fairly complex computational routines. Unfortunately, most of these errors pale into insignificance compared with the coherent interference effects of normal mixer products which share a common port with the RF input and which are terminated at these frequencies in the RF source impedance itself.

The author gives theoretical and experimental data showing the degree of isolation required in broadband measuring systems when resolutions greater than 0.01 dB and 0.1° are required, and examines the inherent weakness of higher order harmonic or sampling mixers when these are used in ANA systems.

NUMERICAL SOLUTION TECHNIQUES FOR GENERAL SCATTERERS
(Special Session)
B-1 Th-PM CR1-46
Chairman: D. R. Wilton, Department of Electrical Engineering, University of Houston, Houston, TX 77004

B1-1
1400

INTRODUCTION TO THE SPECIAL SESSION ON NUMERICAL SOLUTION TECHNIQUES FOR GENERAL SCATTERERS

D.R. Wilton
Department of Electrical Engineering
Cullen College of Engineering
University of Houston
Houston, Texas 77004

The rapid expansion in capabilities of digital computers over the last fifteen years has had a dramatic impact on the way researchers solve boundary value problems of all types. In electromagnetics, this revolution was heralded by the appearance of a now-famous monograph on the so-called method of moments (R.F. Harrington, Field Computation by Moment Methods, Macmillan, 1968). The solution of problems involving scattering by truly arbitrarily shaped bodies has proved quite elusive, however, and good progress has only been made in recent years. In this session, some recent new and important advances in this area will be examined for both conducting and penetrable scatterers. Emphasis will be on problems formulated as integral or integro-differential equations.

As with most numerical algorithms, the procedures presented can each be analyzed with regard to the following steps in their development.

1. Formulation of an integral or integro-differential equation.
2. Modeling of the geometry.
3. Representation of the unknown equivalent currents or fields.
4. Enforcement of the statement of equality in the equation.

In the introduction, each of these aspects are discussed, the important issues in each are summarized, and the interelationships are explored. Each paper presented in the session will be related back to these aspects as it is introduced.

B1-2
1420

POLYGONAL PLATE MODELING

E. H. Newman
Department of Electrical Engineering
Ohio State University
1320 Kinnear Rd.
Columbus, Ohio 43212

The purpose of this paper is to present and illustrate a technique for the electromagnetic modeling of complex or realistic perfectly conducting objects. The basic idea is to model the open or closed surface of the body as an interconnection of polygonal plates. There are two problems which must be solved in order to implement the polygonal modeling technique into a user oriented method of moments (MM) computer code.

The first problem is an isolated polygonal plate. The user inputs the coordinates of the polygonal plate and also the maximum allowable MM segment or mode size. Next the code implements an automated procedure to segment the polygonal plate into a series of quadralateral overlapping piecewise-sinusoidal modes.

The second problem is the interconnection of polygonal plates. Plates are connected through the use of overlap modes which enforce continuity of the normal component of current at the plate/plate junction. Again an automated scheme determines which plates are touching and defines the overlap modes. For multiple plate junctions, the routine determines which plates to connect via the overlap modes so as to allow current to flow between any two plates, and yet not create any linear dependencies.

An important feature of polygonal plate modeling is that the user specifies the geometry in terms of several plates, the corners of which can usually be easily determined from a drawing or a scale model of the body. Thus, one need not be concerned with the complicated way in which possibly hundreds of skew modes in space outline the body. It is this feature which permits realistic shapes to be modelled with relative ease by polygonal plate modeling. The method will be illustrated by examples which show the magnitude and phase of the RCS for the Concorde and Boeing 747 aircraft, and a rocket shape.

B1-3
1440

ELECTROMAGNETIC SCATTERING BY ARBITRARILY SHAPED BODIES

Allen W. Glisson
Dept. of Elec. Engr.
University of Mississippi
University, MS 38677

Donald R. Wilton
Dept. of Elec. Engr.
University of Houston
Houston, TX 77004

Daniel H. Schaubert
Dept. of Elec. & Comp. Engr.
University of Massachusetts
Amherst, MA 01003

Sadasiva M. Rao
Dept. of Elec. Engr.
Rochester Inst. of Tech.
Rochester, NY 14623

Numerical procedures for treating problems involving electromagnetic scattering from arbitrarily shaped bodies are discussed. For arbitrarily shaped, perfectly conducting bodies, a surface equation formulation employing the electric field integral equation with the method of moments is used. To apply the method of moments the body surface is modeled by planar triangular patches and vector, subdomain-type basis functions which represent the induced surface current are defined on each pair of adjacent triangular patches. An efficient testing procedure is used to generate a matrix equation which may be solved to obtain the induced current distribution on the body. Scattered fields or other quantities of interest may be calculated from knowledge of the surface currents.

Problems involving the calculation of electromagnetic scattering from and the electromagnetic field distribution within arbitrarily shaped, inhomogeneous, dielectric bodies are also considered. In this case a volume integral equation is solved via the method of moments. The inhomogeneous body is modeled by tetrahedral volume elements within which the electrical parameters are assumed to be constant. Subdomain-type basis functions representing the electric flux density are defined within each pair of adjacent tetrahedrons. The matrix equation is again obtained by an efficient testing procedure and is solved for the electric flux density distribution within the body. The electric flux density may then be used to calculate other quantities of interest.

Examples are presented for problems involving scattering both by perfectly conducting bodies and inhomogeneous dielectric bodies. These examples illustrate the types of problems to which the methods described may be effectively applied and indicate the accuracy of the numerical solution which may be expected. The relative merits and limitations of these numerical solution procedures are discussed and are compared with other existing solution procedures.

B1-4
1500

SOLUTION OF THE E-FIELD INTEGRAL EQUATION FOR ELECTRICALLY SMALL BODIES

Roger F. Harrington and Joseph R. Mautz
Department of Electrical and Computer Engineering
Syracuse University
Syracuse, NY 13210

Computational difficulties arise when the method of moments is used in the conventional way to solve the E-field integral equation for conducting bodies very small compared to the wavelength. This is because, when the wavelength is sufficiently large, the magnetic vector potential contributions to the elements of the moment matrix are insignificant compared to the scalar potential contributions. As a result, the magnetic vector potential contributions are lost, and the matrix becomes ill conditioned. The remaining scalar potential contributions depend only on the divergence of the current, which is not sufficient to determine the current. All of the previously published E-field solutions fail in the very low frequency portion of the Rayleigh region. In this region knowledge of both current and charge is required to calculate the scattered field because the charge cannot be accurately calculated from the divergence of the current.

The solution of the E-field equation can be extended into the low frequency portion of the Rayleigh region in the following way. Two sets of vector expansion functions are chosen, one set having no divergence and the other set having divergence. The first set must be suitable for expanding the magnetostatic current. It gives the first current term in the Rayleigh series. The second set must have a divergence such that the charge associated with it forms a basis for expanding the electrostatic charge. It gives the charge term in the Rayleigh series. The testing functions are chosen similar to the expansion functions. The result is a moment matrix that remains well conditioned as the frequency approaches zero.

The solution obtained in this manner gives accurate values of current and charge not only in the Rayleigh region, but in the resonance region as well. It turns out that the solution is no more complicated than previous solutions, being basically a recombination of terms to form the moment matrix. A computer program for conducting bodies of revolution has been written and documented. Using this program, we have obtained accurate numerical solutions for conducting disks and spheres of radii 10^{-15} wavelength. These solutions continue to be accurate at larger wavelengths, where the previous E-field solutions also give accurate results. These previous solutions deteriorate when the radii of the bodies become sufficiently small.

B1-5
1540

SCATTERING CALCULATIONS WITH THE BOUNDARY ELEMENT METHOD

A. Wexler
Department of Electrical Engineering
University of Manitoba
Winnipeg, Manitoba, Canada R3T 2N2

The boundary element method (BEM) is a moment method that employs higher-order modelling of both surfaces and surface currents.

Surfaces and sources are defined in terms of elements or patches with several nodes per element/patch. In this way curved surfaces are modelled as curved surfaces rather than as piecewise polygons (in two-dimensional problems) or planar facets (in three-dimensional problems).

Two types of modelling - Lagrangian and cubic spline methods - will be described and compared. Details are available elsewhere (M.H. Lean, Electromagnetic Field Solution with the Boundary Element Method, Ph.D. dissertation, Electrical Engineering Technical Report TR81-5, University of Manitoba, 1981 and S. Bilgen, Cubic Spline Elements for Boundary Integral Equations, Ph.D. dissertation, Electrical Engineering Technical Report TR82-5, University of Manitoba, 1982). Scalar problems have been published elsewhere (M. H. Lean and A. Wexler, IEEE Trans. Mag., 331-335, Mar. 1982).

This talk will present results on the analysis of scattering from conducting and dielectric two-dimensional and three-dimensional objects. An approach to the three-dimensional data preparation problem (Y.B. Yildir and A. Wexler, MANDAP A FEM/BEM Data Preparation Package - User's Manual, Electrical Engineering Technical Report TR82-3, University of Manitoba, 1982) will be described.

B1-6
1600

AN ITERATIVE EXTENDED BOUNDARY CONDITION METHOD FOR CALCULATING SCATTERING AND ABSORPTION BY ELONGATED DIELECTRIC OBJECTS:

Magdy F. Iskander, Department of Electrical Engineering, University of Utah, Salt Lake City, Utah 84112

The Extended Boundary Condition Method (EBCM), which is a popular procedure for solving scattering and absorption by dielectric objects, is based on integral equation formulation which utilizes spherical expansions to solve for the unknown fields. Such a procedure is known to be limited and inadequate for elongated dielectric objects and particularly those of large complex permittivities. As the shape of the object deviates from that of a sphere, a large number of terms in the vector spherical harmonics expansion of the unknown fields is required, which forces the matrix formulation to include Hankel functions of large arguments and orders and, in turn, results in an ill-conditioned system of equations.

In this paper we describe a new procedure, the Iterative Extended Boundary Condition Method (IEBCM), for improving the solution stability and extending the frequency range of the EBCM. The new procedure has two main features including (a) it involves dividing the internal volume of the dielectric object into several overlapping regions and employing separate field expansions in each of the overlapping subregions, and (b) it is iterative since it starts with a known solution that approximates the scattering problem. We utilized the new IEBCM method to calculate scattering and absorption by high-loss dielectric objects of large aspect ratio. The initial assumption of the surface fields in this case was obtained by approximating the object by a perfectly conducting one of the same size and shape. Numerical results were obtained for frequencies up to seven times the resonance of these objects. Up to nine overlapping subregions were found necessary to describe the internal fields of these objects. We also extended the calculations to low-loss elongated dielectric objects commonly encountered in optical applications. In this case the initial assumption was obtained by approximating the object's geometry, rather than its properties, by a spherical one and Mie theory was used to obtain the approximate surface fields. Numerical results for spheroids having aspect ratios as large as 10:1 were obtained, thus illustrating the feasibility of using the IEBCM for highly elongated low-loss objects at frequencies at and beyond the resonance frequency range. We also examined the application of the IEBCM to solve for composite bodies. In a capped cylindrical object, the interior volume was first divided into several overlapping spherical subregions and alternatively partitioned into a finite cylindrical subregion and two spherical end caps. Spherical expansions were used in the spherical subregions and a cylindrical expansion was utilized for the cylindrical subregion. Numerical results illustrating the importance and the computational advantages of using different basis functions as well as the various features of the new IEBCM will be presented.

B1-7 Discussion
1620

PROPAGATION IN RANDOM MEDIA
(Special Session)
B-2 Th-PM CR2-28
Chairman: K. C. Yeh, Department of Electrical Engineering,
University of Illinois at Urbana-Champaign,
Urbana, IL 61801

B2-1
1400

WAVE PROPAGATION IN A TURBULENT MEDIUM - A REVIEW

K. C. Yeh
Department of Electrical Engineering
University of Illinois at Urbana-Champaign
Urbana, IL 61801

The study of wave propagation in a turbulent medium is an old but still very active field. This is so because of its wide applications in remote sensing, communication, radio navigation, radar, etc. All too often the medium through which the signals propagate is rendered turbulent. In many applications, one is then interested in either the effects of turbulence on propagating signals or on ways of probing the stochastic properties of the turbulent medium itself by scattering or propagation experiments. Over the years, many techniques have been developed to solve the problem. Some of these techniques are reviewed.

B2-2
1420

APERTURE ANTENNA EFFECTS ON RADAR OBSERVATIONS THROUGH STRONGLY DISTURBED RANDOM MEDIA

Dennis L. Knepp
MISSION RESEARCH CORPORATION
735 State Street, P.O. Drawer 719
Santa Barbara, California 93102

A strongly disturbed anisotropic layer of ionization irregularities that is used as a propagation channel for radar signals can degrade the propagating wave and thereby affect the resulting radar measurements. The antenna aperture itself also affects measurements of the received signal by its inherent averaging process. Here an analytic solution to the two-position, two-frequency mutual coherence function, valid in the strong-scatter limit, is used to characterize the propagation channel. The channel itself consists of a thick slab of anisotropic electron density irregularities that are elongated in the direction parallel to the earth's magnetic field.

Analytic expressions are obtained that give the effect of the radar antenna on measurements of received power, decorrelation time (or distance), mean time delay, time delay jitter and coherence bandwidth. These quantities are determined as functions of the aperture diameter and of the angle between the magnetic field and the direction of propagation. It is shown that in strong turbulence aperture averaging can be a significant factor in reducing the received power by angular scattering loss, increasing the observed signal decorrelation time via aperture averaging, and reducing the time delay jitter by suppression of signals received at off-boresight angles.

This work is directly applicable to the problem of signal propagation through a highly disturbed transionospheric channel and to the effect of the channel on measurements made with large aperture antennas as could be used for space based radar.

B2-3
1440

THE EFFECTS OF TARGET AND SOURCE MOTION AND BEAM SLEWING ON SPECKLE PROPAGATION THROUGH TURBULENCE[1]

J. Fred Holmes and V. S. Rao Gudimetla
Department of Applied Physics and Electrical Engineering
Oregon Graduate Center
19600 N.W. Walker Road
Beaverton, OR 97006

Atmospheric turbulence and target induced speckle can have a significant and deleterious effect on the performance of optical systems. One method that is used to overcome these effects is to take averages in space and/or time. However, the reduction in signal fluctuation due to averaging are affected by target, receiver and source motion and by beam slewing. Consequently, formulations for the mutual intensity, the time delayed covariance and the power spectral density that include these effects are needed. Formulations for these statistical measures have been developed that include the effects of source, receiver and target motion and beam slewing as well as the effects of the speckle and turbulence. Utilizing the extended Huygens-Fresnel formulation, expressions for the mutual intensity, the time delayed covariance, and the power spectral density have been developed that are valid at all levels of turbulence. A TEM_{00} monochromatic laser in conjunction with a perfectly diffuse target is used to generate the speckle field. The formulations obtained are reduced to numerical data for illustrating the magnitude of the effects.

[1]This material is based in part upon work supported by the Army Research Office under Contract DAAG 29-83-K-0077 and the National Science Foundation under grant number ECS-8300221.

B2-4
1520

RANDOM WAVE PROPAGATION IN THE PRESENCE OF SYSTEMATIC REFRACTION: A CRITICAL REVIEW

Ioannis M. Besieris, Department of Electrical Engineering, Virginia Polytechnic Institute and State University
Blacksburg, VA 24061

It is well known that in the absence of a deterministic profile and within the domain of validity of the pure Markov approximation exact equations can be derived for all moments associated with the stochastic complex parabolic equation. Exact solutions, however, are available only for the single frequency mutual coherence function. The integration of the higher order moment equations can be done only approximately using asymptotic techniques which are applicable either for very short or very long ranges of propagation. A solution to the fourth-order moment equation at intermediate ranges, where intensity fluctuations can be substantial, particularly at high frequencies, has been found recently by Macaskill (Proc. R. Soc. Lond. A 386, 461, 1983) by means of a two-scale expansion method.

The problem is compounded significantly in the presence of systematic refraction, a situation arising naturally in underwater sound propagation and electromagnetic wave propagation in graded lightguides, the ionosphere, planetary atmospheres, etc. Of particular interest in this case is the effect of noise in the vicinity of (geometric) focal points. The latter can be assessed by establishing caustic corrections due both to the profile and scattering.

Again, the pure Markov approximation yields exact equations for all moments. Unfortunately, in this case, even the single frequency second moment equation cannot be solved exactly, except for highly specialized deterministic profiles (M. J. Beran and A. M. Whitman, J. Math. Phys. 16, 214, 1975; I.M. Besieris, W.B. Stasiak and F.D. Tappert, J. Math. Phys. 19, 359, 1978; I.M. Besieris, J. Math. Phys. 19, 2533, 1978). Approximate results for the mutual coherence function which incorporate realistic channels have been presented recently by Macaskill and Uscinski (Proc. R. Soc. Lond. A 377, 1981), Beran, Whitman and Frankenthal (J. Acoust. Soc. Am. 71, 1124, 1982) and Clarke (NOAA Techn. Memo. ERL AOML-51, 1982). It is our goal in this exposition to discuss the relative merits of the various techniques underlying these results, with particular emphasis on their applicability to the computation of higher order single and multifrequency moments.

B2-5 1540 BACKSCATTERING FROM ANISOTROPIC RANDOM MEDIA: Stanford P. Yukon, Rome Air Development Center, Electromagnetic Sciences Division, Hanscom AFB, MA 01731

Cross sections for backscattering from anisotropic random media are calculated in the scalar approximation for arbitrary angles of incidence and exit from a semi-infinite slab oriented either parallel or perpendicular to a symmetry axis. The backscatter cross sections are determined using an eikonal Green's function which includes multiscatter effects in conjunction with deWolf's (IEEE AP19, 254, 1971) cumulative forward scatter, single backscatter approximation. The correlation function for the turbulence is assumed to have either a Kolmogoroff or a Gaussian spectrum with unequal scale lengths parallel and perpendicular to the symmetry axis. Cross sections for scattering into forward directions are calculated as well but are not directly addressed by the approximations adopted in the model and represent lower bounds for the cross section.

B2-6
1600

GENERALIZED BOOKER-GORDON FORMULA INCLUDING THE EFFECTS OF MULTIPLE SCATTERING AND FRESNEL DIFFRACTION

C. C. Yang and K. C. Yeh
Department of Electrical Engineering
University of Illinois at Urbana-Champaign
Urbana, Illinois 61801

The Booker-Gordon formula has been used for three decades to calculate scattered power from a random dielectric volume. Basically, this formula is obtained under the joint assumption of the single scattering approximation and the Fraunhofer diffraction condition. However, recent research has shown the importance of the multiple scattering effects. Especially, under certain conditions, the cumulative forward scattering, which is known to cause the scintillation phenomenon, can drive the signal statistics into the saturated regime in which the complex amplitude becomes a complex Gaussian process. These cumulative or multiple scattering effects on bistatic radar scattering are investigated by applying the cumulative forward-scatter single-backscatter (CFSB) approximation. Additionally, the effects caused by the Fresnel diffraction instead of the Fraunhofer diffraction condition are considered. Such considerations allow us to take into account the phase variation across the irregularity, an important generalization when the size of the irregularity is comparable or larger than the first Fresnel zone. This problem is formulated in terms of propagators which are expressible as Feynman's path integrals. Such integrals are used to derive a generalized Booker-Gordon formula including effects of both the multiple scattering and the Fresnel diffraction. The results show that the Fresnel diffraction pattern appearing clearly around the forward direction under the single scatter limit tends to be smeared out by the multiple scattering. Also, both multiple scattering and Fresnel diffraction effects make the forward-scattered beam weakened and broadened, and the backscattered power reduced, when compared with the single scattering and Fraunhofer diffraction case respectively. In some situations, an enhancement effect, which is attributed to the coherence gained when the wave propagates through the same random medium twice in making a round-trip, can be seen around the backward direction.

B2-7
1620

RETROREFLECTANCE FROM A DENSE DISTRIBUTION OF SPHERICAL PARTICLES

Yasuo Kuga and Akira Ishimaru
Department of Electrical Engineering
University of Washington
Seattle, WA 98195

The sharp increase of the brightness at the retroreflection direction from some objects has been known for a long time. This is sometimes called the opposition effect. The glory appearing around the shadow of an airplane on a cloud, when viewed from the airplane, is an example of the peak in reflectivity. In astronomy it is well known that the reflectivity of the moon increases sharply at full moon. The enhancement of backscattering from a turbulent medium has also been noted in the past.

The sharp peak in the retroreflection direction may be caused by the following: 1) Mie scattering pattern, 2) high density effect when the density is above 1%, 3) mutual coherence effects due to double passage of waves which are not included in the radiative transfer theory.

In this paper we show experimental results of the backscattered intensity within the phase angle of -7.5° to 8°. The data are obtained for five different particle sizes ranging from the average diameter of 0.091 μm to 45.4 μm and at least seven different densities up to 40% in some cases. In all cases the peak of the refectivity at 0° phase angle is observed at high densities, and we found the following results: 1) when the particle size is smaller than the wavelength (λ_w = 0.475 μm in the water), the peak at 0° phase angle is small and appears at densities higher than a few percent; 2) when the particle size is 2 to 4 times greater than λ_w, a sharp peak appears at 0° phase angle and it becomes larger as the density increases; and 3) when the particle size is 10 to 100 times greater than λ_w, the effect of the Mie scattering pattern becomes apparent even in a dense medium, and the sharp peak at 0° phase angle is superimposed upon the Mie scattering pattern.

B2-8 Discussion
1640

SPREAD SPECTRUM COMMUNICATIONS
C Th-PM CRO-38
Chairman: Laurence B. Milstein, Department of Electrical Engineering and Computer Science, University of California, La Jolla, CA 92093

C-1
1340

SPREAD SPECTRUM OVERLAY SYSTEMS

George R. Cooper
William W. Chapman
School of Electrical Engineering
Purdue University
W. Lafayette, IN 47907

A spread spectrum overlay system is one in which a conventional multi- channel narrowband system and a multi-user spread spectrum system share the same portion of the frequency spectrum in the same geographic area in an attempt to improve spectral utilization. An important consideration in such cases is that acceptable quality of performance be maintained for both systems.

The use of a differential phase-shift-keyed frequency hopped system has been proposed for civilian mobile radio applications. In an overlay mode, this system would share the spectrum with cellular narrowband FM systems that are currently being built in many metropolitan areas. It is this type of overlay system that is being considered here.

The first part of the analysis considers the interference offered by the narrowband FM system to the spread spectrum system in a cellular environment. While neither direct nor numerical evaluation of the n-fold integrals resulting from the analysis are feasible, very tight bounds can be obtained. The results show that the spread spectrum system could operate quite well even if every time slot in a user's hopping pattern were exposed to a narrowband interfering signal comparable in power to that of the desired transmission.

The analysis then considers the interference offered to the narrowband system by the spread spectrum system. It is shown that by appropriate design of the spread spectrum signal structure it is possible to keep the interference to the narrowband system down to an acceptably small value. Thus, it appears that the overlay mode of operation is entirely feasible in a cellular mobile radio system.

C-2
1400

NARROWBAND INTERFERENCE REJECTION IN DIRECT SEQUENCE SPREAD SPECTRUM COMMUNICATION SYSTEMS

Laurence B. Milstein, Department of Electrical Engineering and Computer Sciences, University of California at San Diego, La Jolla, CA 92093

Pankaj K. Das, Department of Electrical, Computer and Systems Engineering, Rensselaer Polytechnic Institute, Troy, NY 12181

Two techniques which are useful in enhancing the performance of direct sequence spread spectrum receivers when used to reduce the effects of narrowband interference are discussed. An overview of each of the techniques is presented, along with recent results on system performance.

The first technique makes use of the so-called chirp transform to perform a real-time Fourier transformation on the received waveform. Narrowband interference rejection is then achieved by "notched-filtering" using an on-off switch.

The second technique uses prediction-type filters to estimate the current value of the interference and then subtract that value from the actual received sample. For each of these interference rejection schemes, both analytical and experimental results of system performance will be presented.

C-3
1420

ACQUISITION AND TRACKING OF FREQUENCY-HOPPED SPREAD-SPECTRUM SIGNALS

Dr. Ray W. Nettleton
Staff Scientist, Amecom Division
Litton Systems, Inc.

Acquisition and tracking of frequency-hopped systems has received less attention in the literature than the corresponding problem for direct sequence transmissions. Nevertheless, the problem is distinctly nontrivial when the channel exhibits adverse properties such as frequency-selective fading and time dispersion, and when jamming may be present.

This tutorial paper examines the important parameters for consideration in the design of an acquisition and tracking system, and some of the alternative techniques for realizing these functions.

C-4 1520 LOW PROBABILITY OF INTERCEPT PERFORMANCE BOUNDS FOR SPREAD SPECTRUM SYSTEMS: Edward W. Chandler, EECS Dept., Milwaukee School of Engineering, Milwaukee, WI

An important application of spread spectrum (SS) in military communication systems is that of making the signal difficult to intercept by unauthorized receivers. Error correction coding techniques may be employed to reduce the required input signal-to-noise ratio at the receiver, allowing the system to operate at a lower power level, hence resulting in a lower probability of interception. In the absence of error correction coding, a specified message bit rate, transmitted signal bandwidth, and required bit error probability at the receiver will yield a required signal-to-noise ratio for each type of spread spectrum system. When coding is employed, a specified decoder delay time implies a specified code complexity, and can be used to determine bounds on the required receiver signal-to-noise ratio. These performance bounds are evaluated as functions of the specified parameters. In addition, one may specify a burst interference environment in that the system must operate. Presented is the evaluation of the increase in the lower bound on signal-to-noise ratio as a result of the specification of a correctable single burst time. This increase indicates an anti-intercept/anti-jam trade-off.

C-5
1540

AN APPLICATION OF SINGULAR VALUE DECOMPOSITION TO THE SPECTRAL ESTIMATION OF REAL DATA

S. Avery, R. DeGroat, R.A. Roberts
Department of Electrical and Computer Engineering
University of Colorado
Boulder, CO 80309

Singular Value Decomposition (SVD) is used with forward-backward linear prediction to improve the frequency estimation of sinusoids in noise. The improvement is especially significant for short data records and low signal-to-noise ratio (SNR). The SVD is used to obtain a less noisy, lower rank approximation to the original full rank data matrix. The lower rank approximation is found by eliminating the noise subspace with a projection onto the signal subspace. Since the noise components are reduced, the SNR is effectively increased and the frequency resolution improved. This new technique is applied to wind data obtained from the MST (mesosphere-stratosphere-troposphere) radar at Poker Flat, Alaska. The radar is operated by personnel in the Aeronomy Laboratory of NOAA (National Oceanographic and Atmospheric Administration). It is used for studying atmospheric wind motions. A comparison of SVD and the traditional FFT methods will be made.

C-6
1600

PSEUDONOISE GENERATOR DESIGNS

Dr. Robert A. Scholtz
Communication Sciences Institute
Department of Electrical Engineering
University of Southern California
Los Angeles, CA 90089-0272

Spread spectrum systems use pseudonoise generators for a number of different purposes. Each of these objectives suggests certain nice properties which the PN generator's output sequence should possess. This paper reviews these properties and indicates the extent to which several well-known PN generator designs achieve these goals. Two new families of PN generators employing nonlinear feedforward logic will be described and comparisons made. Unsolved problems in PN sequence design will be posed.

C-7
1620

APERIODIC CORRELATION PROPERTIES OF SEQUENCES

Dilip V. Sarwate
Coordinated Science Laboratory and the
Department of Electrical Engineering
University of Illinois at Urbana-Champaign
Urbana, Illinois 61801 (USA).

The aperiodic autocorrelation and crosscorrelation properties of sequences are of importance in many engineering applications such as spread-spectrum multiple-access communication systems, synchronization systems, ranging and tracking systems, and radar systems. This paper presents a survey of recent results on the aperiodic correlation properties of shift-register sequences. It is shown that the out-of-phase aperiodic autocorrelation for any maximal-length linear feedback shift register sequence (PN sequence) of length N is no larger than $1 + (2/\pi)(N + 1)^{\frac{1}{2}} \cdot \log(4N/\pi)$. It is also shown that for any given offset, careful choice of the initial loading of the shift register enables one to obtain a PN sequence for which the aperiodic autocorrelation for that offset is at most $\frac{1}{2} N^{\frac{1}{2}}$. Similarly, careful choice of the initial loading enables one to obtain a PN sequence for which the merit factor (i.e. the ratio of the square of the signal energy to twice the sidelobe energy) is at least 3.

Other results surveyed include a new construction for complementary sequence sets (sets of sequences whose aperiodic autocorrelations sum to zero for every nonzero offset) which shows that any coset of a PN sequence code forms a complementary sequence set. As a special case of this result, it is shown that the Gold sequences form a complementary sequence set. The aperiodic crosscorrelation properties of these sequences are also studied, and it is shown that the Gold sequences have very desirable properties for spread-spectrum multiple-access applications.

C-8
1640

ADDRESS SEQUENCES FOR FREQUENCY HOPPING MULTIPLE ACCESS

Unjeng Cheng, Charles L. Weber,
Communication Sciences Institute
University of Southern California
Los Angeles, CA 90089-0272

The criteria for developing good sets of Address Sequences for Frequency Hopping Multiple Access (FHMA) depend upon the signal format. Nonoverlapping, Partial Overlapping and Multi-level MFSK signal formats are considered. Lower bounds on the maximum number of hits are developed in all of the above cases in a non-synchronized environment; they are dependent on the number of address sequences in the set, the period of the sequences, and the alphabet size, i.e. the number of candidate carrier frequencies.

The utility of Reed-Solomon (RS) codes in the nonsynchronized frequency hopping multiple access environment is discussed, in particular RS codes can be partitioned so that excellent sets of FHMA address sequences result.

STORMS, PRECIPITATION, SATELLITE TRANSMISSION,
AND PROFILE RETRIEVAL
F Th-PM CR1-42
Chairman: A. T. Waterman, STAR Laboratory,
Stanford University, Stanford, CA 94305

F-1
1340

AUTOMATIC DETECTION OF MESOCYCLONIC SHEAR

D.S. Zrnic', D. Burgess, and J. Gal Chen
National Severe Storms Laboratory
1313 Halley Circle
Norman, OK 73069

We report on an algorithm that detects mesocyclonic shear in storms. Large intense tornadoes are always spawned in regions of high shear. The algorithm uses decision thresholds to discriminate between mesocyclonic and other shears in Doppler radar data. We have observed that distant mesocylonic features become elongated in the beam's azimuthal direction. Thus, an asymmetry criterion that checks the radial and azimuthal extent of the mesocyclone must be range dependent. Data from sixteen different mesocyclones were subjected to the algorithm. For these data the overall probability of false alarm per storm cell was 10% and the probability of detection was 90%.

F-2
1400

MONTHLY RAIN RATE STATISTICS FOR THE CONTINENTAL UNITED STATES

W. F. Bodtmann and K. Y. Eng
Bell Laboratories
Crawford Hill Laboratory
Holmdel, New Jersey 07733

Using a complete record of all rain events that occurred in 19 major United States cities during a 5-year period from 1966 to 1970, we have studied the monthly distribution of severe rain storms relevant to satellite communications. Our results show that generally more than half of the heavy rain storms (leading to deep rain fades) are confined to only two months in a year, and these two "worst" months are generally in the summer (June to August) almost everywhere in the continental U.S. except the Burbank, California area where they tend to be in the winter. A summary of these "worst" monthly statistics is given below:

City, State	Threshold 5-min Rain Rate (mm/hr)	Two "Worst" Months	Combined Percentage Of Annual Rainy Time In The 2 Months When Rain Rates ≥ Threshold
Burbank, California	40	Nov, Dec	67
Denver, Colorado	40	Jun, Jul	67
Miami, Florida	100	May, Jun	47
Atlanta, Georgia	70	Jul, Aug	57
New Orleans, Louisiana	100	Apr, Aug	54
Columbia, Missouri	70	Jun, Jul	52
Helena, Montana	40	Jun, Aug	100
Hudson, New Hempshire	40	Jun, Jul	70
Newark, New Jersey	50	Jul, Aug	65
Buffalo, New York	40	Jul, Aug	59
Bismarck, North Dakota	40	Jun, Jul	71
Columbus, Ohio	60	Jun, Aug	59
Portland, Oregon	40	Aug, Sep	50
Memphis, Tennessee	80	May, Jul	50
Dallas, Texas	70	Apr, Oct	49
El Paso, Texas	40	Jul, Aug	69
Salt Lake City, Utah	40	Jul, Aug	86
Lynchburg, Virginia	50	Jun, Jul	58
Milwaukee, Wisconsin	50	Jun, Jul	59

F-3
1420

A DIAGNOSTIC PROBE TO INVESTIGATE PROPAGATION AT MILLIMETER WAVELENGTHS

E.J. Violette, R.H. Espeland and K.C. Allen
U.S. Department of Commerce
NTIA/ITS
Boulder, CO 80303

A diagnostic probe to fully describe the propagation characteristics of a millimeter wave channel by near simultaneous recording of an impulse response, frequency spectra, amplitude response, and bit error rate is discussed. A 30.3 GHz carrier accommodates the subcarriers and baseband modulation modes in a fully coherent network. Signal-to-noise determining components will permit BER performance of better than 10^{-8} at a 500 MB/s rate with a 25 dB fade margin through a clear air 50 km distortion free path.

Back to back operation of the terminals and a short atmospheric path are used to establish the reference performance level of the hardware. Controlled multipath tests are reported to demonstrate probe capabilities and to obtain reference data to better classify the fades and resulting distortion which occur on terrestrial links at millimeter wavelengths. With dual reflectors, multipath data sets were compiled to aid in predicting bit error rate performance resulting from a combination of signal-to-noise ratio change and intersymbol interference. Included with the above data are corresponding measurements of the impulse response and amplitude distortion on the channel.

Three additional coherent cw channels, 11.4, 28.8, and 96.1 GHz are operated with the 30.3 GHz probe to aid in analyzing selective fades which fall outside the bandpass and to evaluate frequency dependent properties of the link. Examples of performance over a 27.2 km LOS link are presented.

F-4
1440

OBSERVATIONS OF ATTENUATION BY PRECIPITATION AT 11.4, 28.8, AND 96.1 GHz

K.C. Allen, E.J. Violette, and R.H. Espeland
U.S. Department of Commerce
NTIA/ITS
Boulder, CO 80303

Observations of attenuation by precipitation at 11.4 and 28.8 GHz on a 27.2 km path during March through September 1983 have been analyzed. Cross-plots of the signal level during the fading indicate that the ratio of the attenuation at 28.8 GHz to that at 11.4 GHz tends to remain constant for intervals of time during each precipitation event. The ratios vary widely from one rain event to another. Although ratios in the range of 6 to 9 would be expected based on popular rain drop size distributions, ratios as small as 1 and greater than 30 were measured. The average ratio for rain was 4.9, below the range predicted by the popular rain drop size distributions.

No correlation was found between the attenuation ratio and the time of day of the event, the type of rain, or the fade depth. There was a decrease in the range of ratios observed in the summer with all the ratios observed in July below 6.

Although fades due to snow on the path were usually less than 1 dB at 28.8 GHz, on occasion significant fading (sometimes more than 30 dB) occur with air temperatures from 0.4 to 3.1°C. The ratio of attenuation for these fades were distinctively different from those for rain. The average ratio was 2.8 and it only varied from 2 to 3.5 indicating that the microstructure of the snow (rain) and its distribution along the path must have been similar for every significant fade during snow. That is, a specific meteorological event or process must be occurring when snow causes deep fading, presumably the same process associated with the so called bright band observed by meteorological radar.

Data at 96.1 GHz for a few rain events in August and September 1983 are also available.

F-5
1540

TEMPERATURE PROFILE RETRIEVAL BY TWO-DIMENSIONAL FILTERING

K.S. Nathan*, P.W. Rosenkranz and D.H. Staelin
Research Laboratory of Electronics
Massachusetts Institute of Technology
Cambridge, MA 02139

Satellite borne radiometers have been used with increasing success to monitor geophysical parameters. The majority of the statistical retrieval schemes currently in use for estimating atmospheric temperature profiles are one-dimensional (1-D), that is, they consider correlations only in the dimension perpendicular to the surface. Here, a two-dimensional (2-D) spatial filter, optimum in the minimum-mean-square sense, is used to retrieve atmospheric temperature profiles from Microwave Sounder Unit measurements. Horizontal correlations along the orbital track are taken into account. This additional statistical information results in lower root-mean-square errors for the 2-D filter compared to that of its 1-D counterpart, implying that some of the energy to be retrieved is correlated horizontally with the observed energy. The reduction in error is especially true in the troposphere and tropopause, and in radiosonde rich regions, i.e., regions where the verification datasets are more reliable. The previously unstudied behavior of retrieval errors as a function of spatial frequency along the orbital track is also investigated. A large part of the improved performance of the 2-D filter is due to the reduction of short spatial wavelength components in the error. In addition, retrievals over a severe storm front were carried out. The 2-D technique yielded substantially lower errors than the 1-D approach. The latter does not perform so well over such fronts because of the loss in vertical correlation due to the presence of layers of air with different lapse rates.

* was with Research Laboratory of Electronics, Massachusetts Institute of Technology. Is currently with Jet Propulsion Laboratory, California Institute of Technology, Pasadena CA 91109

F-6
1600

A BALLOON EXPERIMENT SIMULATING LAND MOBILE SATELLITE TRANSMISSIONS

W. J. Vogel and G. W. Torrence
Electrical Engineering Research Laboratory
The University of Texas at Austin
10100 Burnet Road
Austin, TX 78758

An experiment has been carried out in which a transmitter operating at 869 MHz was carried by a stratospheric balloon to an altitude of about 40 km. A motor vehicle was driven within line-of-sight from the transmitter. Measurements of the received signal strength were made every $\lambda/8$ for a travelling distance of several hundred miles. This scenario was to simulate a satellite system providing mobile communications to rural areas.

The statistics of the sampled field, consisting of a combination of direct wave, specular reflection and diffuse components, are presented as a function of elevation angle and parameters such as type of road driven or type of landscape and vegetation encountered.

For some of the time, the transmitter was narrow band fm voice modulated. The received audio signal was recorded to allow a qualitative evaluation.

IONOSPHERIC MODIFICATION AND HEATING
G Th-PM CRO-30
Chairman: M. C. Lee, Regis College Research Center,
Weston, MA 03193

G-1
1340 ENHANCED UNDERDENSE RADIOWAVE HEATING THROUGH IONOSPHERIC HOLES

Paul A. Bernhardt and Lewis M. Duncan
Atmospheric Sciences Group
Earth and Space Sciences Division
Los Alamos National Laboratory
Los Alamos, New Mexico 87545

Most high power HF heating experiments use frequencies below the maximum plasma frequency in the ionosphere. This overdense mode of ionospheric heating produces large electric fields near the region of reflection in the ionosphere. Parametric instabilities are excited with the high power HF electromagnetic radiation acting as a pump that stimulates the longitudinal electrostatic electron plasma wave, and the ion-acoustic wave. The parametric decay instability can occur only when the wave frequency (ω) is near the plasma frequency (ω_p).

Other instabilities are possible for wave frequencies much above the local plasma frequency. For instance, the two-plasmon decay instability ocurs for $\omega = 2\omega_p$. This instability has never been stimulated in the ionosphere using ground-based heating facilities because the threshold electric fields for the instability have never been exceeded.

Using an ionospheric hole to focus high power HF waves will permit the stimulation and study of new instabilities in the ionosphere. The chemical release of H_2O, CO_2, H_2 or similar material into the ionosphere promotes rapid, localized plasma reduction, forming an ionospheric hole. The ionospheric hole acts like a convergent lens to HF radio waves. The intensity of the HF radio beam can be enhanced by 20 dB or more. The increased power levels will stimulate airglow emissions and thermal self-focusing, as well as new instabilities.

G-2
1400

THE HF-ENHANCED PLASMA LINE IN A STABLE PLASMA

J.A. Fejer and M. Sulzer
Arecibo Observatory
P.O. Box 995
Arecibo, Puerto Rico 00613

A powerful HF transmitter about 15 miles from the Arecibo Observatory can produce electric fields near the reflection height of the ordinary magnetoionic mode that greatly exceed the threshold for the parametric excitation of Langmuir waves. The excited waves are usually detected by 430 MHz radar backscatter.

During the experiments to be described the power of the HF transmitter was purposely reduced to a level below the threshold for the parametric excitation of Langmuir waves. According to existing theory the spectral intensity of Langmuir waves under below-threshold conditions can exceed by almost 30 db the thermal Langmuir wave level. The Langmuir waves result from scattering of the HF pump wave by the ion acoustic waves responsible for incoherent backscatter, into Langmuir waves. The shape of the Langmuir wave backscatter spectra, centered on the two frequencies differing from 430 MHz by the HF frequency, is double-humped just like the ion-line spectrum of incoherent backscatter.

These theoretically predicted spectra have been confirmed experimentally by the present observations. The theoretical prediction that the intensity of the spectra for a given transmitted power is sensitively dependent on the local height-gradient of electron density (on account of the standing wave nature of the pump field) appears also to be confirmed experimentally.

Even when the threshold is exceeded weakly for Langmuir waves propagating in directions forming small angles with the magnetic field, the Langmuir wave detected by the Arecibo radar are not unstable; the theoretically predicted spectrum for that case is also confirmed experimentally by the present observations.

G-3
1420

GENERATION OF ENERGETIC ELECTRON FLUXES BY POWERFUL HF RADIO WAVES

S. P. Kuo
Polytechnic Institute of New York
Long Island Center
Farmingdale, N. Y. 11735
M. C. Lee
Regis College Research Center
Weston, Mass. 02193

Energetic electrons with a broad energy spectrum can be generated in the ionospheric F region that is illuminated by a powerful HF radio waves. The early evidence was deduced from the enhanced plasma line measurements at Arecibo that indicate the generation of a large flux of energetic electrons with energies exceeding 20 ev (c.f. the thermal electron energy is of order of 0.1 ev). The in situ particle measurments performed later at Tromsφ confirm the electron acceleration and show that electrons with energies greater than 25 ev can be produced by the EISCAT heating facilities. Theories, supported by observations, suggest that various parametric instabilities may be excited by HF heater waves. The intense fields of the excited electrostatic waves have been invoked to explain the acceleration of electrons up to a few ev that are responsible for the 6300 Å and the 5577 Å airglow enhancement. In this paper, we investigate the nonlinear Landau damping of Langmuir waves proposed as the process that may accelerate electrons to acquire energies of a few tens of ev and distort the electron energy distibution with a broad, flat tail.

G-4
1440 MODULATION OF AURORAL CURRENTS BY HF HEATING

M. Shoucri, G. J. Morales and J. E. Maggs
University of California at Los Angeles
Los Angeles, California 90024

The Ohmic heating produced by powerful (megawatt range) HF waves radiated by ground-based transmitters (HIPAS in Alaska, and HEATER in Norway) causes local changes in the electrical conductivity of the high-latitude ionosphere. These changes modulate pre-existing auroral (Birkeland) currents. A model is presented for the generation of very low frequency waves due to this effect.

G-5
1500

CHARACTERISTICS OF IONOSPHERIC ELF RADIATION GENERATED BY HF HEATING OF THE IONOSPHERIC D-REGION

A. J. Ferraro, H. S. Lee, R. Allshouse, K. Carroll, R. Lunnen and T. Collins
Department of Electrical Engineering
The Pennsylvania State University
University Park, PA 16802

This paper describes new observations of the characteristics of ELF generation produced by modulation of the dynamo current system from HF heating of the ionospheric D-region. A model of the ELF antenna structure embedded in the D-region is described and stepped ELF frequency observations are shown to generally support the model assumptions. Presented are data on the phase height of the ELF ionospheric antenna versus ELF frequency, polarization of the downgoing wave and relationship to the dynamo current direction, correlation of ELF field strength with percent cross-modulation, power linearity tests, and duty cycle results. All observations used the high power heater facility of the Arecibo Observatory.

G-6
1540

OBSERVED RELATIONSHIPS BETWEEN DIFFERENT HF-INDUCED PHENOMENA AT ARECIBO

A. J. Coster
Georgia Institute of Technology, EES/RAIL
Atlanta, Georgia 30332

F. T. Djuth
The Aerospace Corporation, P.O. Box 92957,
Los Angeles, California 90009

R. J. Jost
Lyndon B. Johnson Space Center,
Houston, Texas 77058

A primary motivation for ionospheric heating experiments is to determine the mechanisms by which energy is transferred from the HF wave to and through the plasma. To understand this energy-transfer process, HF-heating experiments at Arecibo have been performed coordinating observations of three HF-induced F region phenomena: the enhanced plasma line echo and large scale ($\geq$1 km) striations, both detected with the 430 MHz radar at Arecibo; also three meter field-aligned striations, detected with a portable 50 MHz radar located on the island of Guadeloupe. The timing was coordinated by the simultaneous measurement of the HF signal at both the 50 MHz radar site and at the Arecibo Observatory.

This paper reviews relationships observed between different HF-induced instabilities. First, a direct correspondence between the plasma line overshoot and the growth of three meter striations has been detected. The plasma line overshoot is not, however, always observed following HF turn-on, and a reason for this will be suggested. Second, a relationship is noted between the formation of the three meter irregularities and plasma line ringing, or strong periodic fading (1 Hz) in the enhanced plasma line. Finally, observations of another type of plasma line fading associated with the formation of large scale striations will be presented and discussed.

G-7
1600

ORDINARY MODE IONOSPHERIC MODIFICATION AND HEATING: THE ROLE OF Z-MODE COUPLING

T. A. Seliga
Atmospheric Sciences Program and
Department of Electrical Engineering
The Ohio State University
Columbus, OH 43210

The most significant ionospheric heating by intense radiowaves occurs with ordinary (O)-mode excitation. This mode can excite an extraordinary (X)- or Z-mode near the reflection level of the O-mode. The resultant X-mode electromagnetic wave may be either upgoing or downgoing. Resultant upgoing waves are either reflected at a higher height where $X = 1 + Y$ or penetrate the peak of the F-layer. This latter condition occurs when X_p, corresponding to the maximum plasma frequency of the layer, is less than $1 + Y$. Both the penetrating and downgoing X-waves experience strong absorption and coupling to plasma waves, since their propagation constants become very large (plasma resonance). This resonance condition occurs just below the $X = 1$ level and may be responsible for the strong plasma wave excitations observed in this region. The basic theory of this classical magnetoionic theory of mode coupling and its role in ionospheric modification by intense radiowave heating will be presented.

G-8
1620

SOLITON FORMATION DURING IONOSPHERIC MODIFICATION

G. L. Payne, J. P. Sheerin, and D. R. Nicholson
Department of Physics and Astronomy
University of Iowa
Iowa City, IA 52242

In previous two-dimensional numerical solutions of the Zakharov equations (J. Weatherall et al., J. Geophys. Res., 87, 823, 1982), we have demonstrated that at the exact reflection point of a typical modifier wave where the parametric decay instability cannot occur, the oscillating two-stream instability produces a set of collapsing, collisionally damped, three-dimensional entitites which we call solitons. We have now (G. Payne et al., Bull. Am. Phys. Soc., 27, 992, 1982) numerically studied the one-dimensional Langmuir wave evolution at the point of maximum heater strength, somewhat below the exact reflection point. We find that the oscillating two-stream instability dominates the parametric decay instability, again saturating in a collection of solitons. This finding is in contrast to previous theories which invoked a weak turbulence cascade involving only the parametric decay instability.

G-9
1640

OBSERVATIONS OF PROMPT PHENOMENA DURING IONOSPHERIC MODIFICATION

J. P. Sheerin, D. R. Nicholson, and G. L. Payne
Department of Physics and Astronomy
University of Iowa
Iowa City, IA 52240

L. M. Duncan
M.S. 466
Los Alamos National Laboratory
Los Alamos, NM 87545

Previous analytical and numerical work (J. C. Weatherall et al., J. Geophys. Res., 87, 823, 1982) indicate that during ionospheric modification, the oscillating two-stream instability leads to regions of intense, localized electric fields which evolve into collisionally damped, collapsing solitons. For incoherent scatter from a collection of these collapsing solitons, an intense plasma line is predicted (J. P. Sheerin and D. R. Nicholson, Phys. Lett. A, in press). Certain 'prompt' phenomena in the incoherent scatter spectrum (e.g., plasma-line overshoot) may be explained by this process. Experiments using the HF Facility and 430 MHz radar at Arecibo have been conducted to investigate these prompt, intense plasma lines. Recent results from these experiments and further theoretical developments will be presented.

G-10
1700

RADIO WAVE SELF-ACTION EFFECTS IN THE IONOSPHERE

L. M. Duncan, Los Alamos National Laboratory, Los Alamos, New Mexico 87545; J. P. Sheerin, Dept. of Physics and Astronomy, University of Iowa, Iowa City Iowa 52242; and W. E. Gordon, Office of the Vice President, Rice University, Houston, Texas 77001

Radio wave propagation through a plasma is inherently a nonlinear process. As a radio wave modifies the plasma medium through which it propagates, numerous wave self-action effects may be produced. High-power, high-frequency (HF) electromagnetic radiation incident on the F-region ionosphere modifies the background plasma temperature and density, generates strongly enhanced plasma wave oscillations at both the ion-acoustic and electron-resonance frequencies, and indirectly drives energetic electron production, detectable airflow enhancements, and local electron currents.

This paper describes experimental observations of several wave self-action effects, using the HF ionospheric modification facility and incoherent backscatter radar system of the Arecibo Observatory. Measurements of HF-enhanced plasma lines are used to study the HF thermal self-focusing instability, showing both large-scale structuring of the HF beam and focusing of the HF power into numerous 0.5-1.5 km striations. Enhanced plasma line height variations imply density fluctuations within the striations of $\Delta n/n \sim 1\text{-}10\%$. Dual frequency, multiple-height plasma line measurements suggest a beam-aligned irregularity geometry below the HF reflection height. In natural spread-F, however, the striations clearly become field-aligned, and the plasma line observations exhibit self-quenching "bursts" of HF-induced enhancements.

Immediately following turn-on of the high-power HF radio waves, the ionospheric interaction region is observed to rise several kilometers. This rise occurs on a time scale of a few seconds and is attributed to thermal expansion of the interaction region under the influence of anomalous wave energy deposition. Frequency and amplitude modulation of the incident HF radiation can be used to control the parametric instability, usually excited near the wave reflection height. The parametric wave-plasma interaction may be suppressed by frequency or amplitude modulations generating multiple pump waves, each below instability threshold. However, when the multiple pump separation frequencies correspond to a natural plasma resonance, such as the ion-acoustic frequency, the parmetric instability is enhanced. The effects of these modulation schemes on the enhanced plasma wave spectra are also detectable.

ANTENNAS IN PLASMAS

H Th-PM CR2-26

Chairman: W. W. Taylor, TRW Space and Technology, Redondo Beach, CA 90278

H-1 1340 IMPEDANCE AND EFFICIENCY OF A SPACE SHUTTLE BASED ELECTRIC DIPOLE ANTENNA: U. S. Inan and T. F. Bell, STAR Laboratory, Stanford University, Stanford, CA 94305; and R. W. Fredericks, TRW Defense and Space Systems, Redondo Beach, CA 90278

The radiation characteristics of a long (300m) stem-type VLF electric dipole antenna proposed to be used on the Space Shuttle for the Waves In Space Plasmas (WISP) experiment are studied. Combining a probe model for the sheath impedance with a separate model for the radiation resistance of a dipole in a magnetoplasma (Wang and Bell, 1972) a circuit model of the antenna terminal impedance is obtained. Using this model the efficiency and terminal impedance is evaluated over a wide range of parameters expected to be encountered during a typical flight. The total radiated power available at various frequencies is then compared to power levels that are injected into the magnetosphere using ground based VLF transmitters. It is concluded that the dipole antenna contemplated for the WISP experiments would be a useful tool for studying VLF wave-propagation and wave-particle interactions in the magnetosphere.

H-2 NUMERICAL SIMULATION OF ANTENNA-PLASMA INTERACTIONS:
1400 A. C. Calder and J. G. Laframboise, CRESS, York University, Downsview, Ontario, Canada M3J 1P3

We have developed a computer model for simulating a cylindrical or spherical antenna in an unmagnetized nonflowing Vlasov plasma. A Maxwellian plasma distribution is approximated by a multiple water bag distribution consisting of a sum of step functions. The boundaries and step heights of an n-bag distribution are optimized by equating the first 2n moments of the Maxwellian and water bag distributions. The bag boundaries in the simulation region are defined by chains of phase space particles whose equations of motion are solved by the leapfrog method. Potentials and fields are obtained by self-consistently solving the Poisson equation at each timestep. The program can treat ions as fixed or include ion dynamics for ideally small ion/electron mass ratios (e.g. $m_i/m_e = 16$). We present results of runs simulating sheath-plasma response to applied signals in the frequency range 0.1 ω_{pe} to $2\omega_{pe}$ and with amplitudes varying from 1 to a few times kT_e/e. We see a resonance peak in the d.c. probe current at $\omega \lesssim \omega_{pe}$ for both cylindrical and spherical probes. We also present comparisons of runs with and without ion dynamics taken into account.

H-3
1420

EFFECTS OF VARYING PLASMA DENSITY AND TURBULENCE ON THE OPERATION OF A LARGE VLF DIPOLE ANTENNA

G. B. Murphy and J. S. Pickett
Department of Physics and Astronomy
University of Iowa
Iowa City, IA 52242

Recent measurements made by the Plasma Diagnostics Package on STS-3 indicate that a large dipole antenna transmitting in the VLF range, would encounter several sources of plasma irregularities which could effect its operation. The transition between ambient conditions and the region of the near Orbiter wake sees the plasma density changing by as much as six orders of magnitude. The wake boundary region exhibits strong plasma turbulence at frequencies of up to several tens of kilohertz which is enhanced by water dumps and thruster operation. The operation of the RCS thrusters provides large perturbations to the plasma density in a region near the Orbiter for typically several seconds at a time. Operation of a large dipole antenna at VLF frequencies and characterization of its impedance function in the local plasma, may prove difficult under these continuously varying conditions. Likewise, operation of the antenna outside of these wake and turbulent regions may not always be consistent with magnetic field alignment or pointing requirements.

H-4 VIRTUAL ANTENNAS IN PLASMAS: PRINCIPLES AND TESTS: W. W. L.
1440 Taylor, TRW Space and Technology, One Space Park, Redondo
Beach, CA 90278

Virtual antennas are antennas which are electromagnetic waves from current modulated charged particle beams. Virtual antennas are thought to radiate like physical antennas which conduct currents in metals electrons are the most easily available charged particles and can be used to produce loop and electric monopole antennas. A modulated electron beam emitted perpendicular to the magnetic field in a plasma will gyrate and form a current loop. Parallel emission of a modulated electron beam will act as an electric monopole.

Recent tests of virtual antennas have occurred space shuttle missions OSS-1 and SL-1. On OSS-1 a 100 mA beam of electrons from VCAP was modulated at frequencies from a few Hz to above 1 MHz. A nearby receiver detected waves at all transmitted frequencies. Long distance reception was not observed. Spacelab 1 flew SEPAC, which had an electron beam with currents up to 1.5A. SL-1 results will be discussed including reception by near and remote locations.

H-5
1500

THE EXCITATION OF SHEAR ALFVEN WAVES BY A MOVING FINITE SOURCE

C.E. Rasmussen
Radioscience Laboratory
Stanford University
Stanford, CA 94305

The era of the space shuttle opens up a range of new possibilities for performing active experiments in space. One of these possibilities is the use of an electrodynamic tether to excite very low frequency waves in situ in the ionosphere. This paper looks into this possibility by studying the waves excited by a very long source moving with respect to the background plasma. It is found that the motion of the source has a dominant influence on the excitation of the shear Alfven wave. Radiation by very long sources is treated by an approximation that predicts waves propagating in two dimensions. The amplitude of the radiated waves is found in the far-field zone by the application of the method of stationary phase. The distance to the far field is also found for waves propagating in two dimensions.

H-6
1540

LONG WIRE DIPOLE MEASUREMENT OF SHORT WAVELENGTH ELECTROSTATIC WAVES

D. L. Gallagher
Department of Physics
University of Alabama in Huntsville
Huntsville, AL 35899

Observations with the ISEE-1 215 meter dipole antenna of an apparent bandwidth modulated emission in the Earth's dayside magnetosheath will be discussed. The upper frequency cutoff in the frequency-time spectrum of the emission has a characteristic curved or "festoon" shape and is modulated at twice the spacecraft spin period. The low frequency cutoff ranges from 100 Hz to 400 Hz, while the high frequency limit ranges from about 1 kHz to 4 kHz. The phase of the bandwidth modulation is not related to the local magnetic field direction, bulk plasma flow direction, or the spacecraft-sun line.

The observed frequency spectrum results from the spacecraft antenna response to a Doppler shifted wave vector spectrum, which is tightly collimated in direction. At a slightly negative potential, the spacecraft antenna is determined to be effectively capacitively coupled to the ambient plasma. Constraints are imposed on the possible plasma rest-frame wave vectors and frequencies of the observed emission, with a modeled antenna response to a spectrum of wave vectors. The rest-frame emission is deduced to consist of frequencies from about 150 Hz to 1 kHz and wavelengths between about 300 meters and 600 meters. An analysis of these constraints strongly suggest that the "festoon-shaped" emissions are in the ion-acoustic mode. The small group velocity of ion-acoustic waves and observed wave vector directions are consistent with wave generation upstream at the bow shock and convection downstream to locations within the outer dayside magnetosheath.

H-7
1600

SHORT WAVELENGTH ION ACOUSTIC WAVES UPSTREAM OF THE EARTH'S BOW SHOCK

S. A. Fuselier and D. A. Gurnett
Department of Physics and Astronomy
The University of Iowa
Iowa City, IA 52242

Examples of ion acoustic waves observed in the plasma wave data from the region upstream of the Earth's bow shock are presented to illustrate short wavelength antenna interference effects. The antenna interference effects are easily identified in the plasma wave data because the ion acoustic waves in the upstream region are Doppler shifted to frequencies as high as 10 kHz due to the motion of the solar wind. The identification of the antenna interference effects combined with the fact that the solar wind velocity is most nearly in the ecliptic plane, so that $k_z \cdot v_z \simeq 0$ in the equation $\omega' = \omega_o + \vec{k} \cdot \vec{v}$, allows for the accurate determination of the Doppler shift and dispersion relation, $\omega(\vec{k})$, of the ion acoustic waves. It is found that the measured dispersion relation fits the dispersion relation for ion acoustic waves and that the frequency of oscillation in the rest frame of the plasma is on the order of the ion plasma frequency for a wavelength on the order of a few times the Debye length.

H-8
1620

AN ATTEMPT TO MEASURE THE FIELD-ALIGNED DRIFT VELOCITY OF THERMAL ELECTRONS IN THE AURORAL IONOSPHERE

L. R. O. Storey[1] and J. Thiel[2]
Centre National de la Recherche Scientifique
Laboratoire de Physique et Chimie de
l'Environement, 45045 Orléans Cédex, France

A medium-frequency (0.1 - 1.5 MHz) mutual-impedance probe was flown on three rockets in the auroral ionosphere, for the purpose of measuring the field-aligned drift velocity of the thermal electrons. Detailed results are presented from one of these experiments, in which a sensitivity of the order of 1% of the electron thermal velocity was achieved. Downward electron drifts were indicated, but their high apparent velocities cast doubt on their authenticity. Data from this and the other two experiments suggest that the probe was being perturbed by the payload body. This problem needs to be solved, and the sensitivity improved by an order of magnitude, in order for the probe to become a useful measuring instrument.

[1]Present address: STAR Laboratory
Stanford Electronics Laboratories
Stanford, CA 94305

[2]Present address: GREMI
Universite d'Orléans
45045 Orléans Cédex, France

H-9
1640

A LOOP ANTENNA FOR A VLF SATELLITE TRANSMITTER

H. C. Koons, M. H. Dazey and
D. C. Pridmore-Brown
The Aerospace Corporation
P. O. Box 92957
Los Angeles, CA 90009

The Space Sciences Laboratory of The Aerospace Corporation is presently defining an experiment to test a loop antenna configuration as a VLF transmitter in the ionosphere. The experiment is sponsored by the Naval Air Systems Command. The primary objectives of the experiment are to validate existing models for radiation by a loop antenna and to study the performance of the antenna in the ionospheric plasma.

The antenna will be carried into orbit in the payload bay of the space shuttle. During the radiation tests it will be deployed above the payload bay by the remote manipulator system. A VLF receiver aboard a subsatellite will be used to map the radiation pattern of the antenna by measuring the field intensities at distances from 1 to 100 km from the transmitter. Calculations predict that the antenna impedance will only be slightly modified by the plasma and that the link to the receiver can be closed at distances well beyond 100 km.

A one-third scale model of the antenna has been constructed. Impedance measurements have been made on the model in a 5-m diameter space plasma simulation chamber at NASA Lewis Research Center. The measurements confirm that the reactance of the antenna in an ionospheric plasma is essentially identical to its free space self inductance. The effective series resistance of the circuit increases with frequency. The losses are attributed to power transferred to plasma turbulence.

SELF-CALIBRATION AND IMAGE DECONVOLUTION

J Th-PM CR1-42

Chairmen: Ronald J. Ekers and T. J. Cornwell,
National Radio Astronomy Observatory,
Socorro, NM 87801

J-1 1330 A NEW PRACTICAL APPROACH TO THE MAXIMUM ENTROPY METHOD: R. Narayan, California Institute of Technology, Pasadena, CA 91125

J-2 1355 RESTORATION OF BEAM-SWITCHED SINGLE DISH OBSERVATIONS WITH THE MAXIMUM ENTROPY METHOD: Philip C. Gregory, Department of Physics, University of British Columbia, Vancouver, BC V6T 1W5

J-3 TESTS OF A NEW, SIMPLE MAXIMUM ENTROPY METHOD ALGORITHM:
1420 K. S. Evans, California Institute of Technology, Pasadena, CA 91125; and T. J. Cornwell, National Radio Astronomy Observatory, Socorro, NM 87801

J-4 1510 EFFECTS OF IMAGES, IMAGE CONSTRAINTS, AND ALGORITHMS ON VLBI IMAGE RECOVERY: D. G. Steet, M. R. Ito, and P. E. Dowdney, Dominion Radio Astronomy Observatory, Benticton, BC V2A 6K3

J-5 1535 SELF-CALIBRATION OF MILLIMETER-WAVELENGTH INTERFEROMETER ARRAYS: T. J. Cornwell, National Radio Astronomy Observatory, Socorro, NM 87801

J-6 1600 RELAXING THE ISOPLANATISM IN SELF-CALIBRATION: APPLICATION TO LOW-FREQUENCY ARRAYS: E. R. Schwab, National Radio Astronomy Observatory, Charlottesville, VA 22903

J-7 1625 POLARIZATION SELF-CALIBRATION: Lawrence A. Molnar, Center for Astrophysics, Cambridge, MA 02138

J-8 1650 IMAGE RECONSTRUCTION FROM PROJECTIONS AT IRREGULARLY SPACED POSITION ANGLES: Gary Beihl, Department of Electrical Engineering, Durand #112, Stanford University, Stanford, CA 94305

Image reconstruction from line-integral projections has often been employed to enhance resolution in radio astronomy. Many methods of reconstruction from projections are deterministic (e.g., convolution backprojection) because of profound computational advantages. When applied to data taken at irregularly spaced position angles, however, these techniques produce undesirable artifacts. An improved "natural" pixel iterative reconstruction algorithm is presented and shown to have reduced artifact when position angles are not regularly distributed.

NUMERICAL METHODS
B-1 Fr-AM CR2-28
Chairman: N. G. Alexopoulos, Electrical Engineering Department, University of California, Los Angeles, CA 90024

B1-1 0840 ERROR MEASURES FOR NUMERICAL MODELING

E. K. Miller
G. J. Burke
Lawrence Livermore National Laboratory
P.O. Box 808, L-153
Livermore, CA 94550

ABSTRACT

One of the greatest uncertainties involved in computer modeling is that of determining the numerical accuracy of a computed result. Various procedures have been used to estimate the numerical modeling error usually in terms of solution behavior as the number of unknowns is increased. In this paper we study several numerical measures of the modeling error for a set of representative problems.

Among the error measures studied is the class associated with observables such as the far field, input impedance and current distribution. A second class of error measures is provided by boundary condition miss-match and Poynting's vector on the surface of the object being modeled. A third class is given by the admittance matrix and its eigenvalue spectrum. These various error measures are first defined, and then their numerical behavior is examined, with respect to the model order and intended application (for example, radiation vs. scattering). Results are summarized to provide guidance concerning the quality of an error measure relative to its computational complexity.

B1-2
0900

STABILITY OF HYBRID SOLUTIONS AT INTERNAL RESONANCES

L. N. Medgyesi-Mitschang and Dau Sing Wang
McDonnell Douglas Research Laboratories
St. Louis, Missouri 63166

The use of hybrid solutions to solve integral equation formulations in electromagnetics at the internal resonances of closed perfectly conducting scatterers is examined. Hybrid solutions, incorporating the Fock theory Ansatz and the Galerkin representation, are compared with the method of moments (MM) based solutions of the electric, magnetic, and combined field formulations (J. R. Mautz, R. F. Harrington, AEÜ, 32, 159-164, 1978). The sensitivity of these solutions to the discretization inherent in the Galerkin (MM) process is investigated. The limitation of the condition number, based on the infinity norm, as a sensitive indicator of a spurious MM solution is assessed. Numerical results are presented for spheres and right circular cones and compared with experimental data. Generalization of these results to coated scatterers will be discussed.

B1-3
0920

DYADIC GREEN'S FUNCTION FORMULATIONS FOR USE IN METHOD OF MOMENTS FORMULATIONS

L. Wilson Pearson and J. Patrick Donohoe
Department of Electrical Engineering
University of Mississippi
University, MS 38677

The dyadic Green's function formalism is an attractive approach for the computation of fields produced by known source configurations because it provides a means to catalog systematically the Green's functions associated with a variety of geometries in a given coordinate system and to derive the Green's function for a new configuration from that of a geometrically simillar configuration. Almost all of the work which has been reported until now has focused on the Green's dyadic for electric and magnetic fields and as a result suffers from the difficulty associated with singularities in the source region. Several approaches that address field computation in the face of this singularity have appeared, but the singularity nevertheless proves awkward.

An attractive method of moments formulation for computation of current distributions on both wires and surfaces is the approach due to Glisson and Wilton (IEEE Trans. on Ant. & Propag., v. AP-28, pp. 593-603), which we shall term the "explicit scalar potential formulation." This formulation is based on the electric field integral equation and uses finite-difference approximations to the differential operators so that piecewise-constant basis functions and collocation with their incumbent simplicity can be applied. Because of this, one is interested in the computation of the magnetic vector potential and the electric scalar potential due to a given source configuration.

This presentation deals with the issues outlined above in a brief overview and proceeds to address the construction of the magnetic vector potential dyadic Green's function. The source region difficulties are not present in the potential representation, and, indeed, it may be applied to surface currrent density functions as well as to volume densities. On the other hand, it is somewhat more difficult to derive the vector potential dyadic than the electric field dyadic when an obstacle is present. This difficulty arises through the order in which one applies boundary conditions and executes the integration with respect to one of the spectral variables. These points are discussed and illustrated by way of an expansion for the magnetic vector potential dyadic radiating in the presence of an infinitely long perfectly conducting cylinder.

B1-4
0940

COMBINATION OF FFT AND CONJUGATE GRADIENT METHOD FOR EFFICIENT SOLUTION OF LARGE ELECTROMAGNETIC PROBLEMS

T.K. Sarkar and A.R. Djordjević*
Rochester Institute of Technology
Department of Electrical Engineering
P.O. Box 9887, Rochester, N.Y. 14623
*on leave of absence from University of Belgrade, Department of Electrical Engineering, P.O. Box 816, 11001 Belgrade, Yugoslavia

The spectral iterative approach is only a partly successful method for solving electromagnetic problems. It uses the fast Fourier transform to evaluate the convolution associated with Green's function in the spatial domain. This is quite advantageous as the convolution operation is highly time consuming. The method then utilizes a linear iterative approach to solve the electromagnetic problem. This technique, however, unnecessarily solves for extra unknowns in addition to the currents. Typically, with this iterative approach one solves a problem which has almost twice as many unknowns as the original problem. Thus this method is highly inefficient and does not always converge.

In this paper we propose to replace the spectral iterative method by the highly efficient conjugate gradient method. We utilize the fast Fourier transform to perform the convolution operation between the currents and Green's function, which is otherwise a time consuming procedure. The conjugate gradient method is then applied to solve the electromagnetic operator equation. The conjugate gradient method is always guaranteed to converge to the true solution, for any initial guess, in a finite number of steps. The spectral iterative technique, in contrast, gives no such guarantee. Example will be presented to illustrate the superiority of the conjugate gradient method over the spectral iterative technique.

B1-5
1000

A NOVEL TIME-DOMAIN DIAKOPTIC ANALYSIS OF ELECTROMAGNETIC SYSTEMS WITH NONLINEAR LUMPED LOADS

A.R. Djordjević* and T.K. Sarkar
Rochester Institute of Technology
Department of Electrical Engineering
P.O. Box 9887, Rochester, N.Y. 14623
*on leave of absence from University of Belgrade, Department of Electrical Engineering, P.O. Box 816, 11001 Belgrade, Yugoslavia

A novel time-domain method is presented for analysis of electromagnetic radiation and scattering from arbitrary electromagnetic structures with nonlinear lumped loads. This analysis differs fundamentally from the conventional time-stepping procedure in that the diakoptic approach is used to analyse the structure. Thus, we first consider the linear part of the structure as a multiport network and compute its numerical Green's functions (i.e., impulse responses). These responses can be obtained by using any technique, including the frequency-domain analysis. The nonlinear load is, however, analyzed in the time domain, so to obtain its terminal voltage-current characteristic. The time-domain response of the whole system to a given excitation is then computed by convolving the numerical Green's functions with the voltages at the structure ports. Thereby, the linear part of the system can be represented with respect to the nonlinear load as an equivalent voltage generator, with a time-constant dynamic resistance.

The new method differs from the Volterra series approach since the latter method solves for each intermodulation component separately, while the proposed method obtains the complete solution at once.

Examples of wire antennas with nonlinear loads will be presented to illustrate the application of the proposed technique.

SCATTERING AND INVERSE SCATTERING
B-2 Fr-AM CR2-28
Chairman: J. R. Wait, Geo-Electromagnetics Group,
Department of Electrical Engineering,
University of Arizona,
Tucson, AZ 85721

B2-1
1040

SCATTERING BY A SMALL RESISTIVE PLATE

Thomas B.A. Senior
Radiation Laboratory
Department of Electrical and Computer Engineering
The University of Michigan
Ann Arbor, MI 48109

Resistive sheet materials find many applications, not least for purposes of cross section reduction. To replace a thin metallic plate by one made of a composite or other material that can be represented as a resistive sheet can significantly reduce the radar cross section, and analyses and computations for the two-dimensional analogue of a plate, i.e., a strip, have demonstrated the advantages at frequencies in the resonance region and above. To see if these advantages persist as the frequency is lowered, we here examine the low frequency behavior of a resistive plate of finite dimensions.

When an electromagnetic wave illuminates a body whose dimensions are small compared with the wavelength, the far zone scattered field can be expanded as a power series in kL where k is the wavenumber and L is a characteristic dimension of the body. The leading (zeroth order) terms in the expansion are attributable to induced electric and/or magnetic dipoles. For a plate of resistivity R the boundary conditions imply that the electric dipole moment is identical to that for a perfectly conducting plate, and that the magnetic dipole moment is zero. The low frequency expansion is therefore discontinuous in the perfectly conducting limit $R = 0$, and to show how the scattering depends on R it is necessary to include higher order terms in the expansion.

The next (first order) contribution is considered and expressed in terms of potentials. Some implications of the results are discussed, and the explicit solution is obtained for a circular disk.

B2-2
1100

UNIFORM ASYMPTOTIC GREEN'S FUNCTION FOR THE PERFECTLY CONDUCTING CYLINDER TIPPED WEDGE

William Hallidy
Code 3313
Naval Weapons Center
China Lake, CA 93555

Uniform asymptotic expressions for the Green's functions for scattering of TM or TE plane waves by a perfectly conducting cylinder tipped wedge are calculated from the Watson transform of the appropriate eigenfunction expansions. These expressions are compared numerically with results obtained from the eigenfunction expansions and compared analytically with the expressions that are obtained by the application of UTD techniques to this object.

B2-3
1120

REQUIREMENTS FOR UNIQUENESS IN INVERSE SCATTERING PROBLEMS

W. R. Stone
IRT Corporation
1446 Vista Claridad
La Jolla, CA 92037

Some workers have expressed concern over the conditions under which the inverse scattering problem has a unique solution. This concern is usually motivated by a fear that a nonunique solution will translate into incomplete and/or inaccurate determination of a refractive index distribtuion in a scattering experiment. This paper considers the problem of how uniqueness considerations affect such a determination. It is generally accepted that all nonuniqueness associated with the problem resides in nonradiating sources. Indeed, this author has presented proofs for the uniqueness of the inverse scattering problem in the absence of nonradiating sources. But what is the meaning of a nonradiating source in the context of an inverse scattering problem?

The analogue of a nonradiating source for the inverse scattering problem is a nonscattering potential (or refractive index). It is known that such potentials exist for the case of a single incident (or probing) monochromatic plane wave field. In contrast, it is also known that a potential is uniquely determined by the fields scattered by an infinite set of incident plane waves (e.g., see the paper by Chapter 3 by B.J. Hoenders in H.P. Baltes (ed.), Inverse Source Problems in Optics, Springer-Verlag, 1978, and references therein). A very important practical case falls between these two extremes: Given a finite number of incident plane waves, over what set of potentials can uniqueness be achieved? This question is investigated in light of the author's results on radiating and nonradiating sources, and a relationship between spatial resolution and uniqueness is obtained. Some consequences of this result for obtaining a limitation on the set of nonradiating sources (and nonscattering potentials) which can be associated with a set of scattering data are pointed out.

B2-4
1140

AN EXAMINATION OF THE BOUNDARY CONDITIONS FOR EQUATIONS SATISFIED BY RADIATING AND NONRADIATING SOURCES AND FIELDS

W. R. Stone
IRT Corporation
1446 Vista Claridad
La Jolla, CA 92037

In a series of papers presented at the last two National Radio Science Meetings, the author has shown the following to be true for sources which, when used as the source term in the inhomogeneous Helmholtz wave equation, produce fields which are valid solutions of this equation (subject to appropriate boundary conditons):

1. A necessary and sufficient condition for a source ρ_R to produce fields which radiate is that ρ_R itself satisfies an inhomogeneous Helmholtz equation; and

2. A necessary and sufficient condition for a source ρ_{NR} to produce fields which do not radiate (i.e., which vanish identically everywhere outside a finite volume containing the source) is that ρ_{NR} satisifes a homogeneous Helmholtz equation.

It was also shown that the Green's functions for the Helmholtz equations satisfied by the fields produced by these two types of sources are necessarily different.

Based on these results, this paper shows that there are fundamental inconsistencies among the properties which a nonradiating source and its associated fields must have (using existing derivations), and the boundary conditions on the wave equation from which these properties are derived. This leads to an examination of the necessary and sufficient boundary conditions which must apply to the Helmholtz equation for radiating and nonradiating sources to exist. Such conditions are presented, and their implications for the existence of nonradiating sources and fields are discussed.

DIGITAL COMMUNICATIONS
C Fr-AM CR0-38
Chairman: Jack Salz, Bell Laboratories
Holmdel, NJ 07733

C-1
0900

DIGITAL TRANSMISSION FOR MOBILE SATELLITE SYSTEMS

D. O. Reudink
Bell Laboratories
Crawford Hill Laboratory
Holmdel, NJ 07733

For the next decade the new 800 MHz land mobile systems using cellular concepts will be introduced in urban areas. There are many non-urban applications where telephone service would be highly desirable, including service to vehicles along the nation's interstate highways and rural residence currently without means of wire line service. Estimates of losses on satellite-mobile paths indicate a need for high power satellites. To make matters worse, the received signal fluctuates with Rayleigh (or Rice) statistics resulting in high bit error rates. Estimates of performance are given for various propagation environments and methods are suggested including space diversity and resource sharing which can significantly improve system performance or alternatively increase capacity.

C-2
0930

LINEAR EQUALIZATION AND CANCELLATION IN DUALLY POLARIZED RADIO CHANNELS

N. Amitay and J. Salz
Bell Laboratories
Crawford Hill Laboratory
Holmdel, NJ 07733

Digital data transmission over dually polarized radio channels could potentially double the data rate of singly polarized transmission. The potential benefit can be realized only if end-to-end orthogonality of the polarized radio waves can be sustained. However, due to multipath fading the two waves become dispersed as well as coupled, resulting in mutual interference. The chief goal of this paper is to investigate an approach which mitigates this phenomenon. Toward this end we introduce and study a cross-coupled linear receiver structure which acts as an equalizer for the individual channels and as a cross-polarization canceler. We find that the optimum structure is comprised of four coupled transversal filters and our theory provides formulas relating the important system parameters for the optimized system. Additionally, we optimize a cross-coupled transmitting filter under an average power constraint. Our numerical examples are based on hypothesized channel characteristics since definitive experimental data is as yet unavailable.

C-3
1030

APPLICATIONS OF COMBINED SOURCE/CHANNEL CODING TO CELLULAR MOBILE RADIO

David J. Goodman
Bell Laboratories
Crawford Hill Laboratory
Holmdel, NJ 07733
Carl-Erik W. Sundberg
University of Lund
Lund, Sweden

We have recently studied several combinations of source codes and channel codes for application to cellular mobile telephony. The source codes are forms of differential pulse code modulation (dpcm) and the channel codes are short-constraint-length convolutional codes.

Using new theoretical work and computer simulations, we have studied the impact of various coding strategies on speech quality and on bandwidth efficiency defined as the number of simultaneous users per cell per MHz of system bandwidth.

Within a 10% outage objective, a variable-bit-rate transmission scheme can increase efficiency by a factor of 4 relative to uncoded transmission. This is achieved at the expense of complicated circuitry and a reduction in the number of users with high-quality reception. With a simpler, non-adaptive, coding strategy it is possible to multiply efficiency by 2.5 relative to uncoded transmission and to slightly increase the probability of high-quality service.

C-4
1100

NEEDED CONTROL CAPACITY FOR STABLE RESERVATIONS DATA TRANSMISSION

Joseph M. Aein
Institute for Defense Analyses
1801 North Beauregard Street
Alexandria, Virginia 22311

Consider a geostationary satellite channel accessed by small, possibly mobile, low-speed (e.g., 75 to 2.4 kbps) remote data users (RU) employing a contention-free reservations protocol. The RUs place their reservations over a dedicated control subchannel using the Slotted-ALOHA access protocol. The inherent propagation delay argues against the use of CSMA methods.

In this presentation the peak delay, throughput, and control subchannel capacity trade-off curves are numerically generated requiring absolute stability for the subchannel. It is shown that the reservations control subchannel utilization can be significantly less than 1/e when the stability requirement is imposed. Consequently, the control subchannel capacity need not be negligible.

HIGH LATITUDE IONOSPHERE
G Fr-AM CRO-30
Chairman: Jules Aarons, Department of Astronomy, Boston University, Boston, MA

G-1
0900

ELECTRON DENSITY IRREGULARITY SPECTRA NEAR AURORAL PRECIPITATION AND SHEAR REGIONS

S. Basu
Emmanuel College
400 The Fenway
Boston MA 02115
W.R. Coley and W.B. Hanson
University of Texas at Dallas
Richardson TX 75080
C.S. Lin
Southwest Research Institute
San Antonio TX 78284

Spectral characteristics of auroral F-region irregularities are studied by the use of high resolution ($\sim$35 m) density measurements made on board the retarding potential analyzer (RPA) of the Atmosphere Explorer-D (AE-D) satellite. The auroral energy input was estimated by integrating the low energy electron (LEE) data on AE-D. It was found that the one-dimensional in-situ spectral index (p_1) of the irregularities at scalelengths <1 km showed considerable steepening in regions of large auroral precipitation with p_1 values $\sim$ -3. This probably indicates the effect of E-region conductivity on F-region irregularity spectra. The regions in between the precipitation structures, where presumably the E-region conductivity is small, are generally associated with large shears in the horizontal E-W drifts. The shear gradient scale lengths are $\sim$10 km which is the resolution of the ion-drift meter on AE-D. The spectral characteristics of irregularities in the shear-flow regions are very different with p_1 being $\sim$ -1. Since these regions are also associated with large irregularity amplitudes, it seems probable that the velocity turbulence acts as a source of irregularities in the auroral F-region ionosphere.

G-2
0920

POLAR CAP SCINTILLATION MEASUREMENTS USING THE HILAT SATELLITE

M. D. Cousins, R. C. Livingston,
C. L. Rino, J. F. Vickrey
SRI International
Menlo Park, CA 94025

The HILAT satellite was launched on June 27, 1983. The main tracking station at Sondrestrom, Greenland became operational on September 6, 1983. Multifrequency radiowave scintillation data, together with simultaneous data from a magnetometer, a particle detector, and a retarding potential analyzer/drift meter, have been obtained on a regular schedule. These data, combined with correlative measurements from the Sondrestrom Incoherent Scatter radar, have provided a number of well-defined polar-cap scintillation events. Such data are particularly interesting because they occur in the absence of a strongly conducting E-layer. We shall present and discuss these data in light of new models that attempt to predict the onset and evolution of the irregularities that cause the scintillation.

G-3
0940

COMPARATIVE MORPHOLOGY OF PHASE SCINTILLATION IN THE AURORAL OVAL AND POLAR CAP

S. Basu and E. MacKenzie
Emmanuel College
400 The Fenway
Boston MA 02115
H.E. Whitney
Air Force Geophysics Laboratory
Hanscom AFB MA 01731

A preliminary study of phase scintillations at high latitudes based on the observations of a quasi-geostationary Air Force Satellite at 250 MHz during an equinoctial period is reported. The measurements were made from Goose Bay, Labrador and Thule, Greenland providing geomagnetic latitude coverage of 65°-70°N (CGL) and 85°-89°N respectively. The study is oriented towards contrasting the morphological behavior of phase and amplitude scintillation magnitudes and their temporal structure in the auroral and polar cap locations. It is shown that intense scintillation events in the polar cap providing phase scintillations in excess of 10 radians (with an 88 sec detrend interval) may be obtained irrespective of the diurnal and magnetic conditions. At Goose Bay, on the other hand, such magnitudes of phase scintillation are generally obtained at night under magnetically disturbed conditions. The phase spectral slopes seem to steepen with increasing phase scintillation magnitude at both stations, the trend being more pronounced at Goose Bay. These results are discussed in the light of current knowledge of particle precipitation and convection.

G-4 1020 AURORAL ABSORPTION--ONE MORE TIME: Vaughn Agy, 1718 Bluff, Boulder, CO 80303

Since the 1950's, users of HF at high latitudes have expected that riometers would provide the data base of a method for the prediction of auroral absorption as it affects the performance of HF circuits. Some half-dozen attempts have been made to develop such a method; all of them--consciously or otherwise--have either ignored some of the available information or have misinterpreted it.

Papers in the literature lead us to conclude that no method yet devised is acceptable and, perhaps, that none ever will be. An analysis of Kiruna riometer data for five years (1970-74) supports this conclusion. The analysis will be described.

G-5 1040 A NEW HF-RADAR FOR STUDYING HIGH LATITUDE F-REGION IRREGULARITIES: R. A. Greenwald, K. B. Baker, R. A. Hutchins, and C. Hanuise, Johns Hopkins University, Applied Physics Laboratory, Laurel, MD 20707

In September, 1983 a new coherent backscatter HF-radar was installed at Goose Bay, Labrador to study F-region plasma irregularities at very high latitudes. This radar uses a phased array of 16 log-periodic antennas to construct 16 beams for both transmission and reception, and operates in the frequency range from 8 to 10 MHz. A multipulse pattern is used to form a 17-lag complex autocorrelation function which provides detailed spectral information about the observed irregularities. Up to 50 ranges can be observed simultaneously along a single beam, providing a spatial resolution of about 2 degrees in azimuth and 15-30 km in range. The narrow beams also provide greater backscattered power which allows time resolution on the order of 5 seconds. The system is controlled by a microcomputer and offers manual, semi-automatic, and fully automatic modes of operation.

In this paper examples of the results obtained in the different operating modes will be presented.

F-REGION WAVE STRUCTURES
H Fr-AM CR2-26
Chairman: S. H. Gross, Department of Electrical Engineering, Microwave Research Institute, Polytechnic Institute of New York, Farmingdale, NY 11735

H-1
0840

LARGE SCALE STRUCTURES IN THE F REGION OBSERVED BY AE-C AND AE-E

Stanley H. Gross
Department of Electrical Engineering
Microwave Research Institute
Polytechnic Institute of New York
Route 110
Farmingdale, New York 11735

Large scale wave structures have been observed at F region heights by in situ measurements on board Atmosphere Explorers C and E of electron density, ion and electron temperatures, neutral densities, temperature and winds.

Scales ranging from tens of kilometers to thousands of kilometers have been found with strong correlations between fluctuations of the various geophysical parameters. The observations will be reviewed, examples will be shown and deductions from the observations will be described. The basis will be explained for claiming that much structure observed by the satellites are quasi-stationary in nature. Difficulties in finding sources from satellite data alone will be described.

H-2
0900 TRAVELING IONOSPHERIC DISTURBANCES OBSERVED IN TOTAL ELECTRON CONTENT NEAR L = 4 AND A SEARCH FOR POSSIBLE SOURCES

Robert D. Hunsucker, Geophysical Institute, University of Alaska, Fairbanks, AK 99701 and John K. Hargreaves, Environmental Sciences Department, University of Lancaster, Lancaster, England LA1 4YQ

Total electron content (TEC) values derived from Faraday rotation measurements of ATS-1, ATS-6, and SMS-1 satellite radio beacon transmissions were obtained during the period November 1978 through July 1981 near Fairbanks, Alaska. The subsatellite point of the ATS-6 path was located at geographic coordinates of ~58°N, 146°W; L = 4.0, and invariant latitude ≈60°, over the Gulf of Alaska. Variations in TEC of 1 to 4% of TEC_{max} with periods of 15-90 minutes (peak occurrence near 50 minutes) were observed virtually every day. From examination of the sequential appearance of the periodic events on the SMS-1 to Fairbanks and ATS-1 to Fairbanks paths (intersection points 350 km apart E-W), we deduce an apparent east-to-west velocity component of 200-700 m/sec. Assuming that these periodic TEC variations are traveling-ionospheric-disturbances (TID's) which are manifestations of atmospheric gravity waves (AGW's), and utilizing recently published material on their propagation characteristics, the results are not inconsistent with some of the TID's travelling approximately along the magnetic meridian which passes through the subsatellite areas, with velocities of ~100-200 m/sec. There does not appear to be any strong correlation between the occurrence of these TID's and large-scale weather features in the Alaskan region, College K-indices, K_p, magnetic disturbances on the Alaska meridian magnetometer chain, AE index, or large features of the auroral oval.

Work is continuing in the search for sources of these TID's using simultaneous Chatanika incoherent scatter radar, Cleary HF radar and other high-latitude aeronomic data.

H-3
0920 GENERATION AND PROPAGATION OF ATMOSPHERIC WAVES BY VOLCANIC ERUPTION OF MOUNT ST. HELENS

C. H. Liu and K. C. Yeh
Department of Electrical Engineering
University of Illinois at Urbana-Champaign
Urbana, IL 61801

The problem of excitation and propagation of acoustic-gravity waves by sources in the lower atmosphere is important in understanding the dynamic coupling of the different regions of the atmosphere. The eruption of Mount St. Helens on May 18, 1980 and the subsequent dynamic responses of the atmosphere offered a good opportunity to study this problem. Global observational data including microbarograph on the ground, HF Doppler and TEC in the ionosphere will be presented. Propagating acoustic-gravity wave modes consistent with the data will be applied to interprete the observed phenomena. Possible inference on the nature of the source will be discussed.

H-4
0940

GRAVITY WAVES PRODUCED BY PRECIPITATION FROM THE OUTER RADIATION BELT

M. G. Morgan
Radiophysics Laboratory
Thayer School of Engineering
Dartmouth College
Hanover, NH 03755

Waves produced by heating from the morning maximum in outer radiation belt precipitation have been studied using close-spaced rapid-run ionosondes to observe the resulting traveling ionospheric disturbances (TID's). Waves from individual sources have been found to travel northward, as well as southward, with identical speeds and on opposite bearings. Parameters of the causative gravity waves, including their height dependence and dispersion, are deduced from those of the TID's by inversion of Hooke's perturbation formula. Delineation of the sources with a close-spaced grid of fan-beam riometers is being undertaken.

H-5 1020 GRAVITY WAVES IN THE F-REGION: N. K. Balachandran, Lamont-Doherty Geological Observatory of Columbia University, Palisades, NY 10964

The Doppler shift of CW high-frequency radio waves reflected from the ionosphere is utilised to detect travelling ionospheric disturbances. By using an array of transmitters and different frequencies, the three-dimensional propagation vector of the T.I.D. is evaluated. The T.I.Ds are interpreted as gravity waves generated by the aurora or tropospheric weather systems. Waves generated by the aurora travel away from the pole with a speed (horizontal) greater than the speed of sound at the ionospheric level, whereas waves generated by tropospheric weather system may travel in any direction with the horizontal speed less than the speed of sound. An interesting example of gravity waves arriving from the direction of a deep upper air low is presented. The waves were travelling with a horizontal trace velocity of about 180 meters per sec. At the time of wave generation, the low was dissipating fast and geostrophic adjustment is suggested as a possible source mechanism.

H-6 ATMOSPHERIC GRAVITY WAVES PRODUCED BY SOLAR ECLIPSES
1040

K. Davies, Author
National Oceanic and Atmospheric Administration
ERL/Space Environment Laboratory
325 Broadway
Boulder, CO 80303

The paper reviews the theoretical and experimental bases for gravity wave production resulting from cooling produced by the moon's shadow. Theoretically, it is reasonable to expect waves from the bow shock after propagation in a dispersive and anisotropic atmosphere and that focusing should be expected from the eclipse geometry. Experimental evidence from the eclipses of 7 March 1970 in North America, 30 June 1973 in Africa and 23 October 1976 in Australia leave doubts as to whether such waves have been observed.

H-7
1100

EFFECTS OF NEUTRAL WIND, WAVES, AND VELOCITY SHEAR ON THE GENERATION AND GROWTH OF PLASMA BUBBLES

R. T. Tsunoda
SRI International
Menlo Park, California 94025
D. P. Sipler and M. A. Biondi
Department of Physics and Astronomy
University of Pittsburgh
Pittsburgh, Pennsylvania 15260

Two interpretations have been suggested to explain the generation and growth characteristics of plasma bubbles; (1) wavelike variations are transferred to the F region plasma by atmospheric gravity waves; and (2) large spatial wavelengths in random plasma perturbations are preferentially amplified by plasma instability processes. The preferential filtering results from the presence of velocity shear in bulk plasma drift. In this paper, we evaluate these interpretations in the light of recent radar backscatter and Fabry-Perot interferometer measurements of F region neutral winds, waves in plasma structure, and velocity shear. East-west scans made with ALTAIR, a steerable incoherent scatter radar, reveal that large wavelike altitude modulations in the bottomside F layer contours of electron density are not a prerequisite to bubble generation; yet there appears to be quasi-periodicity associated with east-west bubble spacing. Associated neutral wind and velocity shear measurements are discussed.

H-8
1120

CHARACTERISTICS OF GROUPED IONIZATION DUCTS:

D.B. Muldrew, Communications Research Centre, Department of Communications, Ottawa, Ontario K2H 8S2 and S.H. Gross, Polytechnic Institute of New York, Farmingdale, NY 11735

It has previously been observed by the authors that ionization ducts, capable of trapping MF and HF waves transmitted by topside sounders, often occur almost uniformly spaced, in a group. This suggests that acoustic gravity waves may contribute, in some way, to their generation. The present study shows that certain characteristics, which have been found to apply to isolated ducts, to spread F and to bubbles, also apply to groups of ducts. If acoustic gravity waves are mainly responsible for generating equally spaced groups of ducts but single ducts and spread F are generated by other mechanisms then it might be expected that the grouped ducts would not have the same characteristics. The seasonal variation of occurrence frequency of grouped ducts shows a well-defined maximum in December-January (near the December solstice) for data recorded near Quito, Ecuador and in July-August (near the June solstice) for data recorded near Orroral, Australia. This effect has been explained previously (for spread F and single ducts) by dynamo current systems. The occurrence frequency of grouped ducts also correlates with lunar phase, the maxima occurring about 6 and 21 days after new moon. Hence lunar tidal induced electric fields in the dynamo region apparently have some influence on the production of grouped ducts. The dynamo region is also where acoustic gravity waves can be reflected by temperature gradients and, consequently, standing acoustic gravity waves may at times be set up explaining the almost constant spacing. It thus appears that the generation of field-aligned irregularities such as spread F and ionization ducts is influenced by various mechanisms such as gravity waves, tides and currents in the dynamo region.

H-9
1140

ACOUSTIC-GRAVITY-WAVE-PRODUCED FIELD-ALIGNED IRREGULARITIES

S.P. Kuo and S.H. Gross
Department of Electrical Engineering
Polytechnic Institute of New York
Route 110
Farmingdale, New York 11735
M.C. Lee
Regis College Research Center
Weston, MA 02193

We study the ionospheric disturbances produced by an acoustic-gravity wave. In the E region, electron-neutral and ion-neutral collisions play the principal role. Thus, the energy carried by the gravity wave can be transferred to electrons and ions through collisions. It seems from observations that field-aligned ionization irregularities may be produced in the presence of an acoustic-gravity wave (Gross and Muldrew, URSI National Radio Science Meeting, Boulder, Colorado, January 1983). In this work we propose a theory to show that a field-aligned purely growing wave and an oscillatory quasi-ion wave can be parametrically excited by an acoustic-gravity wave as a pump. The nonlinear effect responsible for the excitation of a field-aligned purely growing mode is the thermal focusing forces on electrons and ions caused by their collisions with neutrals. But for the oscillatory quasi-ion mode, the nonlinear effect comes from momentum transfer collisions. The threshold energy of the acoustic-gravity wave for this instability is found to be inversely proportional to the square of the scale length and the ion-neutral collision frequency. Therefore, large scale irregularities could be favorably excited, comparable to the scale length of the acoustic-gravity wave.

PLANS FOR RADIO AND RADAR ASTRONOMY FROM SPACECRAFT

J Fr-AM/PM CR1-42

Chairman: Samuel Gulkis, Space Science Division, Jet Propulsion Laboratory, Pasadena, CA 91103

J-1 1020 SUBMILLIMETER-WAVE ASTRONOMY FROM SPACE: Thomas G. Phillips and Peter G. Wannier, California Institute of Technology, Pasadena, CA 91125

J-2 1100 VOYAGER'S PLANETARY RADIO ASTRONOMY PROGRAM: James W. Warwick, Department of Astrophysical, Planetary, and Atmospheric Science, University of Colorado, Boulder, CO 80309

J-3 1140 THE VENUS RADAR MAPPER: Gordon H. Pettengill, Department of Earth and Planetary Science, MIT, Cambridge, MA 02139

J-4 1330 THE INFRA-RED ASTRONOMY SATELLITE (IRAS): Charles Beichman, California Institute of Technology, Pasadena, CA 91125

J-5 1410 THE COSMIC BACKGROUND EXPLORER: Samuel Gulkis, Space Science Division, Jet Propulsion Laboratory, Pasadena, CA 91103

J-6 1450 ORBITING VERY LONG BASELINE INTERFEROMETRY: Bernard F. Burke, Department of Physics, MIT, Cambridge, MA 02139

INCOHERENT SCATTER
G Fr-PM CRO-30
Chairman: C. L. Rino, SRI International, Menlo Park, CA 94025

G-1
1400 **Incoherent Scatter Results from the Arecibo Observatory: A Review**

Richard A. Behnke, National Science Foundation
Washington, D.C. 20550

The progress of Arecibo-based incoherent scatter radar studies of the ionosphere and atmosphere is followed from the late sixties to the present. The emphasis is on how the development of new experimental techniques gives rise to an ever-increasing ability of the Arecibo radar facility to measure the structure and dynamics of the ionosphere as well as to infer many properties of the neutral atmosphere. Examples of techniques that have augmented the power of the Arecibo radar include the use of multiple pulses, Barker codes, very large pulses, special correlators, moving the radar beam, and coordinated optical/radar experiments. Some of the outstanding problems that can be attacked using the present-day capabilities of the Arecibo facility are also discussed.

G-2
1420

RADAR RESULTS FROM CHATANIKA AND SONDRESTROM

V. B. Wickwar, SRI International, Radio Physics Laboratory, Menlo Park, CA 94025

This talk will review some of the research accomplishments made with the SRI-operated, incoherent-scatter radar at high latitude ($\Lambda = 65°$) during a solar cycle and at very high latitude ($\Lambda = 75°$) during the past year. The importance of these locations is the possibility of observing phenomena in the upper atmosphere and ionosphere that are related to the magnetosphere. Recall that the Chatanika radar was under the nighttime auroral oval and the Sondrestrom radar is under the magnetospheric cusp. The studies have included energy inputs, convection, the electrodynamical circuit, thermospheric behavior, and plasma physics. The research approach has varied from point measurements with the radar to global scale phenomena requiring coordinated observations with several radars and other instruments, such as project MITHRAS and the meridional chain of radars. While Chatanika operations are now history and we are looking forward to the future in Sondrestrom, the Chatanika data set remains a valuable asset for current and future research.

G-3
1440

STUDIES OF THE MID AND HIGH-LATITUDE IONOSPHERE WITH THE MILLSTONE HILL RADAR

John C. Foster
MIT Haystack Observatory
Westford, Massachusetts 01886

Recent ionospheric studies at Millstone Hill have utilized the capabilities of the 2.5 MW UHF system coupled to the 150 foot fully steerable antenna to make incoherent scatter measurements over a wide span of latitudes and local times. A combination of azimuth and elevation scanning antenna modes provides coverage over 35^{o}-75^{o} invariant latitude and some 6 hours of local time. In addition, the use of the vertically pointing fixed 220 foot antenna with a variety of pulse modes enables high resolution observations of mid-latitude ionospheric parameters over an altitude range of 70-1500 km. Data analysis is facilitated by a dedicated computer which permits complex interactive data acquisition and display programs to control the radar experiments in addition to supporting an on-line data base of some 120 days of detailed Millstone Hill Radar observations. Both the real time data and the Millstone Hill data base are easily accessed by remote users.

Scientific analysis of the Millstone Hill Radar data has involved detailed studies of individual experiments directed towards examining ionospheric temperatures, convection, and trough formation, the use of the data base in the preparation of global high and mid-latitude empirical ionospheric models, and radar studies requested by external users of specific ionospheric phenomena. An important area for continued research involves the Millstone Hill Radar's position in the meridional chain of U.S. incoherent scatter radars which includes Sondrestromfjord, Millstone Hill, Arecibo and Jicamarca. Experiments designed to investigate the interaction of polar, auroral, mid and equatorial latitude ionospheric phenomena as well as global wave propagation and the ionospheric energy budget are underway.

G-4
1500

EISCAT: OVERVIEW OF SOME OF ITS RECENT SCIENTIFIC ACHIEVEMENTS BY THE EISCAT SCIENTIFIC COMMUNITY

Pierre Bauer
CNET/PAB/RPE 38-40
Rue du General Leclerc
Issy-Les-Moulineaux, France

An Eiscat Workshop held at Aussois (France) in September 1983 gave the opportunity of making the point on the scientific return of the Eiscat operation in conjunction with other ground based or space observations. Several of the highlights of the workshop are presented in this paper. They concern:

- The observation of unequal perpendicular and parallel ion temperatures in the F region at times of large convection electric fields.

- The observation of ion composition changes associated to F region joule heating events and to soft particle precipitations.

- The simultaneous observation of the convection electric field and of F region ionization transport phenomena at Chatanika, Millstone Hill and Eiscat during the Mithras Program.

- The observation of F region electron depletions in the noon sector of the auroral region.

- The observations of hard particle precipitations in the morning sector of the auroral region.

G-5
1540

MITHRAS OBSERVATIONS OF AURORAL ZONE PRECIPITATION BOUNDARIES, O. de la Beaujardiere, SRI International, Radio Physics Laboratory, Menlo Park, CA, and C. Senior, CNET, St. Maur, France

During the MITHRAS campaign, the auroral zone could be probed simultaneously by three different incoherent scatter radars. These observations were performed in order to gain insight on the global behavior of high-latitude phenomena. The observations were conducted over a wide range of latitudes and for 24-hour periods. The poleward and/or equatorward boundary of the auroral precipitation were often within the field of view of the EISCAT and Chatanika radars. The E-region density measured at EISCAT and Chatanika are examined to determine the position of the auroral precipitation boundaries. In addition we study their relationship with the ion convection boundaries, and with the ion convection reversal. We examine the latitudinal motion of the continuous aurora boundaries and how they are affected by substorms.

G-6
1600

THE VERY HIGH LATITUDE IONOSPHERE

V. B. Wickwar, J. D. Kelly, O. de la Beaujardiere
SRI International, Radio Physics Laboratory,
Menlo Park, CA 94025

The Sondrestrom radar is situated at approximately 75° invariant latitude. At this location, it passes under or near several ionospheric regions and boundaries: the poleward portion of the nighttime auroral oval, the polar cap, and the cusp. Regular observations of these little explored regions will provide valuable information about the relationship of the ionosphere, thermosphere, and magnetosphere to one another. These observations, in addition, will provide data that will contribute to understanding the global structure and dynamics of the upper atmosphere. This region has been observed extensively during much of the past year in a series of experiments covering 10° of invariant latitude, with 30-minute time resolution, and for 24-hour periods. An overview of the results is presented, including densities, temperatures, and ion velocities. The emphasis is on the differences found between this higher-latitude portion of the upper atmosphere and the auroral zone latitudes observed from Chatanika.

G-7
1620

SONDRESTROM RADAR MEASUREMENTS OF VERY-HIGH-LATITUDE CONVECTION PATTERNS

J. D. Kelly
Radio Physics Laboratory
SRI International
Menlo Park, CA 94025

Twenty-four-hour experiments have been performed at Sondrestrom each month since April 1983; convection patterns derived from these experiments are presented. A multi-position antenna mode is used, and the convection patterns are determined from the ion-drift-velocity measurements. This technique provides resolved ion velocity as a function of both time (30-min resolution) and latitude ($\sim 10^{\circ}$ Λ). From these data, the polar-cusp convection-stagnation region and the polar-cap boundary can frequently be identified: the first by the rotation of convection and the second from the sharp east-west reversal of the convection. Variations in the location of the polar cusp and polar-cap boundary were examined. These data will be compared with models of convection patterns.

GENERAL ASTRONOMY
J Fr-PM CR1-42
Chairman: Mark A. Gordon, National Radio Astronomy Observatory, Tucson, AZ 85705

J-1 1600 MILLIMETER-WAVE APERTURE SYNTHESIS OF W3 (OH): J. L. Turner, Department of Astronomy, Berkeley, CA 94720

We present results from an aperture synthesis mapping of the compact HII region W3(OH) in the 3.3 mm J=1 -0 transition of HCN. The observations were made with the Hat Creek millimeter interferometer. The 1.4" beam achieved in the synthesis reveals an emission feature near the position of the water masers 7" east of the radio continuum source. The velocity profile of this feature suggests that the HCN is physically associated with the maser emission. The continuum map we obtain reveals a weak continuum feature to the northeast of the main continuum source. For the faint continuum source we infer a size of 0.6" and an electron density of 5×10^5 cm-3. Toward the main continuum source, we see HCN emission with peaks separated in both position and velocity. The locations of the peaks are consistent with gravitationally bound rotation about the exciting star of the bright HII region.

J-2 A 100 GHZ SIS MIXER HAVING GAIN AND WIDE BANDWIDTH

1620

L. R. D'Addario
National Radio Astronomy Observatory
2015 Ivy Road
Charlottesville, Virginia 22903

An SIS mixer has been constructed for the 3 mm wavelength band, using a novel design. By using a double-tuned structure in full-height WR-8 waveguide, the r.f. source impedance presented to the junction can be optimized over a wide bandwidth. This makes possible the realization of conversion gain, leading to the prospect of very low-noise receivers.

The SIS junctions used in this mixer are fabricated using the lead-alloy technology developed by IBM (Greiner et al., IBM J. of Res. and Dev., 24, 195, 1980) and implemented at the National Bureau of Standards in Boulder. Integrated circuits containing the junction, a waveguide coupling probe, an inductor to resonate the junction capacitance, and a simple low-pass i.f. filter are fabricated on crystalline quartz substrates. This arrangement helps to achieve the broad bandwidth which is required to achieve conversion gain at moderate i.f. (Smith and Richards, J. Appl. Phys., 53, 3608, 1982).

Results so far include one device which achieves a conversion efficiency of -2.3 to +0.4 dB (SSB) from 100 to 110 GHz, and a mixer noise temperature (SSB) of 36 to 43K over the same range. These results were repeatable over several thermal cycles between 3K and 300K. The measurements were made at an i.f. of 1.4 GHz, but the instantaneous r.f. bandwidth is estimated to be 10 GHz. Because of the broad bandwidth and single-junction device, this mixer tends to saturate at low input noise temperatures; -0.7 dB compression has been measured at 52K input temperature. Work is in progress to improve this by constructing multiple-junction devices and suitable bandpass filters.

J-3
1640

THE ROLE OF CORE AND CONAL EMISSION IN PULSAR MODE CHANGING AND SUBPULSE DRIFTING

Joanna M. Rankin
Physics Department
University of Vermont
Burlington, Vermont 05405

Studies of polarized average profiles distinguish two types of pulsar emission, conal and core. How do these two types of emission manifest themselves in individual pulse sequences? No general answer to this question is available, but two well known pulsar phenomena provide some very clear suggestions: Drifting subpulses seem to be an exclusively conal phenomenon. No characteristic modulation of core emission has been identified. Moreover, mode changing seems to represent a readjustment of the relative amplitudes and symmetry of the conal and core components. While mode changing may not be restricted to triple (T) and multiple (M) profiles, it is certainly most easily identified in this kind of star.

Condensed Technical Program (cont.)

THURSDAY, 12 JANUARY

0830-1200

F Radar Backscatter: Clear Air and Sea Surface	CR1-42
G Radio Propagation	CR0-30
H Coherent Wave-Particle Interactions in the Magnetosphere	CR2-26
J Solar Radio Astronomy	CR1-42

1400-1700

A Network Analyzers: Accuracy and Standard Test Methods	CR2-6
B-1 Numerical Solution Techniques for General Scatterers	CR1-46
B-2 Propagation in Random Media	CR2-28
C Spread Spectrum Communications	CR0-38
F Storms, Precipitation, Satellite Transmission, and Profile Retrieval	CR1-42
G Ionospheric Modification and Heating	CR0-30
H Antennas in Plasmas	CR2-26
J Self-Calibration and Image Deconvolution	CR1-42

1700

Commission B Business Meeting	CR2-28
Commission C Business Meeting	CR0-38

1800

Reception	Events/Conference Center

FRIDAY, 13 JANUARY

0830-1200

B-1 Numerical Methods	CR2-28
C Digital Communications	CR0-38
G High Latitude Ionosphere	CR0-30
H F-Region Wave Structures	CR2-26

0900

Commission J Business Meeting	CR1-42

1020-1530

J Plans for Radio and Radar Astronomy From Spacecraft	CR1-42

1040-1200

B-2 Scattering and Inverse Scattering	CR2-28

1400-1640

G Incoherent Scatter	CR0-30

1600-1700

J General Astronomy	CR1-42